Lithos 370–371 (2020) 105636

Contents lists available at ScienceDirect

Lithos

journal homepage: www.elsevier.com/locate/lithos

Invited review article

Lawsonite composition and zoning as tracers of subduction processes: A global review

Donna L. Whitney [a,*], Katherine F. Fornash [b], Patricia Kang [a], Edward D. Ghent [c], Laure Martin [d], Aral I. Okay [e], Alberto Vitale Brovarone [f]

[a] Department of Earth & Environmental Sciences, University of Minnesota, Minneapolis, MN 55455, USA
[b] Department of Geological Sciences, Ohio University, Athens, OH 45701, USA
[c] Department of Geoscience, University of Calgary, Calgary, Alberta T2N 1N4, Canada
[d] Centre for Microscopy, Characterisation and Analysis, University of Western Australia, Crawley, WA 6009, Australia
[e] Eurasia Institute of Earth Sciences, Istanbul Technical University, TR-34469 Istanbul, Turkey
[f] Institut de Minéralogie, de Physique des Matériaux et de Cosmochimie (IMPMC), Sorbonne Université, Muséum National d'Histoire Naturelle, UMR CNRS 7590, IRD UR206, 75005 Paris, France

ARTICLE INFO

Article history:
Received 31 January 2020
Received in revised form 3 June 2020
Accepted 7 June 2020
Available online 20 June 2020

Keywords:
Blueschist
Eclogite
Lawsonite
Subduction
Zoning

ABSTRACT

Lawsonite is an abundant hydrous mineral in oceanic crust, sediments, and metasomatic rocks at depths of ~45 to 300 km in most subduction zones, but it is rarely preserved in the geologic record because it commonly transforms to epidote and other minerals during prograde or retrograde metamorphism. Owing to the significance of lawsonite for water and element cycling in subduction zones, occurrences of fresh lawsonite in blueschist and, more rarely, eclogite provide important opportunities to determine lawsonite composition, zoning, and inclusion suites and to use this information to reconstruct reaction history during subduction and exhumation. In this review, we use new and published data to document lawsonite composition in eight of the nine known lawsonite eclogite localities in which fresh lawsonite coexists with garnet + omphacite in the rock matrix, as well as the composition of lawsonite inclusions in six of seven known sites in which lawsonite occurs only as inclusions in garnet in eclogite-facies rocks that lack matrix lawsonite. As lawsonite blueschist is much more common than lawsonite eclogite, we survey the composition of lawsonite in representative localities of blueschist, including blueschist associated with eclogite (lawsonite-bearing, epidote-bearing), and blueschist not associated with eclogite at current exposure levels. Included in this review are metabasaltic rocks, silica- and carbonate-rich metasedimentary rocks, metasomatic rocks, and lawsonite-rich veins. This dataset demonstrates that lawsonite composition is a sensitive indicator of reaction history during subduction and exhumation, and specifically of fluid–rock interaction, with implications for element cycling in subduction zones. Furthermore, most exhumed lawsonite eclogite records slab-surface conditions that correspond to the location where the slab-mantle interface transitions from decoupled to coupled, and therefore provides key insights into the thermal history and dynamics of subduction zones.

Contents

* Corresponding author.
E-mail address: dwhitney@umn.edu (D.L. Whitney).

https://doi.org/10.1016/j.lithos.2020.105636

1. Introduction

Volatiles and other elements are transferred from subducted lithosphere to the overlying mantle wedge, influencing the composition of the mantle and, subsequently, the composition of arc magma, the atmosphere, and oceans. Subducted sediments, oceanic crust, and serpentinized mantle begin to devolatilize at forearc depths (e.g. Hacker et al., 2003a, 2003b; Kerrick and Connolly, 2001; Scambelluri et al., 2019; van Keken et al., 2011). Nevertheless, field, experimental, and modeling studies show that subducted materials in all but the hottest subduction zones retain abundant hydrous and/or CO_2-bearing minerals into the eclogite facies, including at conditions corresponding to the maximum depth from which subducted oceanic crust is typically exhumed (~70–80 km; e.g., Whitney et al., 2014; Collins et al., 2015): e.g., amphiboles, lawsonite, epidote-group minerals, talc, chlorite, phengite, and carbonate minerals. The locations and extent of devolatilization of subducting crust and mantle are controlled by the thermal state and composition of the slab, including degree of pre-subduction hydration/carbonation, and these in turn affect the extent to which slab-derived fluids influence oxidation state of the mantle (e.g., Gerrits et al., 2019; Kelley and Cottrell, 2009). The geologic record of fluid-mediated processes in subducted lithologies is primarily in high-pressure/low-temperature (HP/LT) complexes: in tectonically-exhumed mélange and more structurally-coherent terranes, as well as in rare xenoliths derived from subducted oceanic crust.

Experimental and modeling studies of oceanic crust under the HP/LT conditions of subduction metamorphism predict that the hydrous Ca-Al silicate lawsonite ($CaAl_2Si_2O_7(OH)_2H_2O$) is prevalent at forearc to subarc depths (~45–300 km) in subducted oceanic crust (Grevel et al., 2001; Hacker et al., 2003a, 2003b; Liu et al., 1996; Okamoto and Maruyama, 1999; Pawley, 1994; Schmidt and Poli, 1998) (Fig. 1). Lawsonite also occurs in subducted continental crust, continental margin material, oceanic sediments (metachert, metacarbonate), and metasomatic rocks (e.g. Martin et al., 2011b; Vitale Brovarone et al., 2014a), and therefore has widespread stability in a range of rock bulk compositions during subduction metamorphism, as also predicted by experiments (e.g., Domanik and Holloway, 1996; Martin et al., 2014; Ono, 1998).

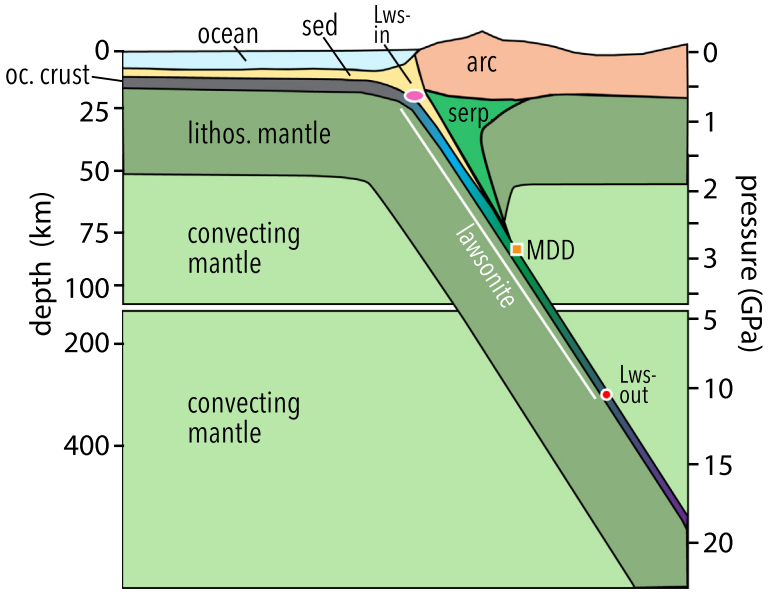

Fig. 1. Schematic illustration of a subduction zone showing the approximate stability region for lawsonite (Lws) in oceanic crust at or near the top of the subducting slab. Also shown is the maximum decoupling depth (MDD) determined from modern subduction zones to be at ~80 km (Wada and Wang, 2009), corresponding to a switch from slab-mantle decoupling (below a serpentinite (serp) 'cold nose') to a coupled interface.

The primary significance of lawsonite for planetary processes is its role in element cycling, including the transport of water through subduction zones. Lawsonite contains ~11.5% H_2O (structurally bound as both H_2O and OH), and is therefore a major carrier of water into forearc, subarc, and deeper parts of the mantle (Forneris and Holloway, 2003; Ohtani et al., 2004; Poli and Schmidt, 2002). At depths at and near ~80 km – corresponding to the depth at which slabs change from decoupled to coupled interaction with the overlying mantle wedge (Wada and Wang, 2009) and the maximum depth from which rocks are typically exhumed in oceanic subduction zones (Agard et al., 2009; Whitney et al., 2014) – lawsonite may be the most abundant hydrous phase in subducted oceanic crust and therefore the most important mineral in the deep-Earth water cycle.

Lawsonite is also a major host of transition metals (Cr, Fe, Ti at weight % levels) and trace elements (REE, U-Th-Pb, Sr), many of which are useful for tracking subduction-zone processes (Fornash et al., 2019; Fornash and Whitney, 2020; Martin et al., 2011a, 2011b, 2014; Pommier et al., 2019; Spandler et al., 2003; Tribuzio et al., 1996; Ueno, 1999; Vitale Brovarone et al., 2014a). Depending on coexistence and reaction relationships with epidote/allanite, titanite, garnet, apatite, calcite, and other minerals, lawsonite can host up to 60% of bulk Pb and 100% of bulk Sr, as well as substantial proportions of U, Th, Y, and REE (30-100% of bulk-rock; Tribuzio et al., 1996; Spandler et al., 2003; Martin et al., 2014; Hara et al., 2018) (Fig. 2). Lawsonite is typically strongly zoned in these elements, providing information about reaction history involving fluids during subduction (Fornash et al., 2019; Fornash and Whitney, 2020; Vitale Brovarone et al., 2014a). In addition, lawsonite-bearing assemblages can be dated with radiogenic isotopic systems (e.g. Lu-Hf, Mulcahy et al., 2011, 2014), and lawsonite may record the isotopic composition of the host-rock protolith (Hara et al., 2018) as well as the composition of syn-subduction metasomatic fluids derived from different protoliths, including sediments (e.g., as seen in a study of Li isotopic signatures of eclogite minerals; Simons et al., 2010).

Previous reviews of lawsonite eclogite and blueschist considered known and potential lawsonite eclogites (Tsujimori et al., 2006) and many examples of lawsonite blueschists (Tsujimori and Ernst, 2014), including localities in which lawsonite is no longer preserved (e.g., present only as pseudomorphs) or cases in which the former presence of lawsonite is inferred from petrologic or geochemical data (e.g., Gao et al., 2012). This paper focuses on occurrences of fresh lawsonite and uses information from lawsonite composition and zoning to interpret conditions and processes recorded in subducted and exhumed oceanic crust.

Unaltered lawsonite is rare, particularly in eclogite, because lawsonite is easily overprinted during prograde and/or retrograde metamorphism and therefore is uncommon in the geologic record

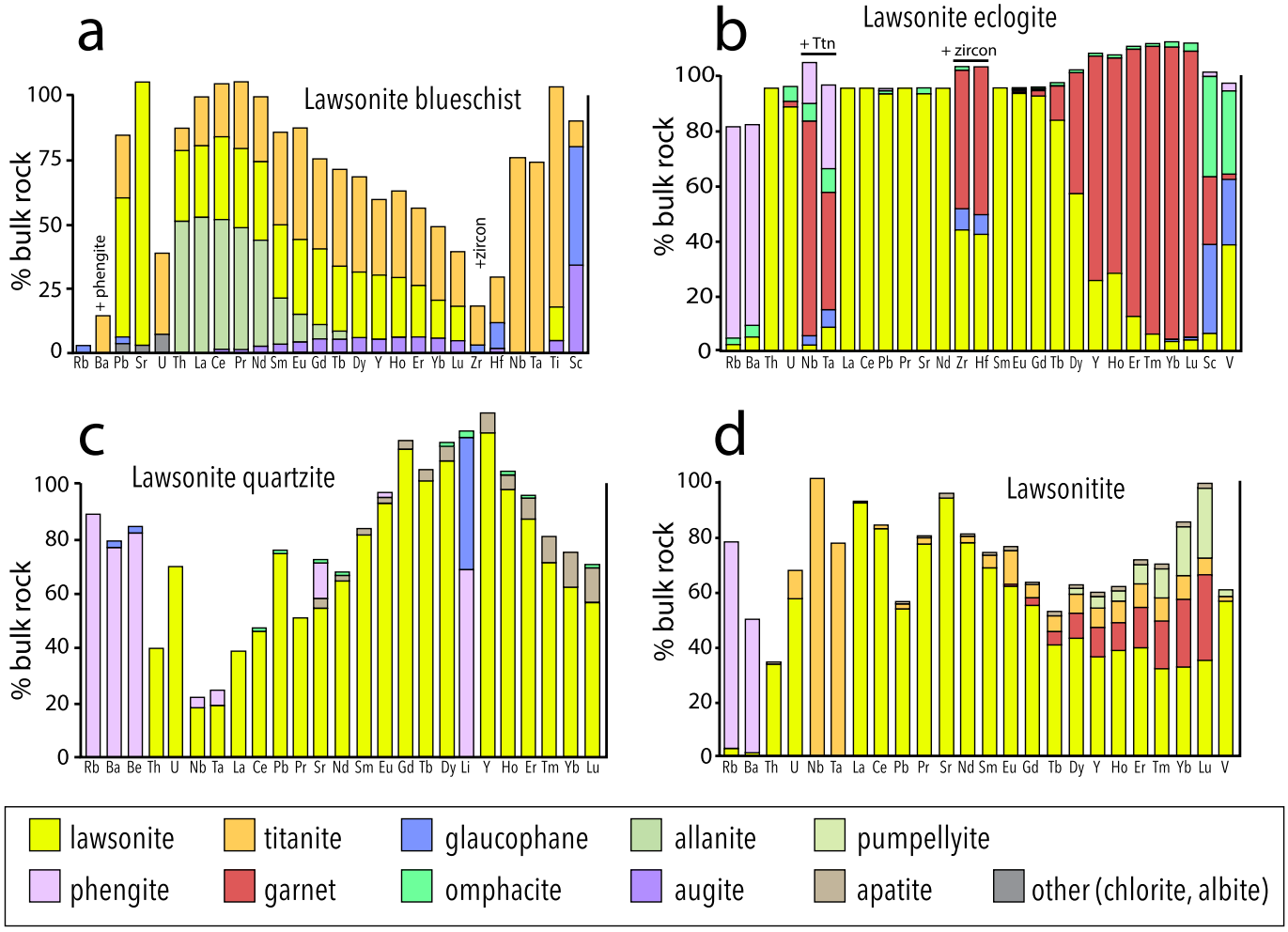

Fig. 2. Trace-element budgets of selected lawsonite-bearing rocks. (a) Lawsonite blueschist, New Caledonia (Spandler et al., 2003); (b) lawsonite eclogite, Guatemala (Hara et al., 2018); (c) lawsonite-bearing quartzite, Sivrihisar, Turkey (Martin et al., 2014); (d) lawsonitite (metasomatic rock), Corsica (Martin et al., 2014). See also Wang et al. (2019) for additional geochemical budget plots of lawsonite-bearing rocks. These diagrams compare the bulk-rock trace-element composition with the trace-element abundance of each mineral (as determined by *in situ* methods). Values of <1 or >100 indicate that the element budget determined by *in situ* analysis of minerals does not correspond perfectly to the bulk composition owing to lack of analysis of some phases (abundance <1), zoning, or presence of inclusions.

(Clarke et al., 2006; Tsujimori et al., 2006; Whitney and Davis, 2006; Zack et al., 2004). Nevertheless, there are excellent examples of lawsonite-bearing eclogite and blueschist-facies rocks preserved in exhumed subduction complexes worldwide (Figs. 3–4), representing a range of P-T conditions (Fig. 5) (Tables 1–3). We have identified nine eclogite localities with preserved (not pseudomorphed) lawsonite that coexists with garnet + omphacite in the rock matrix (e.g., Fig. 4a), and seven sites with preserved lawsonite inclusions (± omphacite inclusions) in garnet (e.g., Fig. 4b) (Fig. 3; Table 1). Blueschist-facies rocks with preserved lawsonite are more common (e.g., Figs. 4c, d). In this paper, we review representative localities of lawsonite-blueschist, including some that are associated with lawsonite or epidote eclogite and some that are not associated with eclogite at current exposure levels (Table 2). We also document lawsonite occurrences in metacarbonate, quartzite, and metasomatic rocks and veins (Table 3).

This review is timely because the significance of lawsonite for understanding subduction processes has stimulated new research into lawsonite composition, including acquisition of detailed major-element, trace-element, isotopic, and microstructural data using *in situ* methods. We survey and discuss what is known about lawsonite composition and zoning in eclogites and selected blueschists and associated metasedimentary and metasomatic rocks, and present new and compiled data and images that show how the petrology and geochemistry of lawsonite can contribute to deciphering the conditions and processes of metamorphism subduction zones, with implications for fluid–rock reaction.

2. Global survey of lawsonite-bearing rocks

In the following sections, we survey lawsonite-bearing rocks that represent a range of bulk compositions and mineral assemblages and a range of recorded P-T conditions (Fig. 5), structural characteristics of the host terrane (mélange, coherent), and age (Neoproterozoic to Neogene). Summary information for these sites (Tables 1–3) also include references to papers with descriptions of the petrology and other aspects of the eclogites and blueschists; additional data are in review papers such as Tsujimori et al. (2006) and Tsujimori and Ernst (2014).

2.1. Lawsonite eclogite

Previous reviews have identified nineteen lawsonite eclogite localities (Tsujimori et al., 2006; Tsujimori and Ernst, 2014; Wei and Clarke, 2011), including some with altered (pseudomorphed) or inferred lawsonite. In some cases, previously proposed lawsonite eclogites are tentatively re-interpreted here because lawsonite is not evidently in equilibrium with garnet + omphacite. Our analysis indicates that there are nine confirmed eclogites in which unaltered matrix lawsonite coexisted in likely equilibrium with garnet and omphacite (e.g., Fig. 4a), and seven localities with confirmed or likely eclogite-facies lawsonite inclusions in garnet (but no matrix lawsonite; e.g., Fig. 4b) (Fig. 3, Table 1). Note that most lawsonite eclogites with matrix lawsonite also have lawsonite inclusions in garnet (e.g., Sivrihisar, Turkey; Pinchi Lake, BC, Canada; Port Macquarie, Australia).

The nine lawsonite eclogites with fresh matrix lawsonite are classified by field structural setting as overall structurally-coherent (C), mélange (M), or xenolith (X). These locations are: (1) the Sivrihisar Massif, Tavşanlı Zone, Turkey (C) (Fig. 6a, 7a–d); (2) the Schistes Lustrés of Alpine Corsica, France (C); (3) Rio San Juan Complex, Dominican Republic (M); (4) South Motagua fault zone, Guatemala (M) (Fig. 6b, 7e–f); (5) Voltri Massif, Western Alps, Italy (M); (6) Port Macquarie, Australia (M) (Fig. 6c); (7) Ward Creek (C), a coherent part of the Franciscan Complex, California, USA; (8) Pinchi Lake, British Columbia, Canada (blocks in glacial deposits, interpreted as M by Ghent et al., 1993) (Fig. 6d); and (9) Garnet Ridge, Arizona, USA (X) (Fig. 6e) (Fig. 3; Table 1). Note that, with the possible exception of the Rio San Juan Complex, in which lawsonite eclogite formed during prograde metamorphism prior to a higher P-T peak phengite-eclogite facies, tectonically-exhumed lawsonite eclogites with matrix lawsonite record peak conditions of 2.4–2.6 GPa at ~500 ± 50 °C (Fig. 5).

Metabasaltic rocks containing garnet with lawsonite and omphacite inclusions but no matrix lawsonite occur in seven localities (Fig. 3; Table 1): (10) the Elekdağ Massif, Central Pontides, Turkey (C), (11) the eastern Shikoku (Kotsu) region of the Sanbagawa belt, Japan (C), (12) the Faro region of the Yukon-Tanana terrane, northern Canadian Cordillera (C). (Fig. 4b), (13) North Qilian, China (C); the Tianshan,

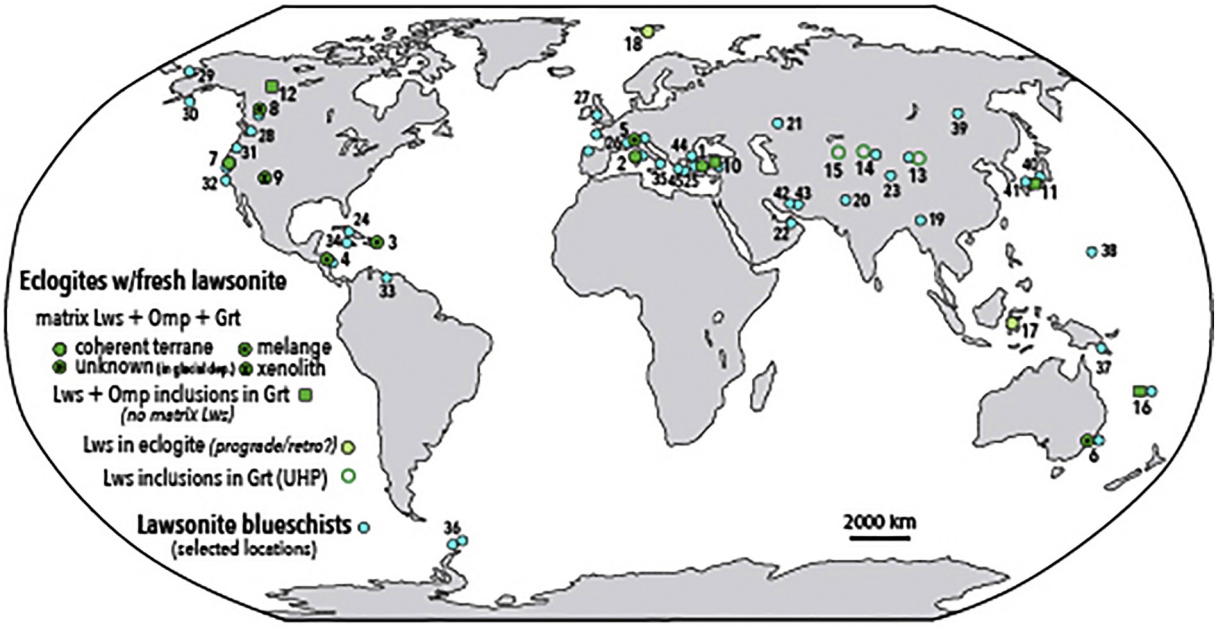

Fig. 3. Locations of eclogite-facies rocks containing fresh lawsonite. Most of these localities also contain lawsonite blueschist and one or more types of lawsonite-bearing metasomatic rocks. Sites are characterized by field occurrence: mélange, coherent, xenolith. Note that Pinchi Lake, BC, Canada, eclogite is categorized here as unknown because it consists of blocks in glacial deposits, but was interpreted as mélange by Ghent et al. (1993). Mineral name abbreviations after Whitney and Evans (2010).

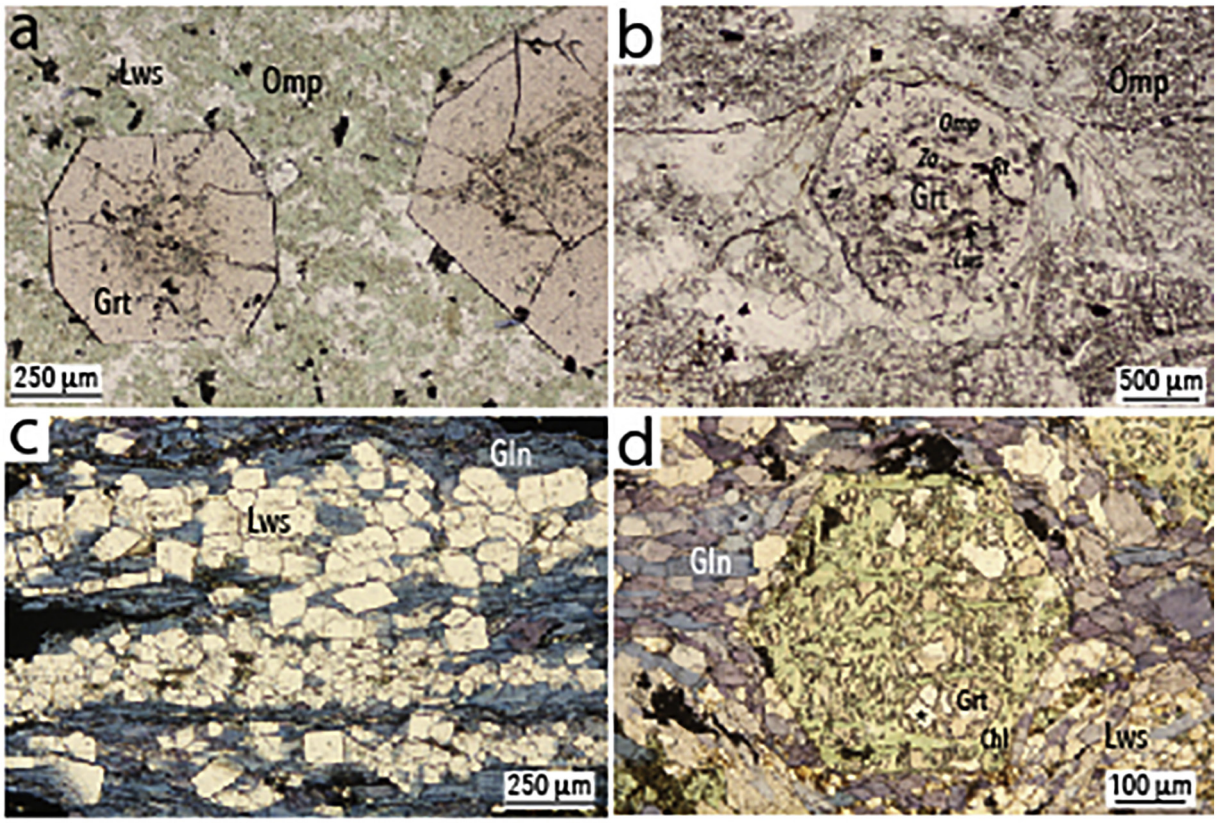

Fig. 4. Photomicrographs of (a) lawsonite eclogite (Guatemala); (b) lawsonite and omphacite inclusions in garnet (Yukon, Canada); (c) lawsonite blueschist (Sivrihisar, Turkey); and (d) lawsonite eclogite retrogressed to lawsonite blueschist; the garnet has been largely pseudomorphed by chlorite, but lawsonite inclusions in garnet were preserved (Sivrihisar, Turkey).

including (14) the SW part of the belt in China (C) and (15) the Atbashi Ridge area, Kyrgyzstan (M); and (16) the Pam Peninsula, New Caledonia (primarily C). In New Caledonia eclogites, lawsonite occurs only as rare inclusions in garnet, in one case in a different domain of garnet than omphacite inclusions (Clarke et al., 1997) and in another case near the garnet rim in a rock with matrix omphacite (Vitale Brovarone and Agard, 2013). Although it is possible that the New Caledonia lawsonite inclusions formed during prograde, blueschist-facies metamorphism, the inclusions in garnet may represent lawsonite eclogite conditions prior to subsequent metamorphism in the epidote stability field, so we include it here as a possible lawsonite eclogite, consistent with the calculation of peak P-T conditions in the lawsonite eclogite facies (Vitale Brovarone and Agard, 2013).

These 16 sites can be analyzed as indicators of lawsonite composition under eclogite facies conditions in oceanic subduction zones, and can be compared owing to their similar major mineral assemblages. In this paper, we use published or new data to document lawsonite composition for eight of the nine sites with matrix lawsonite + omphacite + garnet and six of the seven sites with lawsonite inclusions in garnet in eclogite but no matrix lawsonite.

Two lawsonite-bearing sites (Sulawesi, Spitsbergen; Fig. 3) that have previously been considered as lawsonite eclogites may not contain the equilibrium assemblage lawsonite + garnet + omphacite (based on textural relations of the minerals), and lawsonite may therefore instead be part of a prograde or retrograde blueschist assemblage. Eclogites on the island of Sulawesi, Indonesia, contain texturally-late lawsonite + chlorite domains that appear to be retrograde (Miyazaki et al., 1996), and lawsonite in eclogites on the island of Spitsbergen occurs only as inclusions in garnet, which apparently do not also contain omphacite inclusions (Hirajima et al., 1988). The P-T conditions determined for these two sites are lower than those proposed for other lawsonite eclogites (Table 1; Fig. 5). Additional investigation is needed to determine if these sites contain lawsonite eclogites.

In some UHP localities, including continental subduction terranes such as western Dabieshan, China, the former presence of lawsonite at eclogite-facies conditions is inferred from phase equilibrium modeling. However, there are no lawsonite relics or pseudomorphs yet reported in these rocks (e.g., Wei et al., 2010), so they are not included in this review.

2.2. Lawsonite blueschist

Lawsonite blueschist is much more abundant than lawsonite eclogite. Although lawsonite is commonly pseudomorphed in epidote blueschist (Evans, 1990), there are nevertheless many sites with fresh lawsonite + glaucophane ± garnet (e.g., Figs. 4c–d, 6, 7; Table 2). For this survey, we present a subset of lawsonite blueschist localities and classify them according to whether they are (1) associated with lawsonite eclogite; (2) associated with eclogite that does not contain lawsonite (e.g., epidote and/or amphibole eclogite); or (3) not associated with eclogite at current exposure levels.

All of the tectonically-exhumed lawsonite eclogite localities are associated with lawsonite blueschists. Lawsonite blueschists may be lower-grade/prograde relative to eclogite in the same HP/LT complex or may have formed in a different litho-tectonic unit (e.g., New Caledonia), whereas others may have formed by retrogression of eclogite (e.g., some blueschists in Sivrihisar, Turkey, contain glaucophane rims on omphacite; Davis and Whitney, 2006). Furthermore, some blueschist is co-facial with eclogite; i.e., different mineral assemblages formed owing to differences in bulk composition or oxygen fugacity (e.g., Corsica, Sivrihisar). Lawsonite blueschist also occurs in HP/LT complexes with eclogite in which fresh lawsonite is not preserved but is

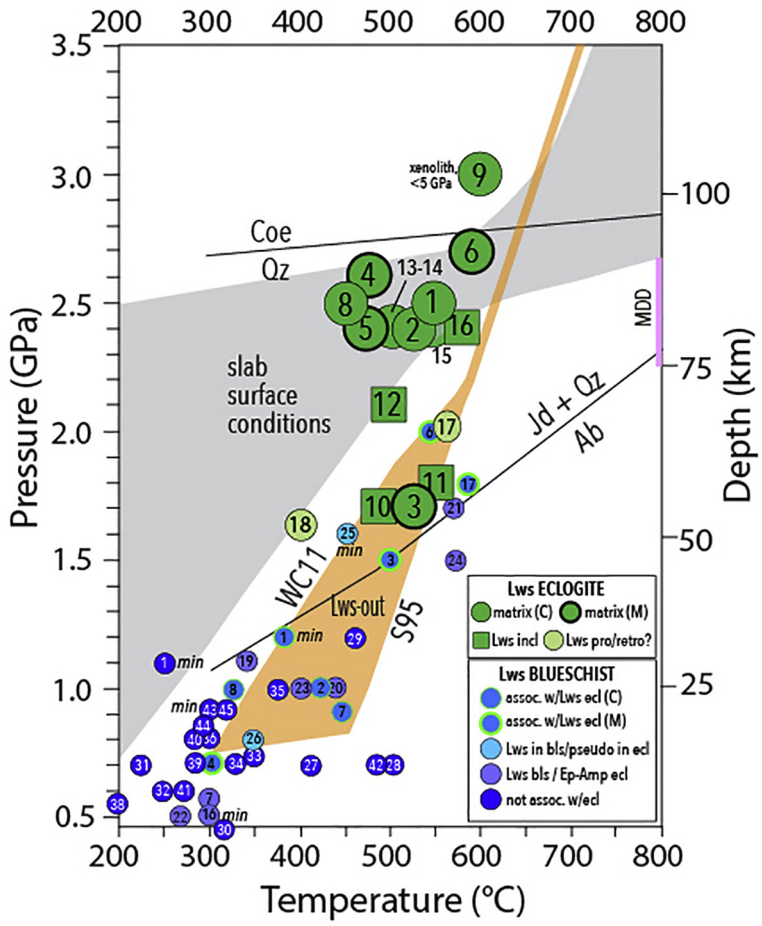

Fig. 5. Peak metamorphic conditions of eclogite and blueschist containing unaltered lawsonite. Green circles indicate lawsonite eclogite; numbers correspond to those in Table 1. Blue circles are selected lawsonite-bearing blueschists; numbers are keyed to Table 2. Also shown are typical slab-surface conditions for modern subduction zones (Syracuse et al., 2010), and proposed conditions for lawsonite-out (epidote/zoisite-in) reactions: S95 = Schmidt (1995); WC11 = Wei and Clarke (2011). MDD = maximum decoupling depth of Wada and Wang (2009). Some lawsonite-bearing rocks plot beyond the proposed stability limit of lawsonite; one possible explanation is that these record a different part of the P-T path than that associated with lawsonite formation.

inferred from tabular pseudomorphs (e.g., Cycladic Islands, Greece; various localities in the Western and Eastern Alps) (Table 2).

Lawsonite blueschist is also common in HP/LT complexes that contain epidote- and/or amphibole-eclogite, such as the Franciscan Complex, New Caledonia, the Indo-Burmese Ranges, NW India, Cuba, and HP/UHP terranes such as those in Tibet/China (e.g., North Qilian, North Qiangtang) (Table 2). In these cases, blueschist may represent a lower-grade unit than the eclogite or, in some cases, may represent retrogressed eclogite.

Lawsonite blueschist with no apparent association with eclogite is abundant in exhumed subduction complexes (Table 2) and typically records very low temperature conditions (<500 °C; Fig. 5). Examples include the Mona Complex, Anglesey, Wales UK (Neoproterozoic; the oldest documented lawsonite-bearing rock), Kodiak Islands and Seward Peninsula, Alaska USA; several sites in the Klamath Mountains, California USA; the Diamante-Terranova unit, Calabria, Italy; Villa de Cura belt, northern Venezuela; the Scotia Arc, Chile and Antarctica; the Emo complex, Papua New Guinea; the Izu-Mariana active subduction zone; the southern Ural Mts, Russia; northern China/Inner Mongolia; HP belts in Japan; Zagros and Makran, Iran; and parts of the Tavşanlı Zone and Thrace, Turkey.

2.3. Other eclogite- and blueschist-facies lawsonite-bearing rocks

Lawsonite occurs in metasedimentary rocks such as metachert and calc-silicate associated with mafic oceanic crust, and in metasomatic rocks such as those formed by interaction between metabasite or metasedimentary rocks with serpentinite at HP/LT conditions (Figs. 8a, b; Table 3). These lawsonite-bearing rocks are typically interlayered with or otherwise spatially associated with lawsonite eclogite and blueschist. For example, layers of lawsonite-bearing quartz-rich metasedimentary rocks occur in the Tavşanlı Zone, Turkey, and are interpreted to be metachert and metatuff (Okay, 1980; Whitney et al., 2014) (Figs. 8a, b), and lawsonite + jadeite-bearing quartzite is associated with the Rio San Juan complex, Dominican Republic (Schertl et al., 2012). Lawsonite in blueschist-facies mafic metasedimentary rocks also occurs in Ladakh, India (Groppo et al., 2016). Some terranes contain lawsonite in blueschist facies rocks with metasedimentary protoliths that are more pelitic (shale/argillite) or semi-pelitic (e.g. Shuksan and associated terranes of NW Washington, USA; Diahot terrane, New Caledonia) (Table 3). Pseudomorphs after lawsonite have also been reported from UHP metasedimentary rocks (e.g., Orozbaev et al., 2015).

Lawsonite has been reported in metacarbonate rocks in some HP/LT complexes (Table 3). For example, lawsonite-bearing calc-schists occur with lawsonite eclogite and blueschist in the Sivrihisar Massif, Turkey (Whitney et al., 2014) (Fig. 8c). These are inferred to have a metasedimentary protolith based on the field setting of marble and calc-schist layers as well as the abundance of calcite ± dolomite in the rocks, although some calc-schists containing lawsonite ± glaucophane ± omphacite may represent deformation and/or fluid-enhanced mixing at the lithologic contacts of metacarbonate and metamafic layers. Lawsonite is also present in HP carbonated metasomatic rocks in Corsica (Piccoli et al., 2016, 2018; Vitale Brovarone et al., 2014a), in carbonated

Table 1
Locations of eclogite with preserved lawsonite.

Site	Field setting[a]	P (GPa)-T(°C)	Age (Ma)	References
Matrix Lws + Grt + Omp (also contain Lws inclusions in Grt)				
1. Sivrihisar Massif, Tavşanlı, Turkey	C	2.5/550	93	Davis and Whitney (2006, 2008), Whitney and Davis (2006), Fornash et al. (2016), Pourteau et al. (2019)
2. Alpine Corsica, France	C	~2.4/520	34	Caron and Péquignot (1986), Ravna et al. (2010), Vitale Brovarone et al. (2013, 2014b)
3. Rio San Juan, Dominican Republic	M	~1.7/520	104-70	Zack et al. (2004). Escuder-Viruete and Perez-Estaun (2006, 2013)
4. S Motagua Fault Zone, Guatemala	M	2.6/480	80-70	Harlow et al. (2004). Tsujimori et al. (2006), Endo et al. (2012)
5. W. Alps, Italy (Voltri Massif)	M	2.4/470	45-34	Scarsi et al. (2018)
6. Port Macquarie, Australia	M	2.7/590	490	Och et al. (2003), Tamblyn et al. (2019)
7. Ward Creek, CA USA	C	#/~320	~152	Shibakusa and Maekawa (1997); Mulcahy et al. (2014)
8. Pinchi Lake, BC, Canada	M[b]	2.5/450	222	Ghent et al. (1993, 1996, 2009)
9. Garnet Ridge, AZ USA	X	~3/600	81-33	Usui et al. (2003, 2006)
Lws + Omp inclusions in Grt (no matrix Lws)				
10. Elekdağ, (Pontides) Turkey	C/M	1.7/490	105	C: Okay et al. (2006), M: Altherr et al. (2004)
11. Sanbagawa, Japan	C	1.8/550	120-80	Tsuchiya and Hirajima (2013)
12. Yukon-Tanana, Canada	C	2.1 /500	260	Faber and Rowe (2019)
13. North Qilian, China	C	2.4/510	490-440	Zhang et al. (2007)
14. SW Tianshan, China	C	2.4/500	320-310	Du et al. (2014), Lu et al. (2019)
15. W Tianshan: Atbashi Ridge, Kyrgyzstan	M	2.4/550	327-324	Shatsky and Usova (1989), Simonov et al. (2008)
16. New Caledonia	C	<2.4/<600	44-37	Clarke et al. (1997), Vitale Brovarone and Agard (2013)
Lws present but possibly not in equilibrium with Omp + Grt				
17. Sulawesi, Indonesia		1.8-2.4 / 580-620 (peak ecl)	120-110	Parkinson (1996)
18. Spitsbergen, Norway	C	1.6 / 400	470	Agard et al. (2005), Hirajima et al. (1988)

[a] C = coherent; M = mélange; X = xenolith ; # pressure of Ward Creek Lws eclogite not known (Lws-pumpellyite rocks in the sequence are 0.7 GPa but other eclogite blocks in the Franciscan are 2.0-2.5 GPa).
[b] Pinchi Lake eclogite occurs as blocks in glacial deposits, so field setting is not well known.

eclogite (Scarsi et al., 2018) and metasomatic rocks (Vitale Brovarone et al., 2020) of the Western Alps, and has been reported in HP marble from Crete (Theye and Seidel, 1987) and schist from the NW Cycladic Islands (Baziotis et al., 2019).

Lawsonite-bearing metasomatic rocks include jadeitite (Guatemala: Harlow et al., 2003; Dominican Republic: Schertl et al., 2012; Iran: Oberhänsli et al., 2007; Tavşanlı Zone, Turkey: Okay, 1997), lawsonitite (Corsica: Martin et al., 2011a; Vitale Brovarone et al., 2011b, 2014b), lawsonite + chlorite ± garnet rocks (Sivrihisar, Turkey, Fig. 8d: Fornash et al., 2019; Corsica:Vitale Brovarone et al., 2014a ; Vitale Brovarone and Beyssac, 2014) (Fig. 8d), and lawsonite-phengite layers, domains, and veins (e.g., Sivrihisar, Turkey; Port Macquarie, Australia; South Motagua Fault Zone, Guatemala, Fig. 8e) (Table 3). In the case of lawsonitite on Corsica, the lawsonite-rich rocks (>75 modal% lawsonite) formed via metasomatic reaction that occurred between meta-mafic, metasedimentary, and ultramafic rocks (Martin et al., 2011; Vitale Brovarone et al., 2014a). Lawsonite in metasomatized metapelites is also reported in the blueschist-facies units of Corsica (Vitale Brovarone et al., 2014a; Vitale Brovarone and Beyssac, 2014).

Lawsonite-bearing omphacitites (lawsonite + omphacite rocks) occur in the blueschist-facies units of Corsica (Vitale Brovarone et al., 2013), in the Port Macquarie mélange (Och et al., 2003), and in the South Motagua Fault Zone locality, Guatemala (Figs. 8f–g; Table 3). In some blueschist and eclogite units of other HP/LT complexes, cm- to dm-scale layers of omphacite + lawsonite (without garnet) occur (e.g., Sivrihisar, Turkey). Omphacite + lawsonite rocks may result from a different bulk composition from typical MORB, either related to protolith composition or syn-metamorphic metasomatism.

Lawsonite-bearing veins have been reported in the Franciscan Complex, California (Davis and Pabst, 1960; Martin et al., 2014); the Tavşanlı Zone, Turkey (Davis and Whitney, 2008; Fornash et al., 2019; Fornash and Whitney, 2020; Okay, 1982); Corsica (Vitale Brovarone et al., 2011a); the Wellington Peninsula, New Zealand (George and Grapes, 1987); the lowest-grade unit of the Schistes Lustrés, Western Alps, France (Ronan et al., 2019); and in the accretionary wedge of SW Japan (lawsonite + quartz pseudomorphs after laumontite; Endo and Wallis, 2017) (Fig. 9; Table 3). Two other localities have possible pseudomorphs after lawsonite in veins: Monviso, Western Alps, Italy (Angiboust et al., 2011) and the Dabie-Sulu UHP belt China (Li et al., 2005).

3. Lawsonite petrography, properties, and microstructure

Because lawsonite is a relatively rare mineral and may in some cases be overlooked owing to its superficial resemblance to plagioclase or owing to its fine grain size in some rocks, we briefly review its appearance and properties.

3.1. Lawsonite appearance in outcrop and thin sections

In outcrop, lawsonite is typically white or pale pink (Fig. 9), the latter owing to the presence of Fe and/or Cr; color may also be affected by the presence of inclusions. In thin section, lawsonite is colorless under plane polarized light (Figs. 4, 7, 8), with high first-order/low second-order interference colors under crossed polars (Figs. 7, 8). Lawsonite has orthorhombic crystal symmetry and commonly occurs as euhedral or subhedral tabular crystals (Figs. 4, 7, 8), in some cases displaying polysynthetic twinning (Figs. 7b, d). Although its tabular shape and twinning may resemble plagioclase, lawsonite can be distinguished by its higher birefringence, its optical properties related to orthorhombic symmetry, and its crystal shape when viewed perpendicular to (001) (Figs. 8e, 9a).

3.2. Inclusions in lawsonite

Common inclusions in lawsonite are titanite, rutile, epidote-group minerals, glaucophane, apatite, sulfides, quartz, carbonates (aragonite, calcite), carbonaceous material, and fluid inclusions (Fig. 10). Other inclusions occur but are less common, e.g., omphacite, tourmaline, and chromite (Figs. 8f–g). Inclusions may be confined to particular textural or compositional domains of a host crystal, providing information about reaction history and changes in P-T conditions during lawsonite

Table 2
Representative list of blueschists with preserved lawsonite.

Locality	Field setting[a]	P (GPa) / T(°C)	AGE (Ma)	References
Lws in blueschist and associated eclogite				
1. Sivrihisar Massif, Turkey	C	1.2-2.6 / 380-520	90-83	Davis and Whitney (2006), Fornash et al. (2016), Pourteau et al. (2019)
2. Alpine Corsica, France	C	1.0 / 420	34	Vitale Brovarone et al. (2014b)
3. Rio San Juan, Dominican Republic	M	1.5 / 500	35-33	Escuder-Viruete and Pérez-Estaún (2006)
4. S Motagua Fault Zone, Guatemala	M	0.7 / 300	125-116	Harlow et al. (2004), Tsujimori et al. (2006)
5. W. Alps, Italy (Voltri)	M	2.4 / 470	45-34	Scarsi et al. (2018)
6. Port Macquarie, Australia	M	2.0 / 550	470	Tamblyn et al. (2019)
7. Franciscan/Ward Creek, CA USA	C	~0.9 / 445	~152	Shibakusa and Maekawa (1997)
8. Pinchi Lake, BC, Canada	C	1.0 / 300	222	Ghent et al. (1996)
10. Elekdağ (Pontides), Turkey	C	1.7 / 490	105	Okay et al. (2006)
17. Sulawesi, Indonesia	M	1.8-2.4 / 580-620 (peak ecl)	120-110	Parkinson (1996)
Lws blueschist in the same terrane/complex as epidote/amphibole eclogite				
7. Franciscan, CA USA (e.g., Ring Mt, Catalina Island)	C/M	0.5 / 300	~145	Bebout and Barton (1993), Mulcahy et al. (2011)
16. New Caledonia	C	0.5-1.7 / 300-510	37	Clarke et al. (1997), Fitzherbert et al., 2005, Vitale Brovarone et al. (2018)
18. Spitsbergen, Norway	C	1.6 / 400	470	Agard et al. (2005), Hirajima et al. (1988)
19. Indo-Burmese Range, India	C	1.1 / 340	80	Ao and Bhowmik (2014)
20. Ladakh, NW India	C/M (kms-scale slices within a 'mélange')	1.0 / 470	100	Groppo et al. (2016)
21. Southern Ural Mts, Russia	M?	1.7 / 570	370-380	Hetzel et al. (1998)
22. NE Oman (Saih Hatat)	M	0.3-0.6 / 250-300	72-80	El-Shazly (1994)
23. N Qiangtang, China	C	0.9-1.1 / 330-415	242	Tang and Zhang (2014)
24. Cuba (Escambray)	C, M	1.5 / 570	70	Schneider et al. (2004), Garcia Casco et al. (2006)
Lws in blueschist, Lws pseudomorphs in eclogite				
25. Cycladic Islands, Greece (rare fresh Lws, mostly pseudo.) - Sifnos, Syros regions	C	1.6-2.4/450-580	50-40	Trotet et al. (2001)
26. Roche Noire Massif, W. Alps, France	C	0.8 / 350		Mevel and Kienast (1980)
Lws blueschist not associated with eclogite				
27. Anglesey Wales UK	M	0.8 / 415	560-550	Gibbons and Mann (1983); Kawai et al. (2006)
28. Easton terrane, WA	C	<0.7 / 500	140-136	Cordova et al. (2019)
29. Seward Peninsula, AK (mostly pseudomorphs, rare fresh Lws)	C	~1.2 / 460	>120	Forbes et al. (1984); Patrick and Evans (1989); Hannula and McWilliams (1995)
30. Kodiak Islands, AK	C	>0.3 / <350	~200	Roeske et al. (1989)
31. Klamath Mts, CA	C	~0.7 / 275	450	Cotkin et al. (1993)
32. Los Ollas Complex, Mexico	M	~0.6/250		Mendoza (2000)
33. Villa de Cura terrane, Venezuela (eclogite in separate, northern belt)	C	<0.75 / 350	80	Smith et al. (1999)
34. Mt. Hibernia Complex, SE Jamaica	C	~0.7 / 310-340	~75	Willlner et al. (2016)
35. Diamante-Terranova, Calabria, Italy	C	0.9-1.1 / 350-390	38-33	Fedele et al. (2018)
36. Scotia Arc, Chile and Antarctica (e.g., Elephant Island, Smith Island)	C	~0.8/300	120-80, 58-47	Trouw et al. (1998)
37. Papua New Guinea	C		35	Worthing and Crawford (1996)
38. Izu-Mariana trench	M	0.5-0.6 / 200	48	Maekawa et al. (1993)
39. Ondor Sum, N China (Lws does not coexist w/Gln)	C	~0.7 / 300	450	Tang and Yan (1993); de Jong et al. (2006)
40. Kurosegawa Complex, Japan	M	0.7-0.9 / <300	280-245	Sato et al. (2014, 2016)
41. Renge Complex, SW Japan	M	0.6-0.7 / 280	280-330	Tsujimori and Liou (2007)
42. Zagros (Seghin Unit), Iran	C	1.7 / 500	64-71	Agard et al. (2006); Angiboust et al. (2016)
43. Makran, Iran	M (km-scale blocks)	0.9-1.4 / 300-380	~88	Hunziker et al. (2017)
1. Tavşanlı Zone, Turkey (other than Sivrihisar Massif)	C	~1.1-2.2 / 250-300	~85	Okay (1980, 1982); Okay and Whitney (2010); Plunder et al. (2013)
44. Thrace, Turkey	C	~0.8 / 300	86	Topuz et al. (2008)
45. NW Cycladic Islands, Greece	C	0.9 / 320	50-40	Baziotis et al. (2019)

[a] C = coherent; M = mélange ; Note: may be different from field setting of associated eclogite.

growth. Some lawsonite crystals contain trails of inclusions that can delineate former foliations comprised of carbonaceous material or Ti-rich minerals (Martin et al., 2014; Vitale Brovarone et al., 2014b) (Figs. 10c–e). In these crystals, the abundance of inclusions may be very high; they can comprise up to 50% of the mineral in some areas. These inclusion-rich zones are commonly associated with trace-element-rich cores, which are very difficult to analyze, even by *in situ* techniques, owing to the abundance of inclusions. It is worth noting that these inclusion-rich lawsonite crystals may be rimmed by an overgrowth of inclusion-free lawsonite (Figs. 10c–e), and also that the inclusion phases may not be preserved in the matrix. Lawsonite crystals can thus record different stages of subduction zone metamorphism though their inclusion populations.

Lawsonite may also contain inclusions that post-date lawsonite crystallization. For example, in some cases, epidote inclusions represent alteration of lawsonite rather than early-formed phases. Similarly, trace element-rich minerals in cracks or altered zones in lawsonite may form via dissolution-reprecipitation processes that modify the composition and texture of the original lawsonite (Martin et al., 2014).

3.3. Lawsonite pseudomorphs

Lawsonite is a very useful index mineral for documenting metamorphic conditions and associated tectonic and geochemical processes, so it is important to know whether lawsonite was ever present in HP/LT rocks that lack lawsonite when exhumed to the Earth's surface.

Table 3
Localities with Lws-bearing metasedimentary rocks, metasomatic rocks, and/or veins

Locality	LWS-bearing rock types	References
Tavşanlı Zone, Turkey	Quartzite, calc-schist, chlorite-lawsonite±garnet rock, omphacitite, lawsonite veins	Okay (1980), Okay and Whitney (2010), Whitney et al. (2014), Martin et al. (2014), Fornash et al. (2019); Fornash and Whitney (2020)
Alpine Corsica (Schistes Lustrés)	Calc-schist, lawsonitite, omphacitites, quartzite	Martin et al. (2011a), Vitale Brovarone et al. (2011a, 2014a), Vitale Brovarone and Beyssac (2014), Piccoli et al. (2016, 2018)
S Motagua Fault, Guatemala	Jadeitite	Harlow et al. (2003)
Rio San Juan, Dominican Republic	Jadeite-quartzite	Schertl et al. (2012)
W. Alps, Italy	Carbonated eclogite, lawsonite veins, metasomatic rocks	Scarsi et al. (2018), Ronan et al. (2019), Vitale Brovarone et al. (2020)
Port Macquarie, Australia	Omphacitite	Och et al. (2003), Tamblyn et al. (2019)
Franciscan Complex, CA, USA	Lawsonite veins	David and Pabst (1960), Martin et al. (2014)
Diahot terrane, New Caledonia	Metapelite	Spandler et al. (2003), Fitzherbert et al. (2005), Vitale Brovarone and Agard (2013)
Ladakh, India	Mafic metasediment	Groppo et al. (2016)
Engadine Window, Switzerland	Metapelite	Goffe and Oberhansli (1992)
Wellington Peninsula, NZ	Lawsonite veins	George and Grapes (1987)
SW Japan	Lawsonite in zeolite veins	Endo and Wallis (2017)
Shuksan, WA USA	Lawsonite-bearing metasediments	Brown and O'Neil (1982)
Crete, Greece	Metacarbonate	Theye and Seidel (1987)

Methods for inferring the former presence of lawsonite include identification of lawsonite pseudomorphs (e.g. Angiboust et al., 2012; Balllevre et al., 2003; Forbes et al., 1984; Hamelin et al., 2018; Hernández-Uribe et al., 2019; Klemd et al., 2002; Lopez-Carmona et al., 2013; Philippon et al., 2011; Sicard et al., 1984, 1986), inference from phase equilibria modeling (e.g., Tian and Wei, 2013), and inference from modeling of trace-element geochemistry (e.g., Sr, LREE; Guo et al., 2013). Phases that commonly comprise pseudomorphs are white mica (phengite, paragonite, muscovite), epidote-group minerals, actinolite, chlorite, quartz, and albite.

In some cases, pseudomorphs after lawsonite exhibit textural zoning in the minerals comprising the pseudomorph (e.g., Philippon et al., 2013). This may indicate former compositional zoning in the original lawsonite or may provide information about reaction history; e.g., the distribution of Ti-bearing phases may indicate former Ti-zoning. Lawsonite may also leave chemical traces in epidote-group minerals that replace it, identifiable as former lawsonite by the tabular shape (Fig. 10b). These compositional 'ghosts' are akin to pseudomorphs and can be used to indicate reaction history.

3.4. Lawsonite crystal structure and related properties

The crystal structure and thermodynamic properties of lawsonite, including the conditions of phase transitions, have been studied over a wide range of P-T conditions using different methods (e.g., Boffa Ballaran and Angel, 2003; Chinnery et al., 2000; Comodi and Zanazzi, 1996; Daniel et al., 2000; Libowitzky and Armbruster, 1995; Libowitzky and Rossman, 1996; McKnight et al., 2007; O'Bannon III et al., 2017; Pawley et al., 1996), with some disagreement about the values of the bulk modulus at particular P-T conditions. At the conditions recorded by exhumed lawsonite-bearing rocks, the mineral remains orthorhombic (space group Cmcm; O'Bannon III et al., 2017).

Owing to the significance of lawsonite for understanding the rheology, seismic properties (e.g. regions of low seismic velocity), and interaction of deformation and dehydration reactions (e.g., generation of earthquakes) in the oceanic portion of subducted slabs. (e.g., Okazaki and Hirth, 2016), the crystallographic orientation and seismic properties of lawsonite along different orientations have been investigated in naturally and experimentally deformed blueschist- and eclogite-facies rocks (Bezacier et al., 2010; Cao et al., 2013, 2014; Cao and Jung, 2016; Fujimoto et al., 2010; Iizuka-Oku et al., 2019; Kim et al., 2013a, 2013b, 2015; Teyssier et al., 2010; Whitney et al., 2014; Zucali and Spalla, 2011).

Lawsonite and associated glaucophane and/or omphacite commonly exhibit a strong crystallographic preferred orientation (CPO), and distinct CPO patterns have been observed in different studies (e.g., Cao and Jung, 2016; Teyssier et al., 2010). In some cases, the difference results from the use of different space groups for indexing lawsonite crystallographic orientation (Ccmm vs. Cmcm). However, different CPOs have also been determined even for the same space group (Cmcm), likely in part because different studies analyzed materials that varied considerably in mineral mode, including relative proportions of lawsonite, glaucophane, omphacite, and phengite, and differed as to whether the deformed material was monomineralic or polymineralic. Other variables that might influence lawsonite CPO include P-T conditions, stress, strain, water fugacity, and rock textural features (e.g., crystal shape, grain size). The major controls on lawsonite CPO and the likely primary CPO in subducted oceanic crust remain unresolved.

4. Lawsonite composition

Analyses conducted by electron microprobe, LA-ICPS, and other *in situ* methods have determined that most lawsonite contains transition elements (Fe, Cr, Ti) (Tables 4–8) as well as lesser and more variable amounts of other elements (Sr, U, Pb, REE) (e.g., Fornash et al., 2019; Fornash and Whitney, 2020; Li et al., 2013; Martin et al., 2011a; Martin et al., 2014; Mulcahy et al., 2011; Spandler et al., 2003; Vitale Brovarone et al., 2014a) (Table 9). The correlation of transition metal abundance with Al^{3+} concentration indicates that these elements substitute for each other in the lawsonite structure (Fornash et al., 2019; Vitale Brovarone et al., 2014a) (Fig. 11a), whereas REE and other large cations may substitute for Ca (e.g., Martin et al., 2011b).

4.1. Transition elements

Lawsonite can contain significant amounts of transition elements; in particular, Fe (up to 8 wt% FeO*; Maekawa et al., 1993), Ti (up to 1 wt%; Vitale Brovarone et al., 2014a; Piccoli et al., 2018; Fornash et al., 2019), and Cr (e.g., ~6–11 wt% Cr_2O_3; Mevel and Kienast, 1980; Sherlock and Okay, 1999; Davis and Whitney, 2006; Vitale Brovarone et al., 2014a; Fornash et al., 2019, Fornash and Whitney, 2020; this study) (Fig. 11b; Tables 4-8), with lesser amounts of V, Sc, and Mn (Fornash et al., 2019). Fe and Ti substitution for Al are most common, and Cr substitution is less so (Fig. 11a). Based on evidence for substitution of Fe for Al, it is likely that Fe in lawsonite is primarily Fe^{3+}. Lawsonite with the highest Ti contents has been reported in metasomatic rocks associated with serpentinites (Fornash et al., 2019; Vitale Brovarone et al., 2014a), and the highest Ni content (tens of ppm) are in Cr-rich lawsonite (Fornash et al., 2019). Cr-rich lawsonite occurs in both blueschist and eclogite but is most common in metasomatic rocks and veins (Fig. 11b). Although some Cr-rich lawsonite also contains substantial Fe, Ti, these are exceptions; more common is for Cr-rich lawsonite to contain low amounts of Fe and Ti or either Fe or Ti but not both (Figs. 11b, S1).

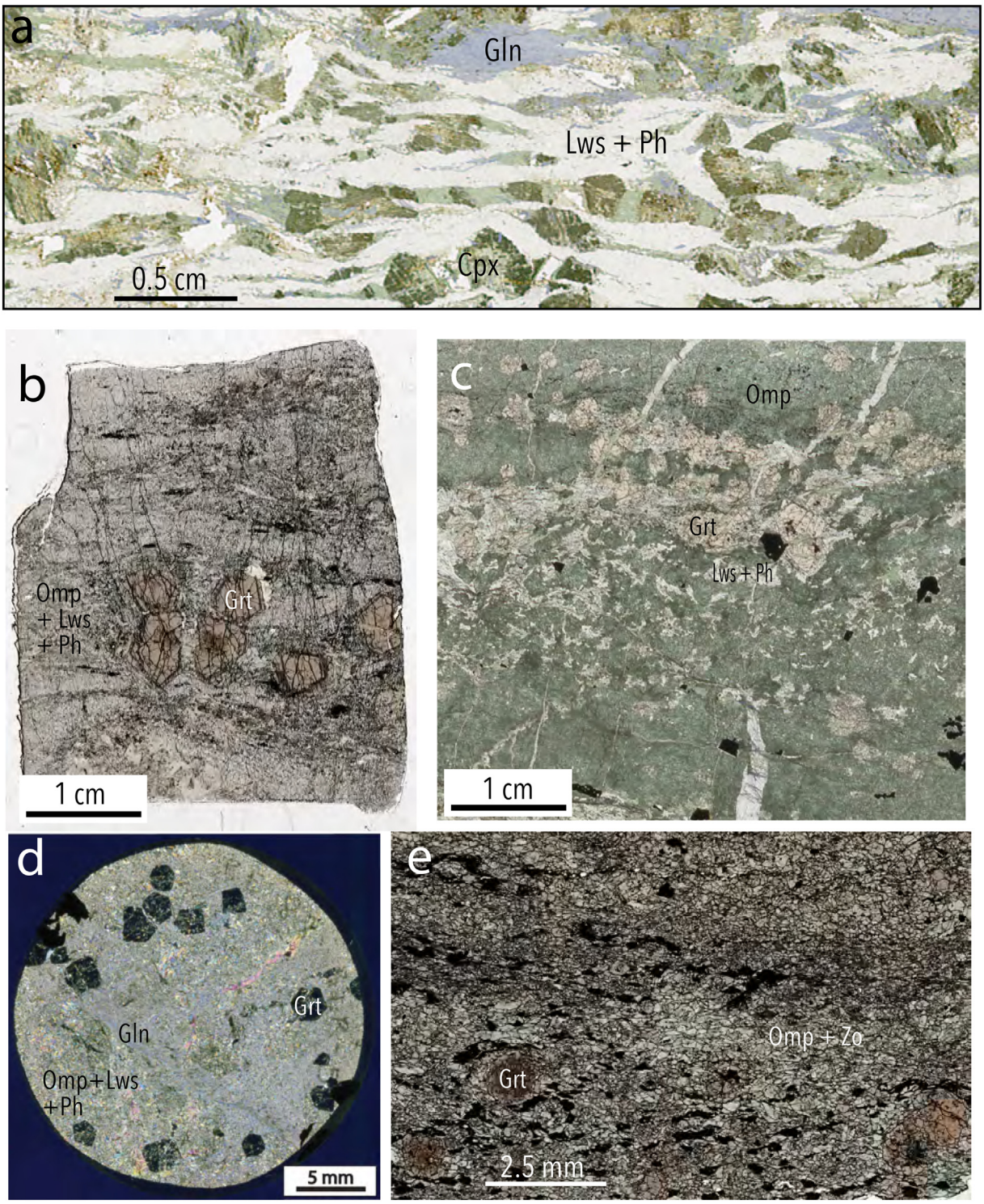

Fig. 6. Thin section scans of representative lawsonite eclogites: (a) Lawsonite-bearing metagabbro, Sivrihisar Massif, Turkey. Note relict augite that has been boudinaged and partially replaced by omphacite. The white area in the matrix are dominantly comprised of fine-grained lawsonite. Garnet is not in the field of view. (b) Eclogite from the South Motagua Fault Zone, Guatemala; lawsonite occurs in the matrix and in small lawsonite-rich veins and layers (sample MVE04-7-2 from Simons et al., 2010). (c) Eclogite from Port Macquarie, Australia. Lawsonite occurs in the matrix and as inclusions in garnet. (d) Crossed-polars scan of Pinchi Lake eclogite; lawsonite occurs in the matrix and as inclusions in garnet (sample BLR5 from Ghent et al., 1993). (e) Garnet Ridge xenolith, consisting primarily of garnet + omphacite + zoisite, with rare relict lawsonite (sample 17GR11 from Hernández-Uribe and Palin, 2019).

4.2. Sr and Pb

Sr, Pb, and other large divalent and trivalent cations substitute for Ca (Martin et al., 2011b; Ueno, 1999). Indeed, there is a Sr end-member of lawsonite, itoigawaite (Miyajima et al., 1999). The abundance of Sr relative to Pb in lawsonite may vary as a function of rock (protolith) type. Previous studies have documented distinct trends in Sr/Pb for metabasaltic vs. metasedimentary rocks: lawsonite in quartz-rich metasedimentary rocks tends to have lower Sr/Pb (4–25) than lawsonite in metabasaltic rocks (>30) (Fornash et al., 2019; Hara

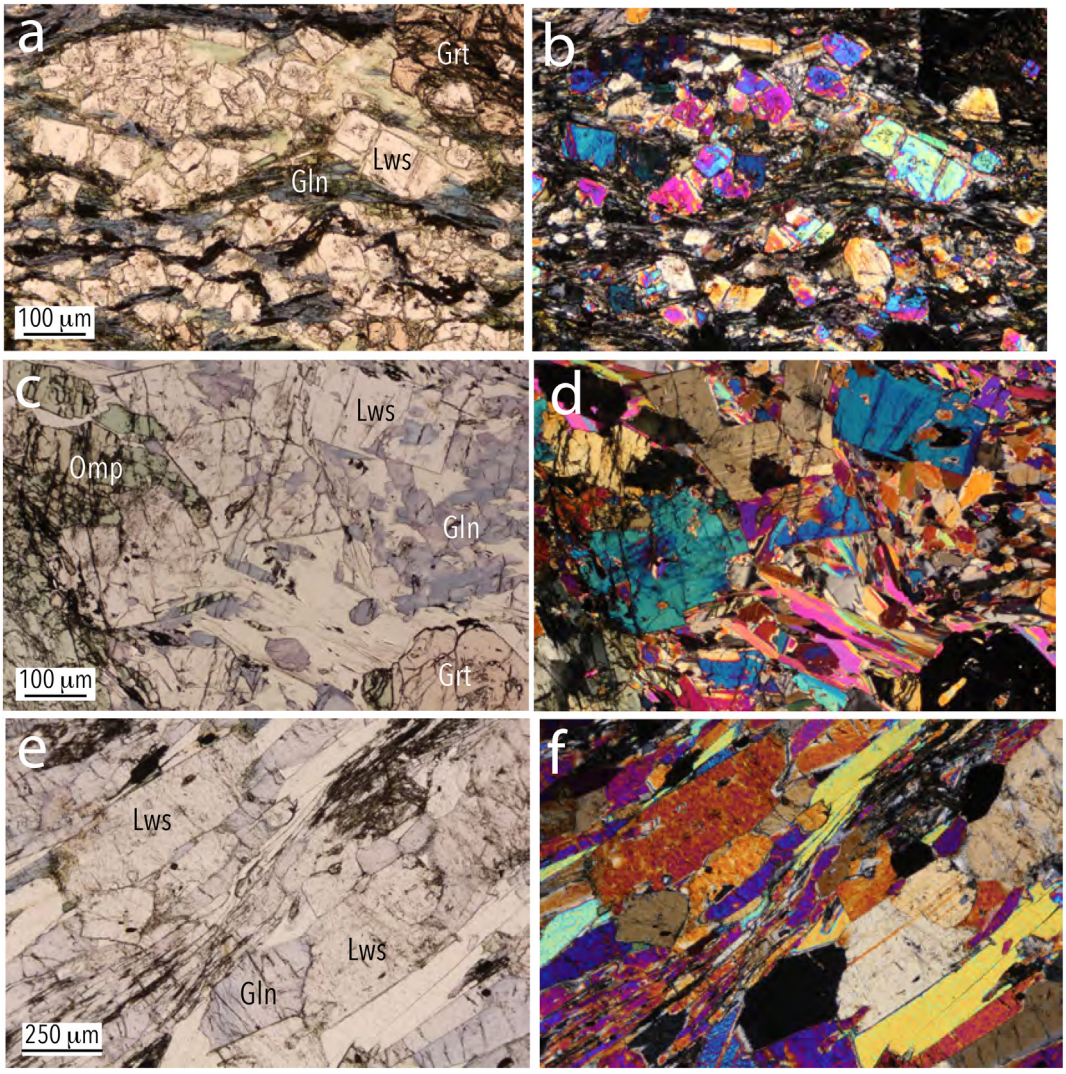

Fig. 7. Photomicrographs of lawsonite in mafic rocks (left panels: plane polarized light, ppl; right panels: crossed polarized light, xpl); some crystals in the xpl images can be seen to display twinning; (a–b) Lawsonite–garnet blueschist, Sivrihisar Massif; (c–d) omphacite–glaucophane–lawsonite–phengite–garnet rock at the blueschist margin of an eclogite pod, Sivrihisar Massif; (e–f) Lawsonite blueschist, South Motagua Fault Zone, Guatemala.

et al., 2018; Martin et al., 2011b, 2014) (Fig. 12). Although data are limited, there are possible indications of two metabasalt trends: one with very high Sr/Pb (>130) and another with more moderate ratios (30–50) (Fig. 12). In the Sivrihisar Massif, Turkey, lawsonite in metasomatic rocks plot along the meta-mafic trend, although metasomatic rocks exhibit a greater range in Sr and Pb than eclogite and blueschist (Fornash et al., 2019) (Fig. 12). Distinct trends in lawsonite Sr/Pb have also been documented for Alpine Corsica, but other lawsonite-bearing terranes do not exhibit these trends, e.g. New Caledonia (Fornash et al., 2019) (Fig. 12). Lack of a trend in Sr/Pb, such as variation in Sr without an accompanying change in Pb, is likely associated with particular mineral assemblages, such as the presence of sulfide minerals that preferentially incorporate Pb but not Sr. Sr and Pb isotopic compositions of lawsonite are also an indicator of protolith type and how protolith composition may change as a result of alteration, metamorphism, and metasomatism (e.g., Hara et al., 2018).

4.3. REE

REEs in lawsonite show great variability in patterns across samples from different localities, bulk compositions of the protolith, and even within a single crystal (Fornash et al., 2019; Martin et al., 2014). Lawsonite is typically enriched in LREE relative to HREE, but also characteristically displays enrichment in MREE relative to HREE and, in some cases, relative to LREE (Fornash et al., 2019; Martin et al., 2014; Spandler et al., 2003) (Fig. 13). Some crystals also show enrichment in the heaviest REE compared to MREE (e.g., Corsica lawsonitite; Martin et al., 2011a). Normalized Dy/Lu ratios in lawsonite are useful to represent the direction and steepness of the MREE-HREE slope in REE patterns.

In general, lawsonite in metasedimentary rocks has higher REE abundance than in metabasaltic rocks (Figs. 13a–d), but there is considerable variability in the abundance of REE and other trace elements in lawsonite within and among different lawsonite-bearing rock types and localities. Variation in REE content in different rock types and within a rock during lawsonite growth (i.e., zoning) is influenced by the bulk composition of the rock and, more specifically, by the presence or absence of other phases such as titanite and apatite for MREE, garnet for HREE, and epidote-group minerals (especially allanite) for LREE (Fig. 2; Martin et al., 2014). In addition to having higher overall REE abundances, metasedimentary rocks tend to be enriched in LREE relative to HREE (average $[La/Yb]_N = 7$- 739). In the case of metapelitic rocks, the higher (L)REE concentrations may reflect the (L)REE-enriched nature of the protolith. However, as quartz-rich metasedimentary rocks such as metacherts are not expected to have very high bulk-rock REE contents,

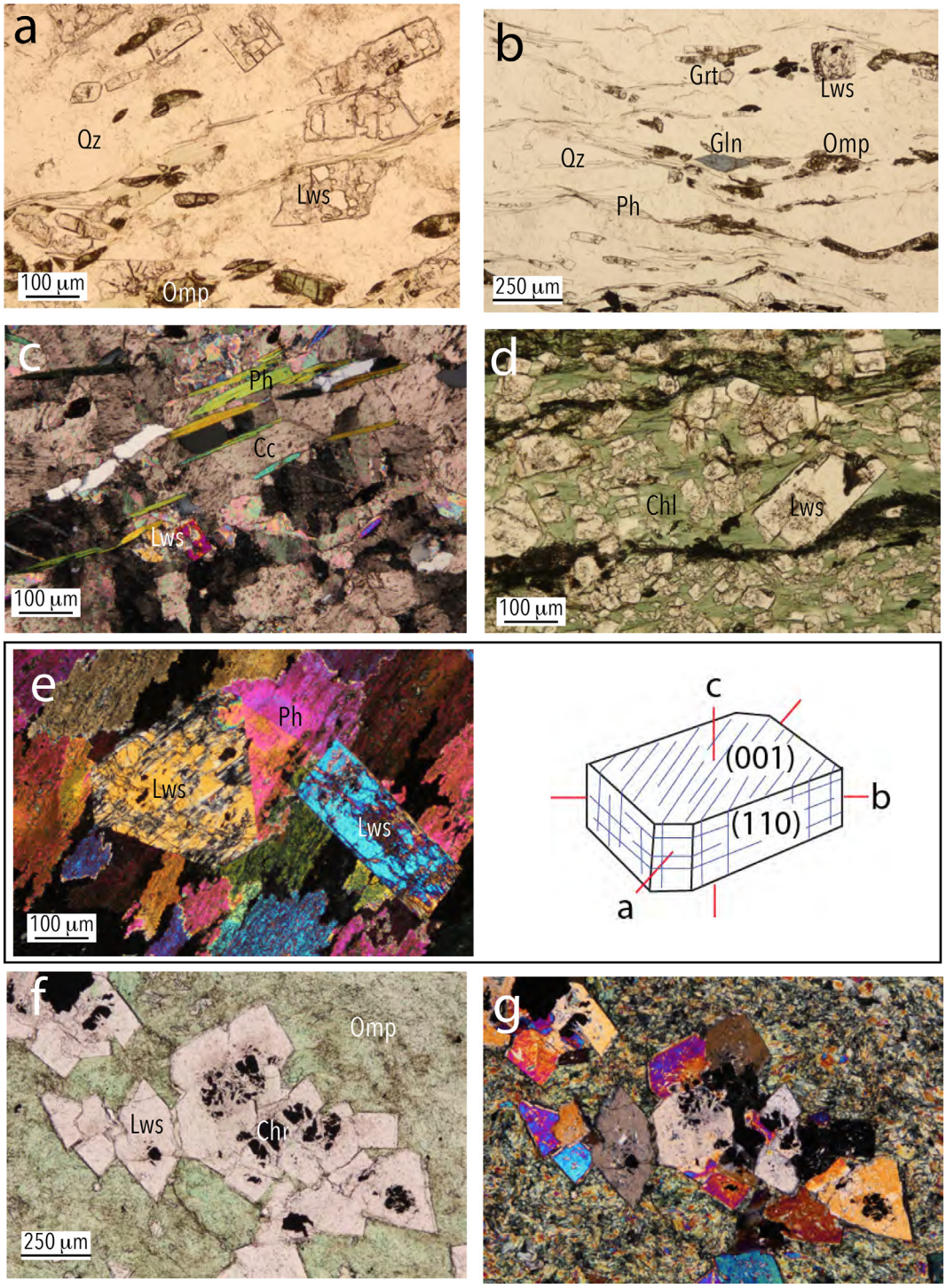

Fig. 8. Photomicrographs of lawsonite in metasedimentary and metasomatic rocks. (a,b) quartz-rich rocks from the Sivrihisar Massif, Turkey: (a) omphacite–quartz rocks; (b) quartzite (metachert) containing omphacite, glaucophane, phengite, garnet, and lawsonite (Sivrihisar, Turkey); (c) lawsonite-bearing calc-schist; (d) lawsonite–chlorite rock, Sivrihisar, Turkey; (e) lawsonite–phengite rocks, Guatemala, including a lawsonite crystal showing a characteristic (001) face and a more tabular crystal cut along a prism face; South Motagua Fault Zone, Guatemala (xpl); a sketch of a euhedral lawsonite crystal with faces labeled is shown for comparison with the lawsonite in the associated photomicrograph; (f–g) lawsonite from a lawsonite-omphacite rock, South Motagua Fault Zone, Guatemala (ppl, xpl); lawsonite contains inclusions of chromite and is zoned from more Cr-rich cores to lower-Cr rims.

the high REE contents in lawsonite in these rocks likely reflect its lower modal abundance and/or a lack of other phases competing for available REE.

Lawsonite-bearing metabasaltic rocks have normalized REE concentrations ranging from ~0.1 to 1000 times chondrite (Fig. 13a, c, d). Although there are no systematic variations in overall REE concentrations between blueschist and eclogite, eclogites show an overall enrichment in LREE relative to HREE (average $[La/Yb]_N = 5 - 537$) and most show a depletion in HREE, likely reflecting the co-existence of lawsonite with garnet. Blueschists show more variation in REE trends. Garnet-absent blueschists range from LREE-enriched (New Caledonia, Sivrihisar) to HREE-enriched (Franciscan, Ligurian Alps) (Fig. 13c). The HREE-enrichment may reflect lawsonite growth after garnet breakdown (Franciscan; Mulcahy et al., 2011) or the lack of another phase

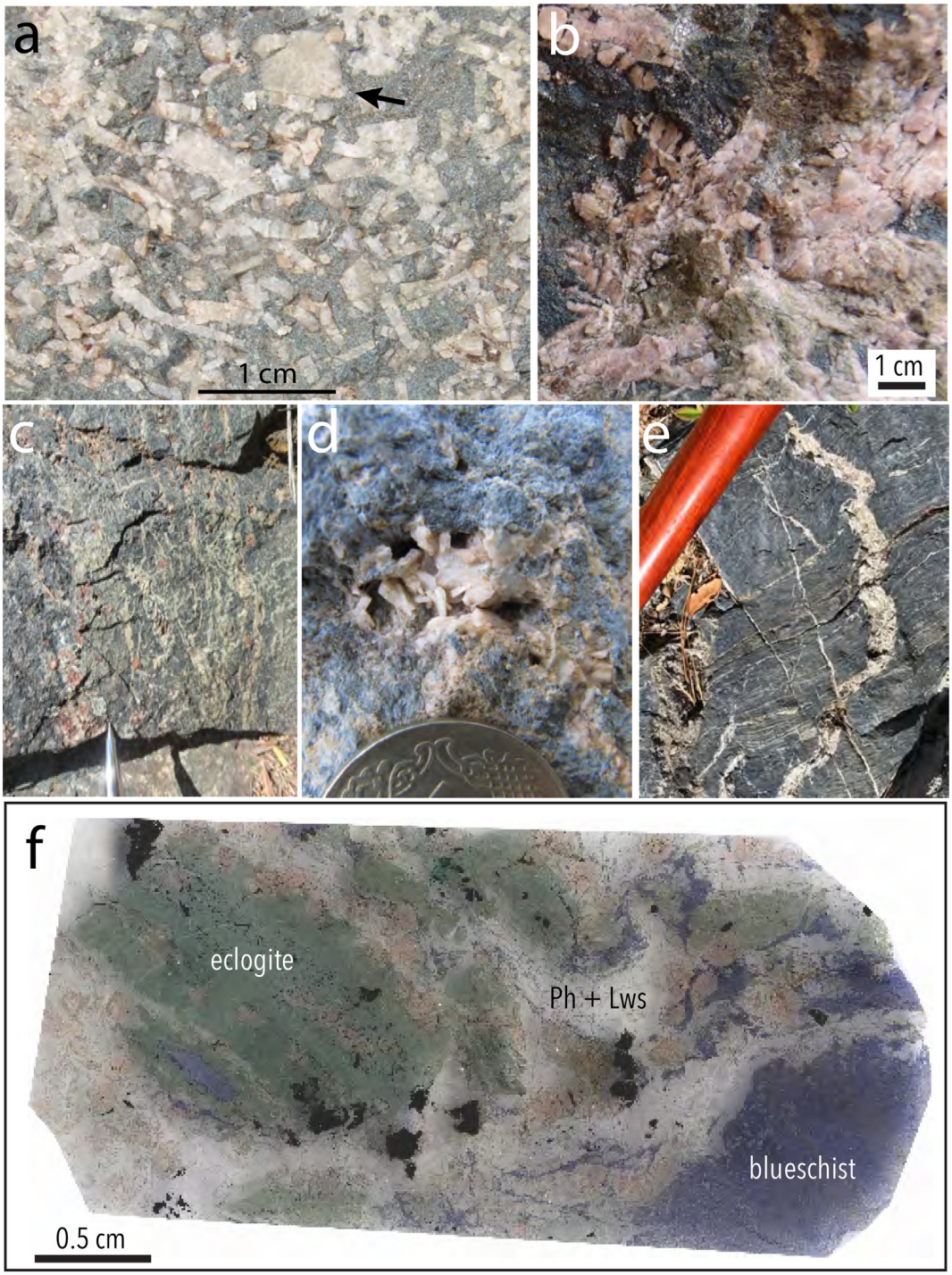

Fig. 9. (a–e) Photographs of lawsonite in outcrop. (a–d) Tavşanlı Zone, Turkey, including (a) a lawsonite–chlorite rock, (b) pink lawsonite (Fe, Cr-bearing), (c) a lawsonite vein network in blueschist, Sivrihisar Massif, and (d) lawsonite vein in blueschist; (e) lawsonite vein in blueschist, Franciscan Complex, USA (North Berkeley Hills, CA); (f) polished slice of mixed eclogite and blueschist with phengite + lawsonite-rich domains, Port Macquarie, Australia.

that competes for HREE. Garnet-bearing blueschists are enriched in LREE relative to HREE and show a depletion in HREE (Fig. 13d), likely reflecting lawsonite growth during or after garnet growth. A unique feature of the lawsonite REE pattern for the blueschist from the Ligurian Alps is the presence of a prominent positive Eu anomaly. In this case, the positive Eu anomaly is likely inherited from the bulk rock, which also has a positive Eu anomaly.

Lawsonite in metasomatic rocks are the most variable (Fig. 13e): e.g., lawsonite in Sivrihisar lawsonite-chlorite rocks has lower trace-element and REE abundance than associated metamafic and metasedimentary rocks (Fornash et al., 2019). In contrast, lawsonite in Corsica metasomatic rocks has higher trace-element concentrations than lawsonite in non-metasomatic rocks (Vitale Brovarone et al., 2014a).

5. Lawsonite zoning

Lawsonite is commonly zoned in Al, transition metals, REE, Sr, Pb, and other elements (e.g., Davis and Whitney, 2006; Fornash et al., 2019; Fornash and Whitney, 2020; Martin et al., 2011a; Piccoli et al.,

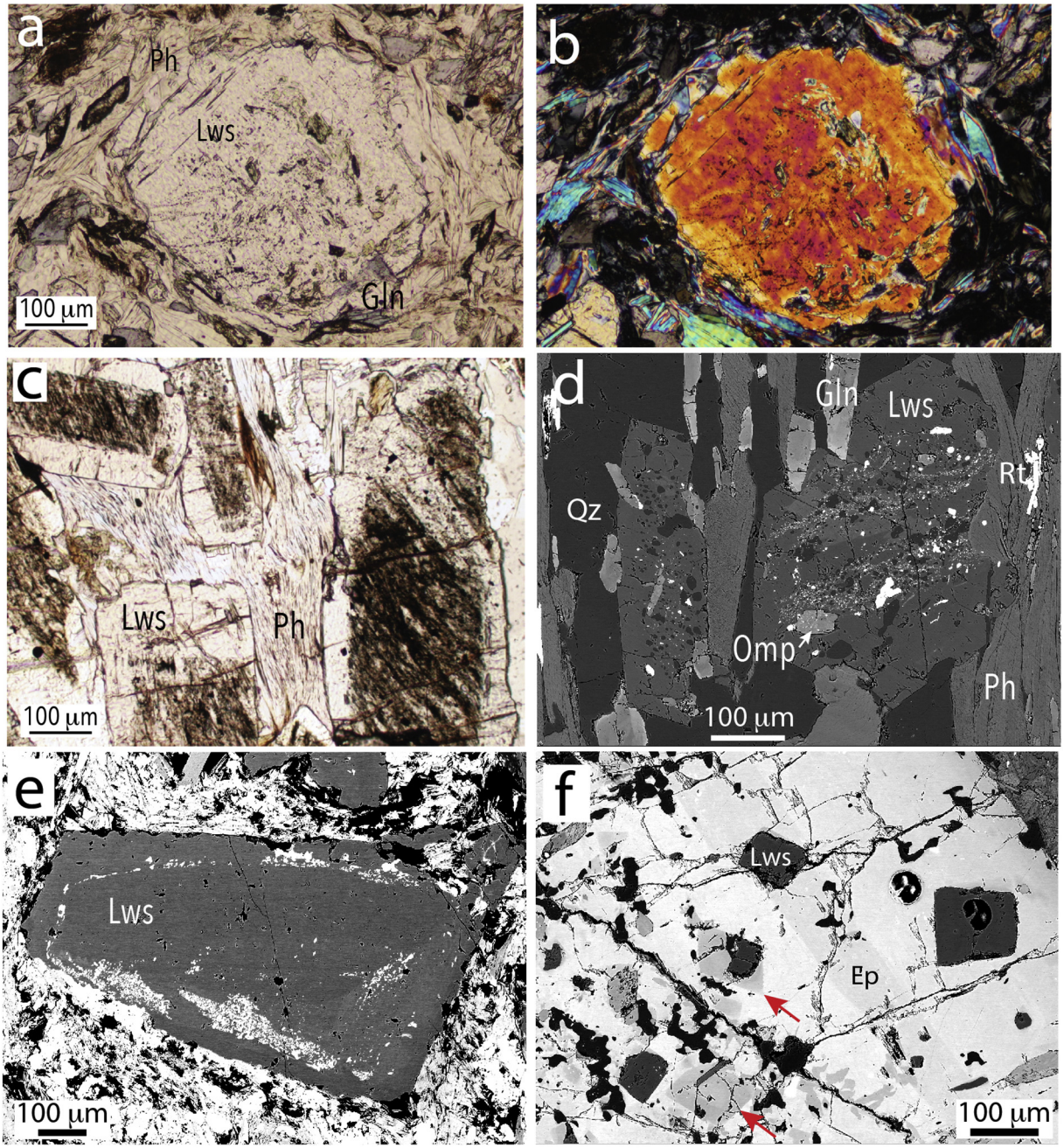

Fig. 10. (a–b) Photomicrographs (ppl, xpl) of lawsonite containing inclusions of epidote (core) and glaucophane (rim), corresponding to compositional zoning seen in the change in interference colors in the xpl image; Sivrihisar Massif, Turkey; (c) inclusion-rich cores in. lawsonite with relatively inclusion-free rims, Corsica; inclusions are dominantly graphite and Fe–Ti oxides; (d) Inclusion trails in lawsonite core region in glaucophane-bearing quartzite, Sivrihisar Massif, Turkey; inclusions are Fe–Ti oxide, quartz, apatite, rutile, and omphacite (modified from Martin et al., 2014); (e) Texturally and compositionally zoned lawsonite with inclusion-rich domains comprised of fine-grained titanite + pyrite, Port Macquarie, Australia; (f) Epidote containing lawsonite inclusions as well as 'ghosts' of former lawsonite, inferred from shape and from relict lawsonite in partially-replaced inclusions; garnet-epidote blueschist, New Caledonia (see also Fig. 2f in Martin et al., 2014; sample 96322B1 is documented in Fitzherbert et al., 2005).

2018; Sherlock and Okay, 1999; Tsujimori and Ernst, 2014; Ueno, 1999; Vitale Brovarone et al., 2014a) (Figs. 14, 15). Lawsonite may also exhibit zoning in some isotopic systems (e.g., $^{87}Sr/^{86}Sr$, $^{207}Pb/^{206}Pb$; Hara et al., 2018), although there have not yet been many studies of the radiogenic isotope systematics of lawsonite, and application of stable isotopes (Li, O, H) in lawsonite is currently in the initial stages of development (e.g., Kang et al., 2019).

5.1. Transition element zoning

Ti, Fe, and Cr display characteristic zoning patterns (Fornash et al., 2019): (1) Ti commonly exhibits hourglass sector zoning (Fig. 14a, 15a), although may also show other types of zoning; e.g., Ti-rich rims, in some cases associated with a change in inclusion assemblages (Figs. 14c, d) or other distinct domains

Table 4
Selected compositions of lawsonite in eclogite.

Locality	Sivri. Turkey	Sivri. Turkey	Corsica France	Pinchi Lk BC *matrix*	Pinchi Lk BC *inclusion*	Rio SJ DR	Motagua GUA *matrix*	Motagua GUA *inclusion*	Voltri Italy	Pt Macq AUS	Pt Macq AUS	Grt Rdg AZ USA
Reference	*1*	*1*	*2*	*3*	*3*	*4*	*3*	*3*	*5*	*6*	*7*	*8*
SiO_2	37.94	38.29	38.28	37.72	38.20	38.30	37.93	38.17	36.75	38.54	37.14	38.56
TiO_2	0.31	0.07	0.13	0.25	0.15	0.04	0.08	0.08	0.15	0.03	0.50	0.12
Al_2O_3	31.21	31.99	31.21	31.51	32.19	31.56	32.01	32.07	30.13	31.42	31.76	30.00
Cr_2O_3	0.02	0.01	bdl	0.11	0.10	0.01	0.08	0.06	0.39	0.19	bdl	0.19
FeO*	1.45	1.47	1.18	0.77	0.65	0.44	0.40	1.07	1.21	0.52	0.25	0.94
MnO	bdl	bdl	0.03	bdl	bdl	0.02	bdl	bdl	bdl	bdl	bdl	0.01
MgO	bdl	bdl	bdl	bdl	bdl	bdl	bdl	bdl	bdl	bdl	bdl	0.02
CaO	17.92	17.86	17.76	18.54	17.45	17.74	17.83	17.94	16.86	16.90	17.32	17.04
Na_2O	bdl	bdl	bdl	bdl	bdl	bdl	bdl	bdl	bdl	0.01	bdl	0.00
K_2O	bdl	bdl	bdl	bdl	bdl	bdl	bdl	bdl	bdl	bdl	bdl	0.00
Total	88.85	89.69	88.59	88.90	88.75	88.11	88.34	89.39	85.49	87.61	86.97	86.88
Cations (8 oxygen basis)												
Si	2.00	1.99	2.01	1.98	1.98	2.00	1.99	1.99	2.01	2.04	1.98	2.06
Ti	0.01		0.01	0.01	0.01	0.01			0.01		0.02	0.01
Al	1.94	1.96	1.93	1.95	1.99	1.98	1.98	1.97	1.94	1.96	2.00	1.89
Cr					0.01				0.02	0.01		0.01
Fe^{3+}	0.06	0.06	0.05	0.03	0.03	0.03	0.02	0.05	0.06	0.02	0.07	0.04
Ca	1.01	1.00	1.00	1.04	0.98	0.98	1.00	1.00	0.99	0.96	0.99	0.97
Ti+Cr +Fe	0.07	0.06	0.06	0.04	0.05	0.04	0.02	0.05	0.09	0.03	0.09	0.06

References: 1 = Fornash et al. (2019); 2 = Ravna et al. (2010); 3 = this study; 4 = Zack et al. (2004); 5 = Scarsi et al. (2018); 6 = Och et al. (2003); 7 = Tamblyn et al. (2019); 8 = Usui et al. (2006).
FeO* (total Fe) reported for Fe-oxide from microprobe analysis; Fe in lawsonite is likely Fe^{3+} and is reported as such in the cation list.
bdl = below detection limit.
Analyses were selected to show a range of compositions within and among HP/LT complexes; owing to zoning, these are not necessarily representative of the complete range of compositions in a crystal, rock, or terrane.

(Figs. 15b, c); (2) Fe is commonly concentrically zoned (Fig. 14b, e), with distinct core and rim domains, although in some cases is entirely or partially oscillatory (Figs. 14f, 15a) or occurs as patchy 'ghost' zoning that may be inherited from a precursor phase (Fig. 14g); and (3) Cr commonly exhibits oscillatory zoning (Figs. 14g, 15a, b), but may also occur in distinct domains. Different zoning types (e.g., hourglass, core-rim, oscillatory) may occur in the same lawsonite crystal for different elements (Fig. 15a, b), indicating the simultaneous operation of crystallographic control (Ti), changing P-T and/or fO_2 conditions (Fe), and/or fluids (Cr) during lawsonite growth.

Growth zoning may be modified by deformation and other processes. For example, in some Sivrihisar rocks, subgrain boundaries and twin planes are enriched in Ti relative to other regions of lawsonite grains (Fornash et al., 2019), and compositional variation in major and trace elements is seen associated with fractures in lawsonite in the Port Macquarie locality, possibly indicating dissolution-reprecipitation processes.

Table 5
Selected compositions of lawsonite inclusions in garnet in eclogite.

Locality	New Caled.	Elekdağ Turkey	Tianshan China	N Qilian China	Sanbagawa Japan	Monviso Italy	Yukon Canada	Pinchi Lk Canada
Reference	*1*	*2*	*3*	*4*	*5*	*6*	*7*	*7*
SiO_2	38.47	38.20	36.76	37.63	38.52	37.43	37.35	38.20
TiO_2	0.05	0.14	0.14	0.08	0.20	nd	0.24	0.15
Al_2O_3	32.29	31.23	30.39	30.75	31.61	30.39	31.37	32.19
Cr_2O_3	0.03	0.03	0.02	0.04	nd	nd	0.05	0.10
FeO*	0.51	0.74	0.80	0.58	0.86	1.98	0.86	0.65
MnO	0.04	0.02	bdl	0.05	0.11	bdl	bdl	bdl
MgO	bdl	bdl	bdl	0.01	nd	bdl	bdl	bdl
CaO	17.14	17.73	17.78	17.91	17.86	17.32	17.73	17.45
Na_2O	0.02	0.03	0.06	bdl	nd	bdl	bdl	nd
K_2O	0.01	0.02	0.03	bdl	nd	nd	bdl	nd
Total	88.56	88.14	85.98	87.05	89.16	87.12	87.60	88.73
Cations (8 oxygen basis)								
Si	2.01	2.01	2.00	2.01	2.02	2.00	1.98	2.00
Ti		0.01	0.01				0.01	0.01
Al	1.99	1.94	1.95	1.94	1.95	1.92	1.96	1.98
Fe^{3+}	0.02	0.03	0.04	0.03	0.04	0.08	0.04	0.03
Ca	0.96	1.00	1.03	1.03	1.00	0.99	1.01	0.98
Ti+Cr+Fe	0.02	0.04	0.05	0.03	0.04	0.08	0.05	0.04

References: 1 = Clarke et al. (1997); 2 = Altherr et al. (2004); 3 = Du et al. (2014); 4 = Zhang et al. (2007); 5 = Tsuchiya and Hirajima (2013); 6 = Groppo and Castelli (2010); 7 = this study; 8 = Ghent et al. (1993); bdl = below detection limit; nd = not determined.

Table 6
Selected compositions of lawsonite in blueschist.

Locality	New Caledonia	Sivrihisar Turkey	Corsica France	Franciscan (Ring Mtn)	Motagua Guatemala	Pinchi Lk Canada	Kurosegawa Japan
Reference	*1*	*2*	*3*	*3*	*3*	*3*	*4*
SiO_2	38.24	37.41	37.73	38.40	38.14	37.71	38.65
TiO_2	0.55	0.80	0.27	0.17	0.13	0.15	0.19
Al_2O_3	31.94	25.79	31.26	31.94	31.41	31.75	30.12
Cr_2O_3	0.04	5.81	bdl	bdl	bdl	0.05	bdl
FeO*	0.47	2.12	0.68	0.96	1.45	0.62	1.77
MnO	0.11	0.01	bdl	bdl	bdl	bdl	bdl
MgO	0.01	0.01	bdl	bdl	bdl	bdl	0.22
CaO	16.98	17.26	17.99	18.39	17.91	17.38	17.09
Na_2O	0.01	bdl	bdl	bdl	bdl	bdl	bdl
K_2O	0.02	bdl	bdl	bdl	bdl	bdl	bdl
Total	88.37	89.21	87.93	89.86	88.43	87.68	88.04
Cations (8 oxygen basis)							
Si	2.01	2.01	2.00	1.99	1.99	1.99	2.04
Ti	0.02	0.03	0.01	0.01	0.01	0.01	0.01
Al	1.97	1.63	1.95	1.95	1.94	1.98	1.87
Cr		0.25					
Fe^{3+}	0.02	0.10	0.03	0.04	0.06	0.03	0.08
Ca	0.95	1.00	1.02	1.02	1.00	0.99	0.97
Ti+Cr+Fe	0.04	0.38	0.04	0.05	0.07	0.04	0.09

References: 1 = Clarke et al. (1997); 2 = Fornash et al. (2019); 3 = this study; 4 = Sato et al. (2016).
bdl = below detection limit

Table 7
Selected compositions of lawsonite in metasedimentary rocks.

Locality	Sivrihisar Turkey	Sivrihisar Turkey	Corsica France	Sivrihisar Turkey	Sanbagawa, Japan	New Caledonia
Rock type	Quartzite	Quartzite	Quartzite	Calc-schist	Metapelite	Metapelite
Reference	*1*	*2*	*1*	*1*	*3*	*4*
SiO_2	37.69	37.55	37.60	37.79	36.90	38.41
TiO_2	0.07	0.17	0.12	0.11	0.65	0.12
Al_2O_3	30.98	31.77	30.97	31.10	31.00	31.82
Cr_2O_3	bdl	bdl	bdl	0.05	0.12	nd
FeO*	1.89	1.42	0.20	0.68	0.32	0.20
MnO	bdl	bdl	bdl	bdl	nd	0.12
MgO	0.02	bdl	bdl	bdl	nd	0.02
CaO	17.74	17.43	17.81	16.53	17.50	16.96
Na_2O	0.01	bdl	bdl	bdl	nd	nd
K_2O	bdl	bdl	0.01	bdl	nd	nd
total	88.40	88.34	86.71	86.27	86.49	87.65
Cations (8 oxygen basis)						
Si	2.00	2.00	2.01	2.02	1.98	2.02
Ti		0.03			0.03	0.01
Al	1.94	1.93	1.95	1.96	1.96	1.98
Cr					0.01	
Fe^{3+}	0.08	0.06	0.01	0.03	0.01	0.01
Ca	1.01	0.97	1.02	0.95	1.01	0.96
Ti+Cr+Fe	0.08	0.09	0.01	0.03	0.05	0.02

References: 1 = this study; 2 = Martin et al. (2014); 3 = Ueno (1999); 4 = Spandler et al. (2003).
bdl = below detection limit; nd = not determined

5.2. Trace-element/REE zoning

Lawsonite is also commonly zoned in other trace elements and REE (Fornash et al., 2019; Fornash and Whitney, 2020; Martin et al., 2014; Spandler et al., 2003; Vitale Brovarone et al., 2014a). In some cases, REE variation correlates with transition-metal zoning (Fig. 16a–b) and in other cases it does not. Lawsonite in metasomatic rocks from Corsica is strongly zoned in REE (Martin et al., 2011b; Vitale Brovarone et al., 2014a) (Fig. 16c). Key features of trace-element composition and zoning of lawsonite from these metasomatic rocks are strong zoning (1-3 orders of magnitude) in Th and REE, core to rim enrichment in Pb relative to Ce and Sr relative to Nd, and an increase in HREE relative to MREE. In Corsica lawsonitite, the cores of lawsonite crystals have Sr/Pb values similar to that of metasedimentary rocks, but the metasomatic rims have Sr/Pb values more similar to metabasaltic rocks (Martin et al., 2014). In contrast, core-to-rim zoning in $^{87}Sr/^{86}Sr$ and $^{207}Pb/^{206}Pb$ zoning in Guatemala lawsonite was interpreted to indicate an increasing sedimentary influence on the fluid present during crystallization of lawsonite rims (Hara et al., 2018).

Lawsonite from the Sivrihisar Massif, Turkey, also commonly records zoning in REE (Fornash et al., 2019). Some grains record a core-to-rim decrease in overall REE concentrations with no change in the overall shape of the REE pattern, whereas other lawsonite records either a core-to-rim increase in REE concentrations and/or a change in the shape of the REE pattern. In one garnet-bearing blueschist, there is a core-to-rim increase in MREE concentrations, likely signifying the breakdown of an MREE-bearing phase such as titanite or apatite during the growth of the lawsonite rim. As there is no concomitant increase in P content between the core and the rim, the most likely phase is titanite.

A change in Eu anomaly from negative in the lawsonite core to positive near the rim was observed in Corsica lawsonitite (Martin et al., 2011a) (Fig. 16c) and interpreted to indicate progressive growth of

Table 8
Selected compositions of lawsonite in metasomatic rocks and veins.

Locality	Sivrihisar Turkey	Sivrihisar Turkey	Sivrihisar Turkey	Corsica France	Corsica France	Corsica France	Corsica France	Motagua Guatem.	Francisc. USA	Francisc. USA	New Zealand
Rock type	Lws-Chl	Lws layer	Lws layer	Lws-Chl	Metasom metased	Metasom metased	Omphacitite	Omphacitite	Lws vein in bls	Lws vein in ecl	Lws vein low-grade
Reference	*1*	*2*	*3*	*1*	*4*	*4*	*1*	*1*	*1*	*5*	*6*
SiO_2	37.83	38.31	38.31	37.65	37.38	38.37	37.34	36.04	37.84	37.48	39.35
TiO_2	0.60	0.41	0.41	0.45	0.17	0.04	0.07	0.40	0.35	0.81	0.03
Al_2O_3	31.00	31.97	31.97	31.04	26.53	31.56	31.47	22.80	30.88	31.24	31.97
Cr_2O_3	0.06	0.08	0.08	0.10	7.11	0.32	0.04	11.38	0.11	bdl	nd
FeO*	1.26	1.45	1.45	0.41	0.27	0.50	0.91	0.46	1.60	1.47	0.14
MnO	bdl	bdl	bdl	bdl	bdl	0.02	bdl	0.06	bdl	bdl	bdl
MgO	bdl	bdl	bdl	bdl	bdl	bdl	bdl	bdl	bdl	bdl	0.02
CaO	17.56	17.67	17.67	17.87	16.86	17.65	17.62	17.01	17.55	17.49	16.83
Na_2O	bdl	bdl	bdl	bdl	0.01	0.01	bdl	bdl	0.01	bdl	nd
K_2O	bdl	bdl	bdl	bdl	0.01	bdl	bdl	bdl	bdl	bdl	nd
total	88.32	89.89	89.89	87.51	88.34	88.47	87.44	88.17	88.34	88.49	88.34
Cations (8 oxygen basis)											
Si	1.99	1.99	1.99	2.00	2.01	2.01	1.99	1.98	2.00	1.98	2.05
Ti	0.02	0.02	0.02	0.02	0.01			0.02	0.01	0.03	
Al	1.92	1.96	1.96	1.94	1.68	1.95	1.97	1.48	1.92	1.95	1.96
Cr					0.30	0.01		0.50			
Fe^{3+}	0.06	0.06	0.06	0.02	0.01	0.02	0.04	0.02	0.07	0.06	0.01
Ca	0.99	0.98	0.98	1.02	0.97	0.99	1.00	1.00	0.99	0.98	0.94
Ti+Cr +Fe	0.08	0.08	0.08	0.04	0.32	0.03	0.04	0.53	0.09	0.09	0.01

References: 1 = this study; 2 = Fornash and Whitney (2020): 3 = Fornash et al. (2019); 4 = Vitale Brovarone et al. (2014a); 5 = Martin et al. (2014); 6 = George and Grapes (1987).
bdl = below detection limit; nd = not determine

Table 9
Trace-element ratios in lawsonite from different rocks types and metamorphic facies.

Rock type	Sr/Pb	$[La/Dy]_N$	$[Dy/Lu]_N$	$[La/Yb]_N$	References
Metabasalts					
Blueschist-facies					
Franciscan (Ring Mt), USA	nd	0.21	0.77	0.15	Mulcahy et al. (2011)
New Caledonia	3063	1.22	3.03	3.49	Spandler et al. (2003)
New Caledonia	166	1.78	5.42	8.42	Spandler et al. (2003)
North Qilian, China	600	0.53	0.45	0.28	Xiao et al. (2013)
North Qilian, China	310	0.72	2.99	1.60	Xiao et al. (2013)
Ligurian Alps, Italy	nd	0.62	nd	0.66	Tribuzio et al. (1996)
Sivrihisar Massif, Turkey	45	12.09	2.57	30.62	Fornash et al. (2019)
Sivrihisar Massif, Turkey	182	2.70	6.10	18.36	Fornash et al. (2019)
Sivrihisar Massif, Turkey	30	2.82	34.43	27.41	Fornash et al. (2019)
Eclogite-facies					
Sivrihisar Massif, Turkey	38	2.58	39.19	11.97	Fornash et al. (2019), Fornash and Whitney (2020)
Sivrihisar Massif, Turkey	43	1.23	12.16	4.57	Fornash et al. (2019), Fornash and Whitney (2020)
S Motagu FZ, Guatemala	49	10.99	27.67	536.97	Hara et al. (2018)
S Motagu FZ, Guatemala	251	1.88	24.70	33.30	Hara et al. (2018)
Garnet Ridge AZ USA	nd	5.69	3.10	16.63	Usui et al. (2006)
Metasediments					
Metaquartzite (eclogite/blueschist facies)					
Sivrihisar Massif, Turkey	7	3.59	5.35	6.63	Martin et al. (2014)
Sivrihisar Massif, Turkey	5	6.46	34.07	106.12	Fornash et al. (2019)
Metachert (eclogite facies)					
S Motagua FZ, Guatemala	16	30.85	34.72	738.92	Hara et al. (2018)
Metapelite (blueschist facies)					
New Caledonia	317	2.74	5.20	11.04	Spandler et al. (2003)
Metasomatic Rocks					
Alpine Corsica, France	46	10.17	6.16	38.48	Vitale Brovarone et al. (2014a)
Alpine Corsica, France	77	12.41	2.55	28.57	Vitale Brovarone et al. (2014a)
Sivrihisar Massif, Turkey	45	1.18	1.91	2.27	Fornash et al. (2019)
Sivrihisar Massif, Turkey	26	0.12	2.07	0.20	Fornash et al. (2019)
Sivrihisar Massif, Turkey	29	0.64	0.83	0.45	Fornash et al. (2019)
Lawsonite-rich veins and layers					
Franciscan, USA	57	0.19	2.22	0.34	Martin et al. (2014)
Sivrihisar Massif, Turkey	41	2.99	26.82	18.17	Fornash et al. (2019), Fornash and Whitney (2020)

nd = not determined

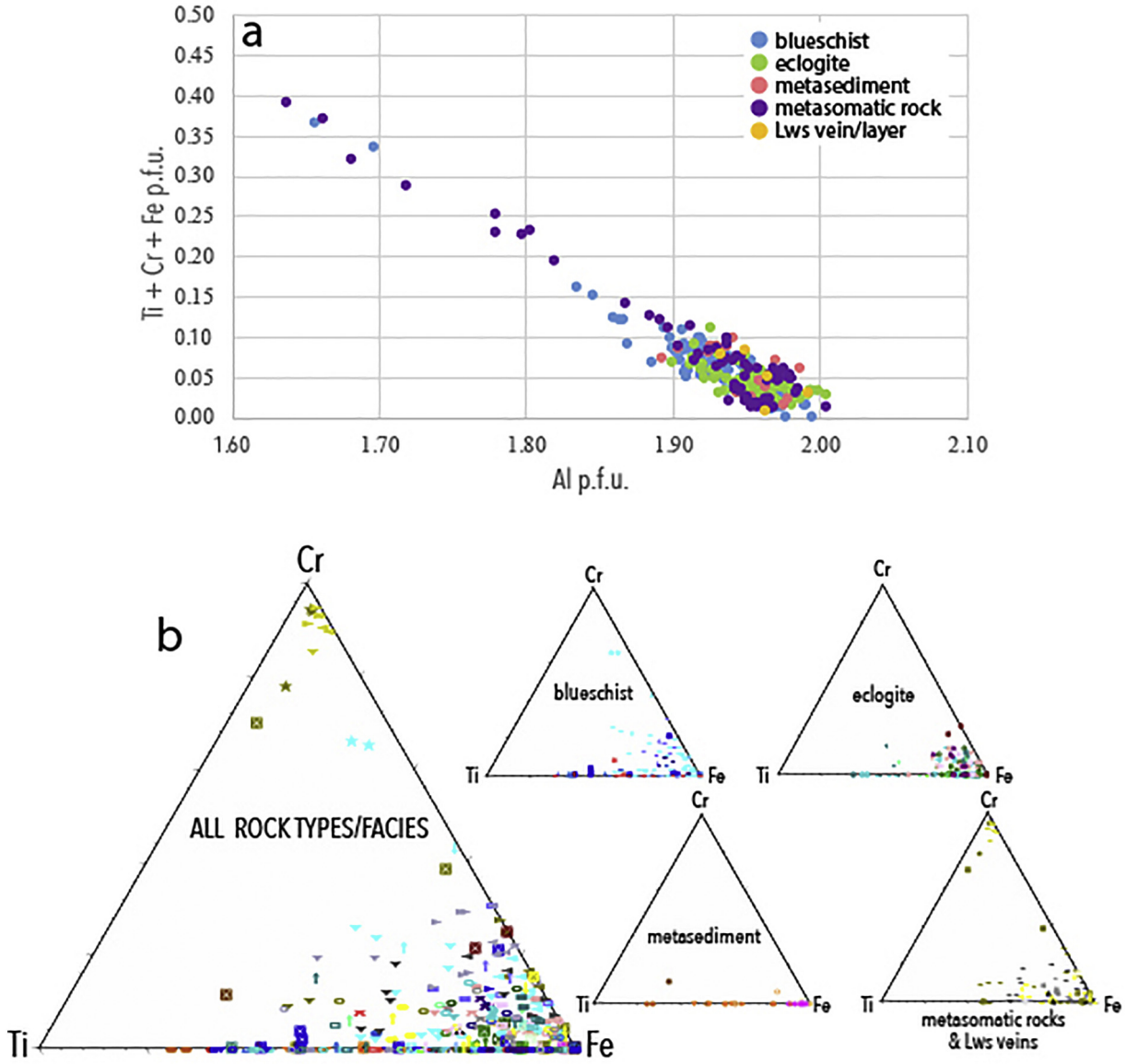

Fig. 11. Lawsonite Al-site composition, with data from a wide range of localities and rock types (complete dataset with references in Table S1). (a) Fe + Ti + Cr vs. Al plot, showing that the transition metals typically substitute for Al in the lawsonite structure; (b) ternary Fe–Ti–Cr plot showing the abundance of these elements in blueschist- and eclogite-facies metamafic (metabasalt, metagabbro), metasedimentary, and metasomatic rocks and veins from 15 different HP/LT complexes. In both (a) and (b), plotted data represent lawsonite in which Fe, Cr, and Ti were analyzed, whether or not they were detected, and in which $1.97 < Al + Fe + Cr + Ti < 2.02$.

lawsonite during plagioclase-bearing blueschist-facies to plagioclase-free eclogite-facies conditions. A systematic change in Eu is not observed in other localities in which lawsonite likely grew over a blueschist to eclogite transition (e.g., Sivrihisar, Turkey; Fornash et al., 2019), indicating that there are other processes (unrelated to plagioclase) that may lead to a negative Eu anomaly, including crystallization of titanite, change in oxygen fugacity, or metasomatic change in Eu in the bulk rock (Fornash et al., 2019; Martin et al., 2014).

6. Lawsonite geochronology

A compilation of ages of lawsonite blueschist and eclogite shows that, with the exception of the Neoproterozoic blueschist of Anglesey (Wales, UK), all others are Phanerozoic (Fig. 17). This may in part be a function of the lack of preservation, as Proterozoic HP/LT rocks in general are rare. However, given the significance of lawsonite for indicating cooler subduction geotherms, it is important to evaluate possible trends in formation of lawsonite-bearing rocks. For example, Tsujimori and Ernst (2014) noted that there is no difference in the occurrence of lawsonite vs. epidote blueschists in Phanerozoic subduction complexes, and therefore no overall global change in subduction geotherms in that time. An apparent "hiatus" in lawsonite formation in the Permian was attributed to processes related to the breakup of Pangaea, although subsequent work has determined Permian ages for lawsonite blueschist and eclogite (Fig. 17).

Most studies of the metamorphic age of lawsonite-bearing rocks have employed methods that did not directly involve analyzing lawsonite. The Lu-Hf isotopic system can be used to determine the age of HP/LT metamorphism through analysis of lawsonite, other HP/LT minerals (garnet, omphacite), and whole-rock composition, but this method has thus far only been applied in a few studies (Mulcahy et al., 2011; Vitale Brovarone and Herwartz, 2013; Mulcahy et al., 2014; Tamblyn et al., 2019). Analyses of Franciscan lawsonite blueschists from two regions of the complex yielded ages of c. 145 Ma (Ring Mountain) and c. 152 (Ward Creek), within the range of 157-141 Ma determined by other methods from HP rocks in the Franciscan

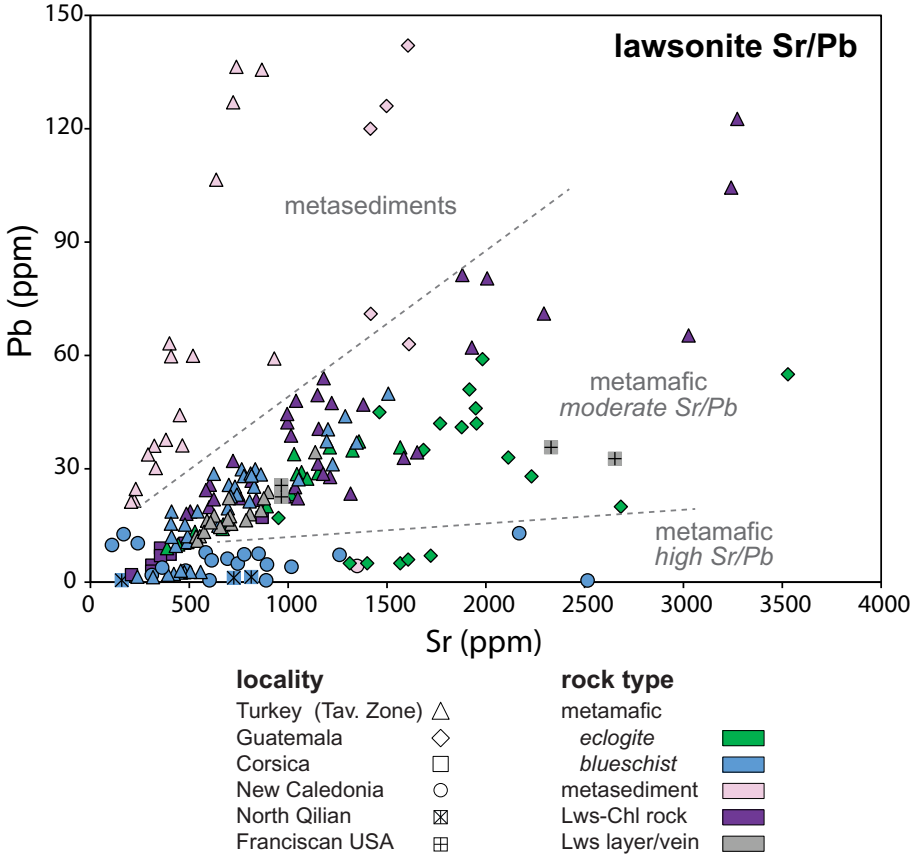

Fig. 12. Pb vs. Sr in lawsonite from six localities including data from eclogite and blueschist-facies mafic rocks (metabasalt, metagabbro), metasediment (quartzite), and metasomatic rocks (lawsonite–chlorite rocks, lawsonite-rich veins and layers) (data and data sources are in Table 9).

(Mulcahy et al., 2011, 2014). Application of the Lu-Hf method to Sivrihisar, Turkey, lawsonite-bearing rocks yielded ages of ~91 Ma for eclogite and ~83 Ma for blueschist (Mulcahy et al., 2014), consistent with the results of ^{40}Ar-^{39}Ar phengite analyses (Fornash et al., 2016; Sherlock et al., 1999) and a Lu-Hf garnet geochronology study (Pourteau et al., 2019) from the same HP unit.

Lu-Hf ages of ~37 Ma for a lawsonite-bearing blueschist (garnet-absent metagabbro) from Alpine Corsica are slightly older than Lu-Hf garnet ages (~34 Ma) obtained for lawsonite eclogite, interpreted to indicate diachronous HP metamorphism in the two units (Vitale Brovarone and Herwartz, 2013). Similarly, the recent work of Tamblyn et al. (2019) on the Port Macquarie mélange indicates that lawsonite eclogite (~480 Ma) is older than associated lawsonite blueschist (~470 Ma), which likely formed by retrogression of eclogite. These studies establish the reliability of the method for determining the age of HP metamorphism and for distinguishing ages of eclogite and blueschist. Owing to technical and other challenges, there have thus far been no studies in which different ages have been determined for lawsonite core vs. rim or for different textural generations of lawsonite within a rock.

7. Discussion

Although somewhat rare in the geologic record, particularly in eclogite, lawsonite is predicted from experiments, thermodynamic modeling, and geophysical data to be an abundant mineral in subducted oceanic crust and sediments. Lawsonite also occurs in metasomatized rocks, including in veins that record HP fluid systems. The discrepancy between predicted occurrence in active subduction zones and preservation in the geologic record has been termed the 'lawsonite paradox' (Clarke et al., 2006), and is important to understand because of the significance of lawsonite for subduction thermal structure and element budgets. For lawsonite to form and then survive continued subduction and subsequent exhumation, lawsonite-bearing rocks must remain relatively cold (<7–10 °C/km thermal gradient, depending on the P-T location of the lawsonite-out reaction; Fig. 5) during prograde metamorphism and exhumation.

A H_2O-rich environment promotes lawsonite crystallization and persistence, and bulk composition of the rock is important in determining whether the presence of CO_2 will contribute to lawsonite or carbonate stability; e.g., in some basaltic bulk-compositions, CO_2 may increase the lawsonite stability field, along with Mg-carbonates (Martin and Hermann, 2018; Poli et al., 2009). However, if quartz is present, the reaction lawsonite + quartz + CO_2 = calcite + pyrophyllite + H_2O may restrict lawsonite to very low f_{CO2} (Okay, 1980).

This set of conditions may be achieved at the top of slabs in normal to cool subduction zones if a slice becomes detached and is refrigerated by continued subduction below it and/or if subduction and exhumation are relatively rapid. Numerical models show that P-T conditions suitable for the growth of lawsonite are easily attained during subduction, and maintenance of sufficiently cold conditions is facilitated in mature subduction zones (e.g., Gerya et al., 2002; Malatesta et al., 2012). In a study of deformation fabrics involving lawsonite, Teyssier et al. (2010) proposed that oblique exhumation below a serpentinized mantle wedge driven in part by rapid pure-shear extrusion in the subduction channel facilitated preservation of lawsonite. However, exhumation need not be rapid (cms/year) as long as a cool thermal gradient is maintained.

In the following sections, we discuss the data and observations presented in this review to develop ideas about how lawsonite can be used as an important archive of information for reconstructing reaction history, fluid–rock interaction, and fluid sources in subduction. We

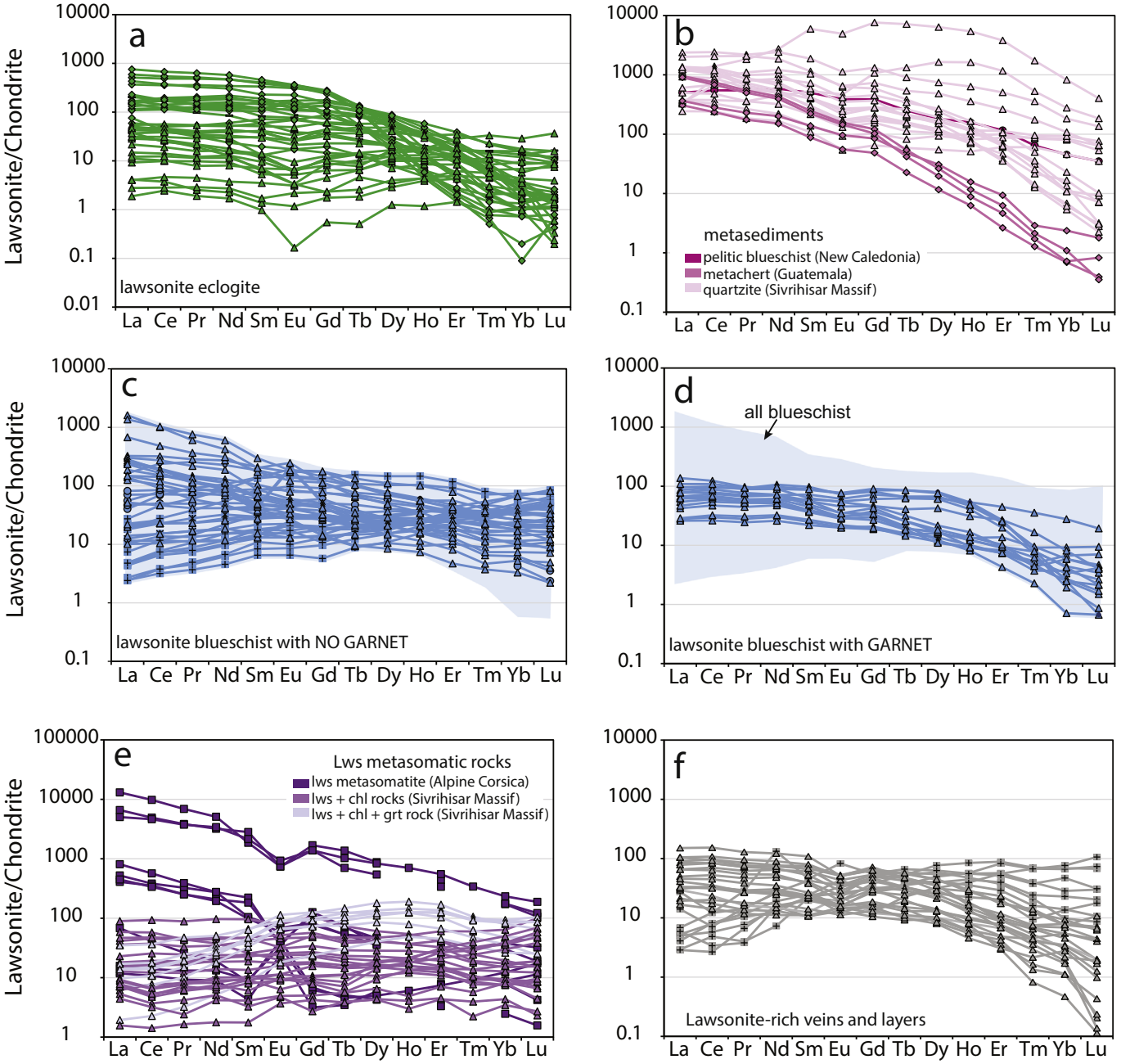

Fig. 13. REE abundance in lawsonite from different rock types and localities (representative data in Table 9; complete data in Table S2), including (a) eclogite (mafic protoliths); (b) quartz-rich metasedimentary rocks; (c) garnet-absent blueschist; (d) garnet-bearing blueschist; (e) metasomatic rocks; and (f) veins and layers.

consider the role of lawsonite in the subduction component of the deep-Earth water cycle and discuss how the geochemistry of lawsonite provides new information about fluid–rock reaction during HP/LT metamorphism. We then use the compositional dataset summarized in this paper to discuss how lawsonite composition and zoning may be used to document subduction conditions and processes.

7.1. Lawsonite and subduction-zone water budgets

The H_2O-rich nature of HP/LT rocks, and eclogite-facies rocks in particular, is important for understanding element cycling as well as the rheology and geophysical properties of subducted crust. There has been much research on subduction zone fluids because dehydration of hydrous minerals in the slab is the key mechanism by which fluids are transferred to the mantle wedge, driving arc magmatism and contributing to the chemical heterogeneity of the mantle (e.g., Bebout, 1991; Scambelluri et al., 2019; Schmidt and Poli, 1998), with implications for the composition of the crust and atmosphere. In addition, fluid release, including by lawsonite dehydration, may trigger intermediate-depth earthquakes in subducted slabs (e.g., Abers et al., 2006; Hacker et al., 2003b; Kirby et al., 1996; Okazaki and Hirth, 2016; Peacock, 2001).

The growth and preservation of lawsonite has significant implications for water and element cycling in the Earth. In metamafic blueschists and eclogites, lawsonite may comprise 20–40% of the mode (e.g., Davis and Whitney, 2006). Owing to its high modal abundance and H_2O content of ~11.5%, lawsonite is a (and in some cases *the*) major contributor to the water and element budget of subduction zones. Some studies have proposed that most of the water in subducted oceanic crust is released at the "wet" blueschist to "dry" eclogite

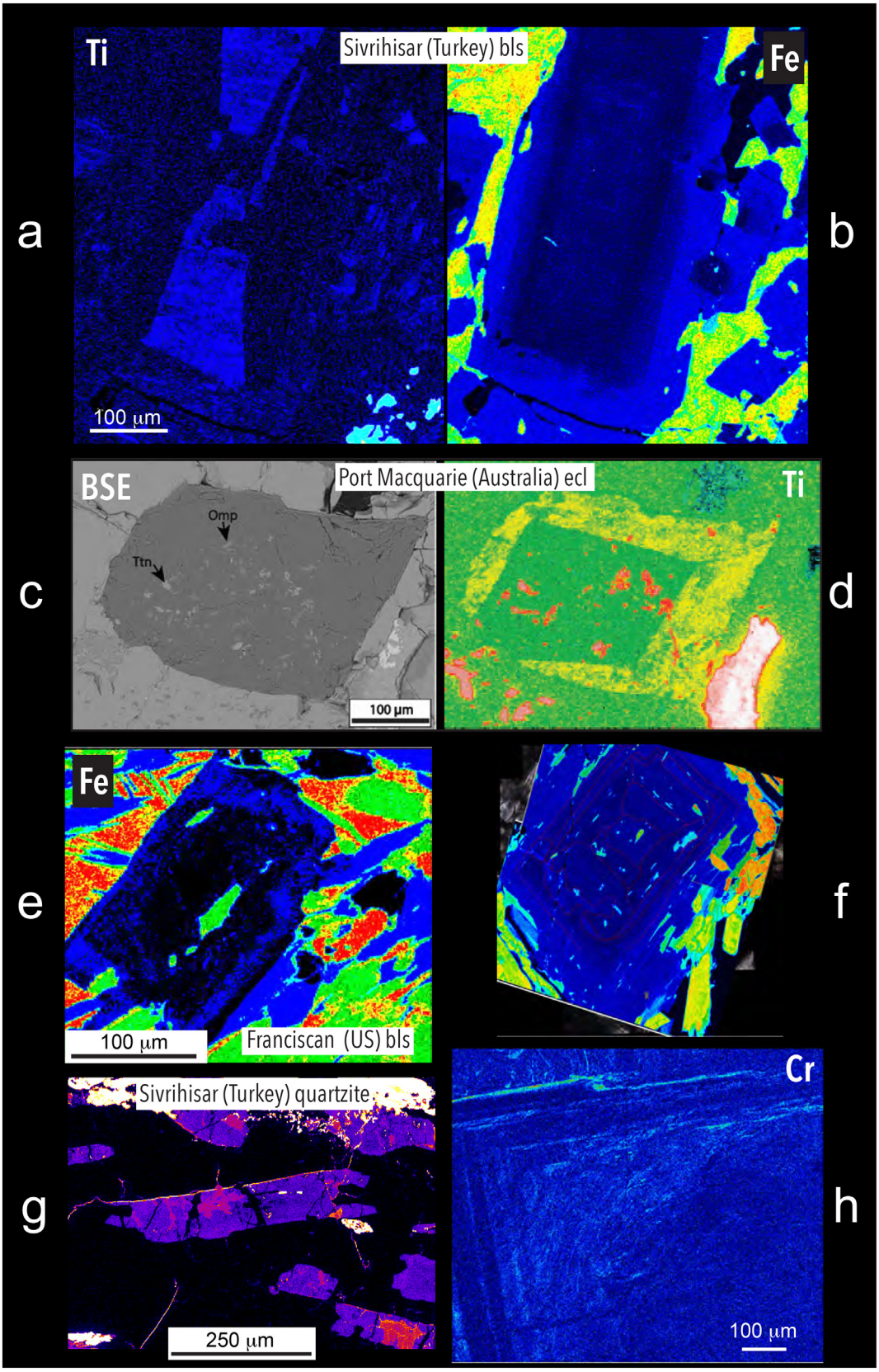

Fig. 14. Transition-element zoning in lawsonite, illustrated with false-color images obtained by electron microprobe: (a) Ti hour-glass zoning and (b) Fe concentric zoning in lawsonite from a blueschist, Sivrihisar, Turkey; (c) BSE image showing titanite and omphacite inclusions in lawsonite and (d) Ti concentric zoning in lawsonite from eclogite, Port Macquarie, Australia; (e) concentric Fe zoning, Franciscan lawsonite blueschist (North Berkeley Hills); (f) oscillatory Fe zoning in a lawsonite blueschist, Sivrihisar, Turkey; (g) patchy Fe zoning characterized by Fe-rich regions in lawsonite from quartzite, Sivrihisar, Turkey; and (h) oscillatory Cr zoning, Franciscan lawsonite blueschist.

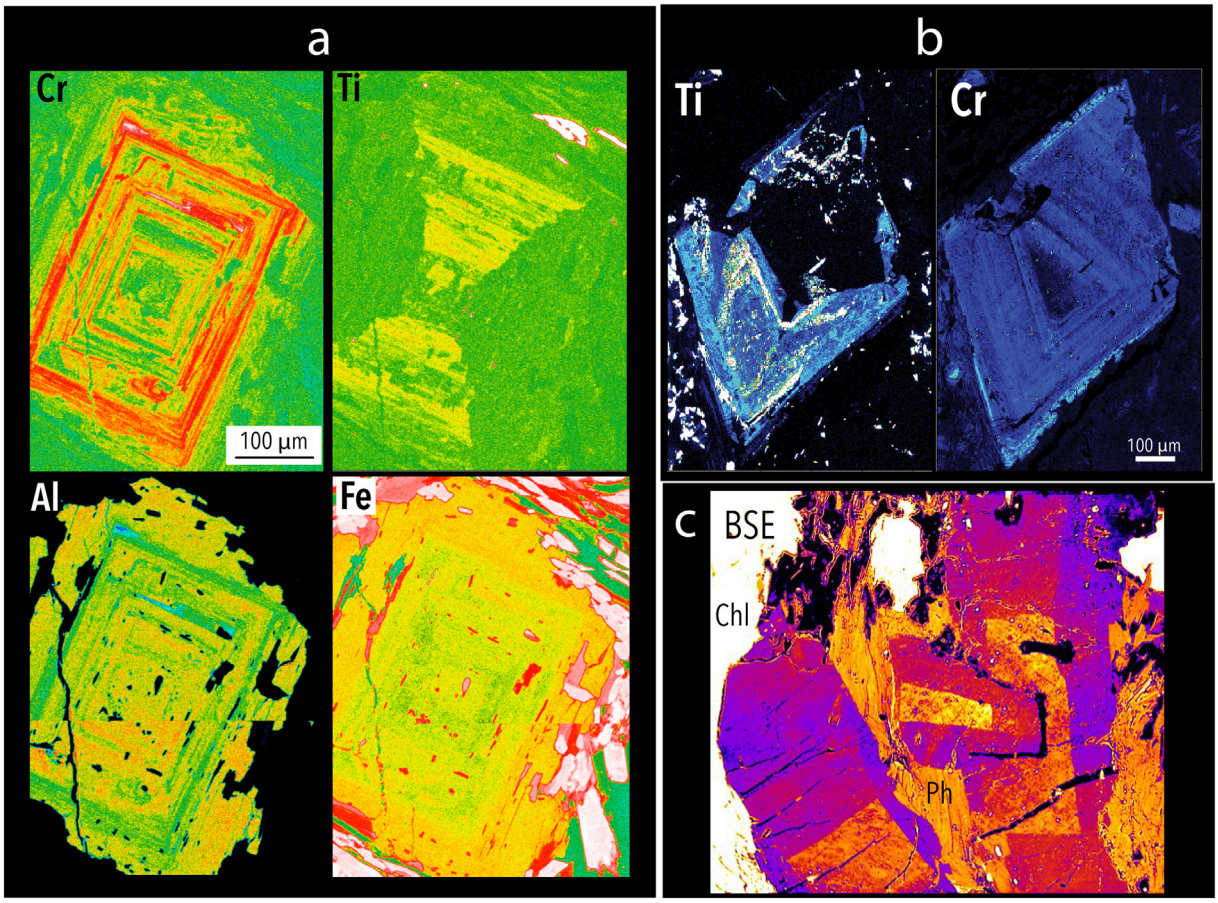

Fig. 15. Transition-element zoning in lawsonite, illustrated by false-color images obtained by electron microprobe: (a) Cr, Ti, Al, and Fe zoning in one lawsonite crystal from a blueschist, Sivrihisar, Turkey; (b) Ti and Cr zoning in a lawsonite crystal from Port Macquarie, Australia; (c) BSE image of zoned lawsonite from a metasomatized blueschist, Alpine Corsica (modified from Vitale Brovarone et al., 2014a); lawsonite crystals in this image show three distinct domains defined primarily by variation in Ti.

transition, but work in the last two decades has shown that hydrous minerals such as lawsonite and phengite may persist to great depths in eclogite and associated metasomatic rocks, and that these rocks are therefore important in ferrying large amounts of H_2O into the deep mantle (Forneris and Holloway, 2003; Ohtani et al., 2004; Poli and Schmidt, 2002).

At ~550 °C, ~2.4 GPa – i.e., conditions corresponding to the maximum depth from which oceanic rocks are typically exhumed from subduction zones (Fig. 5), HP/LT oceanic crust is predicted to have ~2 wt% H_2O (Hacker, 2008; van Keken et al., 2011). According to bulk composition measurements (e.g., loss on ignition, LOI) and estimates from mineral modes and compositions, lawsonite blueschists and eclogites commonly contain 2–7% H_2O (e.g., Coleman and Lee, 1963; Davis and Whitney, 2006; Fujimoto et al., 2010; Groppo et al., 2016; Hara et al., 2018; Sato et al., 2016; Vitale Brovarone et al., 2014a), similar to altered oceanic crust (which may also contain substantial amounts of carbonate) (Hacker et al., 2003a; Kelley et al., 2003; Peacock, 1993; Staudigel et al., 1989).

Results of a survey of ~300 HP/LT metabasaltic rocks from 30 subduction complexes (Fig. 18, Table S3) indicates that epidote blueschist and eclogite have volatile contents (inferred primarily from LOI and assumed to be dominantly H_2O) of ~2.0–2.7%, with most ranging between 0.5 and 5 wt% and with more eclogites than blueschist with <1 wt% H_2O. Lawsonite-bearing metabasites typically have higher H_2O content: most lawsonite blueschists range from ~2.5 to 8.5 wt% (a few are even more H_2O-rich), with an average of ~5%, and lawsonite eclogites range from ~1.2 to 6.4 wt% (average ~3%) (Fig. 18, Table S3). According to this dataset, most lawsonite-bearing metabasalts have more H_2O than predicted by phase equilibrium modeling.

Lawsonite-bearing metagabbro and metatroctolite (e.g., Fig. 6a) are particularly H_2O-rich (~7 wt% H_2O), even under eclogite facies conditions, because plagioclase in the protolith was converted to lawsonite. Lawsonite ± chlorite-rich metasomatic rocks are also very H_2O-rich (~5–11%; Vitale Brovarone et al., 2014a). For example, lawsonitites from Corsica contain up to 10.5 wt% H_2O (Vitale Brovarone and Beyssac, 2014). These data show how the formation of lawsonite-rich rocks facilitates the transfer of H_2O to great depths in subduction zones.

Some lawsonite eclogites have similar amounts or, in some cases, more H_2O than associated blueschists, including co-facial blueschist and eclogite in which difference in peak mineral assemblage is related to difference in bulk-composition and/or fO_2 (e.g., Fornash and Whitney, 2020). For example, the calculated difference in H_2O content of core (lawsonite eclogite) and rim (lawsonite blueschist) of metamorphosed pillow basalts in the Alpine Corsica HP/LT complex is only ~0.7% (Vitale Brovarone et al., 2011a). These observations show that the blueschist-eclogite transition is not necessarily associated with a significant loss of H_2O, particularly if there is an external source of fluids. Similar retention of H_2O in reactions involving lawsonite and chlorite has been proposed for lawsonite blueschists (Sato et al., 2016). Given the likely location of most exhumed HP/LT rocks at or near the top of the subducted slab, fluids derived by dehydration of deeper parts of the slab will infiltrate this physically and chemically dynamic part of the subduction system (e.g., Bebout, 2007; Scambelluri et al., 2001, 2015, 2019; Scambelluri and Philippot, 2001). The high H_2O content of lawsonite-bearing rocks may be an indicator of an open-system fluid regime.

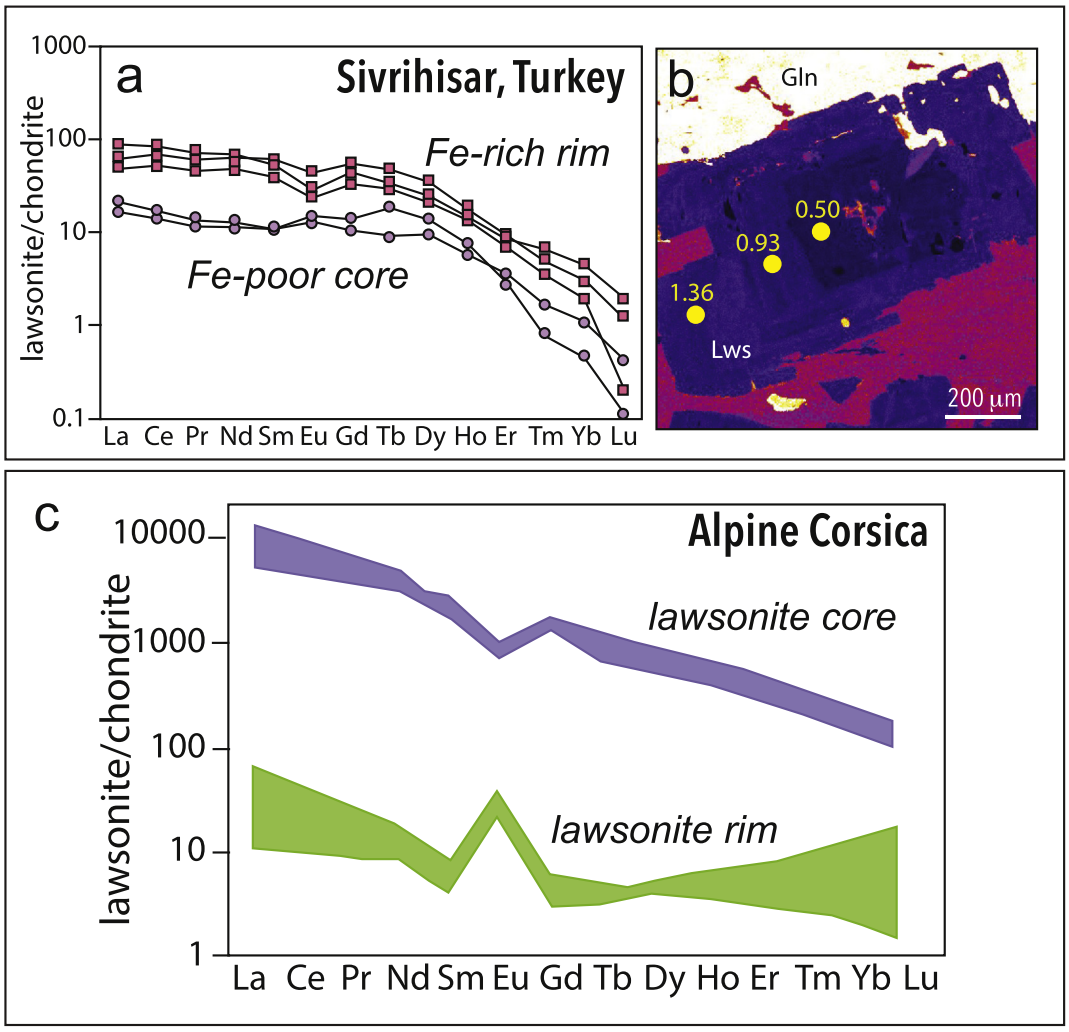

Fig. 16. (a–b) Relationship of Fe and REE zoning in lawsonite, Sivrihisar, Turkey (Fe map modified from Fornash et al. (2019)); (c) variation in REE content, including sign of the Eu anomaly, in lawsonite from a metasomatic rock (lawsonitite), Alpine Corsica; figure modified from Martin et al. (2011b).

7.2. Fluid–rock reaction in HP/LT rocks: Potential contributions of lawsonite studies

From field, experimental, and phase equilibrium-modeling studies of subduction zone P-T-X conditions, the stability of hydrous mineral-bearing assemblages in rocks with mafic, ultramafic, and sedimentary protoliths has been determined, as well as estimates of the amount of fluid released, the nature and magnitude of fluid–rock interactions (if any), the composition of fluids at HP/LT conditions, and the pathways and scales of fluid transport within the subducted slab and between

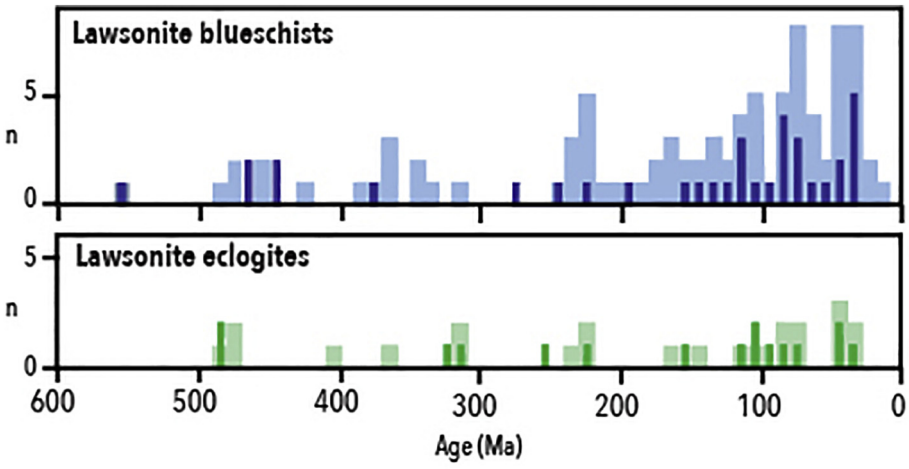

Fig. 17. Histogram showing ages of lawsonite blueschists and eclogites, based on a figure in Tsujimori and Ernst (2014) and showing their data in lighter colors and wider bars; new data are shown in the darker/narrower bars. Sources of data are in Tsujimori and Ernst (2014) and Tables 1–2 (this paper).

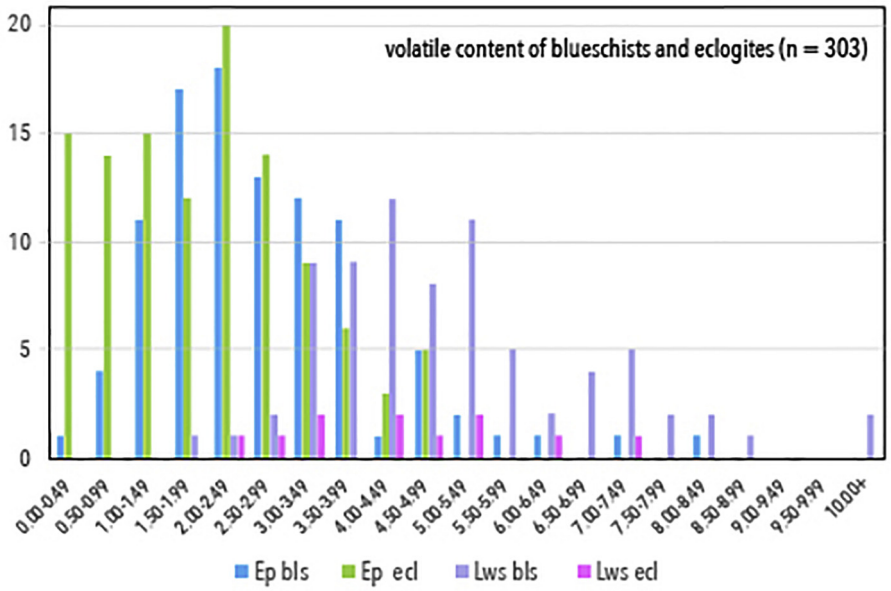

Fig. 18. Histogram showing volatile content (primarily from loss on ignition data) for epidote (Ep) and lawsonite (Lws) blueschist (bls) and eclogite (ecl). Data for this plot are in Table S3.

the slab and the mantle wedge (e.g., Bebout, 2007; Hacker, 2008; Hacker et al., 2003a; Manning, 2004; Peacock, 1993; Poli and Schmidt, 1995; Scambelluri et al., 2001; Schmidt and Poli, 1994, 1998; van Keken et al., 2011). In addition, some studies have documented trace element concentrations of HP/LT rocks to understand element cycling in subduction zones (Bebout, 2007; Bebout et al., 1999; Bebout and Barton, 1993; Becker et al., 2000; El Korh et al., 2009; Rubatto and Hermann, 2003; Rüpke et al., 2004; Sorensen et al., 1997; Spandler et al., 2011; Zack et al., 2001, 2002) or have used the trace element and isotopic compositions of arc rocks (e.g. large-ion lithophile element enrichment, high-field-strength element depletion) to evaluate fluid-related processes that occurred in the slab (Pearce, 1983; Turner et al., 1996), although comparatively few studies have focused on lawsonite-bearing rocks (e.g., Fornash et al., 2019; Martin et al., 2011b; Simons et al., 2010; Spandler et al., 2003). Documenting the composition and zoning of lawsonite in HP/LT rocks can contribute to understanding fluid–rock reaction in subduction zones because compositional characteristics can be related to P, T, and time, and because lawsonite composition may be a sensitive indicator of the source(s) of fluids involved in reactions. Tracking the composition of lawsonite in HP/LT complexes could contribute to mapping and quantifying the extent and nature of fluid–rock reaction at various scales (regional to microscale), as well as the contributions of fluids from ultramafic, mafic, and sedimentary sources (Section 7.3). For example, mapping the chemical and P-T-t conditions of lawsonite crystallization in a subduction complex could be used to track fluid pathways, including sites of significant fluid–rock interaction (metasomatic rocks, veins).

7.3. Interpretation and significance of lawsonite composition and zoning

The composition of subducted oceanic crust preserved in HP/LT terranes may be influenced by processes that occurred: (1) at or near the seafloor (e.g. hydrothermal alteration, which may be localized or pervasive); (2) during prograde metamorphic processes (e.g. interaction with fluids derived from sediments and/or ultramafic rocks in the accretionary wedge, at the slab-mantle interface, or at deeper levels of the subducted slab); (3) at or near the maximum depth attained during subduction (e.g. by interaction with fluids derived from dehydrating rocks at depth in the slab, or by interaction with mantle-wedge serpentinites or interlayered sediments – as in the prograde case); and/or (4) during exhumation (e.g. retrograde hydration of eclogite to blueschist, greenschist, or amphibolite). In most of these cases, changes to rock and mineral composition are related to de/hydration reactions, although it has been proposed that changes in major and trace element composition may be decoupled from volatile cycling (e.g. Spandler et al., 2003).

Some blueschists and eclogites show compelling evidence for interaction with ultramafic or sedimentary host rocks, for example, as seen in large-ion lithophile element (LILE) (K, Ba, Rb, Cs) enrichment in HP/LT rocks that have interacted with subducted sediment in mélange (e.g., Sorensen et al., 1997) or enrichment of HP vein minerals in elements that are characteristic of ultramafic rocks (Cr, Ni) (Spandler et al., 2011). Lawsonite composition and zoning record many of these processes, including sources of metamorphic fluids. The substitution of elements for Ca and Al in lawsonite – transition elements, REE, and other trace elements – and the concentration and variation of elements in several isotopic systems are the basis for the utility of lawsonite as an indicator of subduction zone processes involving fluids at forearc to subarc depths.

Composition and zoning in lawsonite have been related to textural observations such as inclusion distribution to interpret whether lawsonite grew during prograde, peak, or retrograde metamorphism. In some cases, compositional and textural change in lawsonite may indicate a change in mineral assemblage in the host rock, such as occurs during a prograde change from blueschist to eclogite or retrograde transformation of eclogite to blueschist (e.g., Martin et al., 2011a; Vitale Brovarone et al., 2014a). For example, in the Alpine Corsica HP/LT complex, lawsonite crystals record three (blueschist) to four (eclogite) compositional and textural growth zones (Fig. 15c). In some zoned lawsonite, inclusion-rich and inclusion-poor regions correspond to compositional domains, and in others, inclusion-rich regions do not correspond to compositional zoning.

Although more work is needed to understand the parameters that control lawsonite composition and zoning (including fO_2 and crystallographic effects), existing studies of element zoning in lawsonite demonstrate that it is a sensitive indicator of reaction history as well as of the possible source(s) of fluids that reacted with minerals under HP conditions, and can be used to track changes as a function of changing P-T conditions. In order to relate lawsonite composition to conditions, it is essential to assess whether lawsonite grew during prograde, peak, or

retrograde metamorphism. This can be done qualitatively using textural (petrographic) observations, and is ideally complemented by geochronology, including the use of isotopic systems such as Lu-Hf that involve analysis of lawsonite and other minerals (or regions of zoned minerals) that are part of the eclogite or blueschist facies assemblage.

7.4. Fluid–rock interaction in mélange vs. coherent terranes

Lawsonite-bearing eclogite and blueschist facies rocks occur in mélange (used here to indicate a mixture of rock types and facies, typically in a matrix of serpentinite or (meta)sediment) and in more structurally-coherent terranes (typically consisting of interlayered slices of different rock types on the scale of hundreds of meters to kilometers). Most HP/LT terranes contain both coherent and mélange domains, and many are overall dominated by structurally-coherent regions (e.g., Franciscan; Alpine Corsica; Tavşanlı Zone, Turkey; Elekdağ Massif, Central Pontides, Turkey; Diahot and most of the Pouebo terranes, New Caledonia). A significant part of the slab-mantle interface under eclogite and blueschist-facies conditions is characterized by large-scale layers and slices of metamorphosed oceanic crust and associated sediment rather than a mixture of rock types that record different P-T conditions. In HP/LT complexes comprised of large-scale slices in tectonized zones, the distinction between a mélange and a coherent terrane is somewhat arbitrary, as there is an overall structural coherence (i.e., the complex is not a chaotic mixture of blocks) but some displacement and mixing may have occurred, particularly if serpentinite and/or schist is present. Coherent terranes may also bear some resemblance to mélange when metabasaltic rocks are substantially retrogressed (eclogite to blueschist, or eclogite and blueschist to chlorite–actinolite), resulting in blocks of eclogite and/or blueschist in a highly deformed matrix, as occur in local regions of New Caledonia, Port Macquarie, and Sivrihisar.

Of the eight known tectonically-exhumed eclogites (i.e., excluding the Garnet Ridge xenolith) that contain fresh matrix lawsonite, four are in mélange, three are in coherent complexes, and one (Pinchi Lake, BC) is ambiguous because eclogite blocks occur in glacial deposits (although the blueschist part of the sequence is coherent and the eclogite unit has been interpreted as a mélange by Ghent et al., 1993) (Table 1). Three of the four eclogite-bearing mélanges are in Pacific or Caribbean terranes, as is one of the coherent terranes (Ward Creek, Franciscan).

There are no discernible trends in P-T conditions of mélange vs. coherent eclogite or blueschist (Fig. 5), and both coherent terranes and mélange contain metasomatic rocks and HP veins. Lawsonite abundance and characteristics (composition, zoning) also indicate no significant difference in degree of metasomatism or other indicators of fluid–rock interaction between the two types of terranes, at least under lawsonite-stable conditions. Both types of terrane record extensive interaction of different rock types (mafic, sedimentary, ultramafic) as indicated by lawsonite composition and zoning. This likely reflects the fact that both types of terranes, whether largely coherent or largely disaggregated, were exhumed from the slab-mantle interface, the site of significant fluid–rock interaction.

7.5. The record and interpretation of subduction P-T conditions

The observation that most lawsonite eclogites record maximum P-T conditions at or near the global decoupling depth (~80 ± 5 km; Fig. 5) may indicate that the transition from a decoupled to coupled slab-mantle interface induces exhumation at that point. Exhumation occurs under warm (epidote) or cool (lawsonite) conditions depending on the dynamics of the exhuming terrane relative to the rest of the subducting slab.

Although P-T paths of subduction and exhumation may be confined entirely to the lawsonite stability field, it is common for lawsonite in eclogites and blueschists to occur in the same terrane – or even the same rock – with epidote-group minerals that indicate a different (warmer) thermal setting than the lawsonite-bearing assemblage. For example, in the HP/LT complex of New Caledonia, lawsonite occurs in the matrix of low-grade blueschists and is joined by epidote in higher-grade blueschists (both in the Diahot terrane), in some cases occurring as inclusions in epidote (Fig. 10f). In the adjacent Pouebo terrane, lawsonite occurs only locally as inclusions in garnet in eclogites that contain epidote and/or Ca-rich amphibole in the matrix (e.g., Clarke et al., 1997). P-T modeling of the eclogites indicates that maximum pressures and corresponding temperatures were in the lawsonite stability field; the lack of matrix lawsonite in eclogite is the result of exhumation through the epidote-stability field at temperatures higher than the conditions of prograde metamorphism (Vitale Brovarone and Agard, 2013). Widespread retrograde epidote-group mineral formation also occurs in other lawsonite eclogites (e.g. Port Macquarie, Australia, mélange; Garnet Ridge xenolith). The relative lack of fresh lawsonite in eclogite globally is likely related in part to the prevalence of exhumation through the epidote stability field. Although pseudomorphed lawsonite is primarily replaced by hydrous minerals (paragonite, epidote, chlorite), retrogression is driven by P-T changes, not by introduction of fluids; lawsonite eclogites and blueschists that have interacted with fluids that drove retrogression of garnet (e.g., replacement by chlorite) will retain fresh lawsonite if retrograde metamorphism occurred under low temperature conditions (Fig. 4d).

P-T paths in subduction metamorphism may be 'counterclockwise' (i.e., relative to P-T coordinates such as those in Fig. 5) (e.g., South American Cordillera: Willner et al., 2004; Franciscan: Krogh et al., 1994; Sivrihisar: Davis and Whitney, 2006, 2008), in some cases indicating a transition from epidote to lawsonite, such as may occur by continued subduction of colder rocks below a detached slice. This transition may be preserved as epidote inclusions in garnet in a blueschist or eclogite with matrix lawsonite. In such cases, it is important to determine what part of the P-T path is recorded, so as to understand the thermal evolution of the exhumed HP/LT rocks and therefore the subduction zone.

The P-T path of a rock, including conditions of retrogression, may affect the recorded conditions – and, as is true for many metamorphic rocks, different thermobarometric methods may produce different results – leading to some uncertainty about the estimated maximum depth and corresponding temperature. The broad scatter in conditions recorded by lawsonite blueschist (Fig. 5), including some that record conditions beyond the experimentally-determined upper stability limit of lawsonite, may to some extent reflect this uncertainty and/or the effects of retrograde heating during exhumation. There is less scatter in conditions recorded by lawsonite eclogite: most experienced peak conditions between 2.4 and 2.5 GPa and 500 ± 50 °C, corresponding well with modeled slab thermal conditions (Fig. 5) and perhaps indicating preferential exhumation and preservation associated with the maximum decoupling depth of subduction zones, a point beyond which tectonic exhumation and/or preservation of eclogite is unlikely (Whitney et al., 2014).

In recent years, there has been much discussion of the observation that many exhumed HP/LT rocks apparently record higher temperatures than predicted by thermal models (Penniston-Dorland et al., 2015). Indeed, even with a revised P-T dataset that includes more lawsonite eclogites (e.g., Port Macquarie, Australia; central Pontides, Turkey) and that excludes rocks that experienced ultrahigh-pressure conditions of continental subduction (Table S4), results show that most blueschist-facies rocks record higher-temperature conditions than modeled slab-surface temperatures for a typical (normal/cold) subduction zone (e.g., Syracuse et al., 2010) (Fig. 19). However, it is interesting that a majority of HP/LT rocks plot in the lawsonite stability field (>3x as many as in the epidote stability field, though results vary depending on which lawsonite-out reaction is assumed). In addition, most lawsonite eclogites – and all but one with fresh matrix lawsonite – plot in the realm of modeled slab conditions (Figs. 5, 19). Furthermore, some subduction complexes containing high-temperature rocks

(600–700 °C) also contain very-low-temperature rocks, including lawsonite eclogite (e.g., Rio San Juan/Samaná Complex, Dominican Republic), indicating that the thermal conditions of the material exhumed from the subduction zone varied considerably in time and/or space.

8. Suggestions for future research

To make progress with developing lawsonite as a tool for understanding subduction zone processes and evaluating the contributions of fluids from different chemical sources to element cycling and mantle redox conditions, it will be useful to:

(1) **acquire major and trace element data from lawsonite** from more terrains with different structural settings (mélange, coherent), P-T conditions, and geochemical contexts, accompanied by a thorough assessment of whether lawsonite is prograde, peak, or retrograde. Of particular utility are data from terrains with multiple generations of lawsonite in associated rocks, such as lawsonite inclusions, matrix lawsonite, and lawsonite-bearing veins, as well as compositional data from other minerals. When analyzing lawsonite by electron microprobe, it is important to take into account the beam-sensitivity of the mineral, to analyze for Fe, Ti, and Cr, and – although likely not present – to analyze for Mn, Mg, Na, and K as a means of evaluating interference with adjacent/host phases (e.g., Mn from garnet; Na or K from white mica).

(2) **obtain microstructural data for lawsonite**, including systematic study of the crystallographic preferred orientation (CPO) of lawsonite in different rock types recording eclogite- and blueschist-facies conditions, for better understanding of the rheology and geophysical properties and dynamics of subducted oceanic crust at forearc to subarc depths. Electron back-scatter diffraction (EBSD) analysis of lawsonite CPO should be accompanied by information about the overall mineral assemblage (including mode) and an evaluation of the fabric data in the context of textural generation of lawsonite and P-T path. Comprehensive, high-quality datasets that integrate composition with microstructure allow evaluation of the parameters that control trace-element incorporation in lawsonite (crystallographic effects, P-T-X conditions – including fO_2).

(3) **conduct radiogenic isotopic studies of lawsonite**, including development of lawsonite geochronometers, ideally with *in situ* methods, leading to better integration of lawsonite data with other geo/petrochronometers such as those involving garnet, rutile, and/or titanite. As with other compositional analyses of lawsonite, it is important to consider zoning and the interpretation of lawsonite in the context of P-T conditions and path.

(4) **develop methods for stable isotopic (O, H) analysis of lawsonite**, as results could be used to aid interpretation of fluid sources involved in lawsonite growth and fluid–rock reactions in subduction zones (e.g., Kang et al., 2019). In this case, too, lawsonite zoning and P-T conditions/reaction history should be considered, as well as the effects of protolith composition, including those related to seafloor alteration.

Lawsonite has the potential to be a powerful new petrochronometer for subduction processes that are recorded in exhumed HP/LT rocks. Lawsonite composition, zoning, microstructure, and age provide significant information that can be linked to prograde, peak, and retrograde metamorphism to document the conditions, mechanisms, and magnitude of water and element cycling between the subducted plate and overlying mantle, including the contribution of subducted slabs to mantle redox conditions.

Supplementary data to this article can be found online at https://doi.org/10.1016/j.lithos.2020.105636.

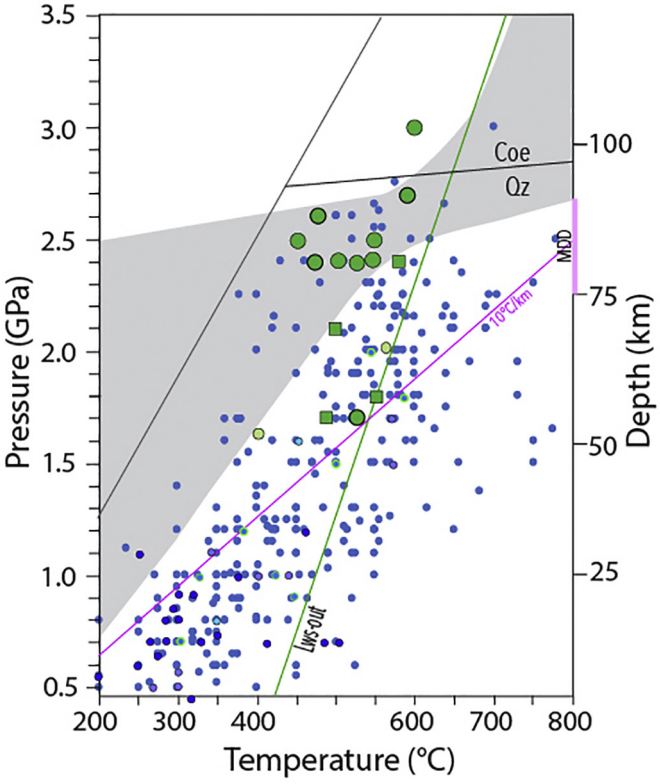

Fig. 19. P-T diagram showing recorded conditions of HP/LT rocks exhumed from oceanic subduction complexes (small blue dots; dataset of Penniston-Dorland et al. (2015), with addition of lawsonite eclogites in this compilation and other data from the literature and subtraction of continental subduction rocks; Table S4). Lawsonite eclogites and blueschists of this paper's compilation are highlighted using the same symbols used in Fig. 5. Also shown are the slab-surface conditions of Syracuse et al. (2010), the maximum decoupling depth (MDD) of Wada and Wang (2009), and the lawsonite-out reaction of Schmidt (1995).

Declaration of Competing Interests

The authors declare that they have no known competing financial interests or personal relationships that could have appeared to influence the work reported in this paper.

Acknowledgements

We thank the following colleagues for sharing lawsonite-bearing samples: Carly Faber (Yukon), George Harlow (Guatemala), Sean Mulcahy (Franciscan), Tatsuki Tsujimori (Franciscan, Guatemala), and Richard Palin and David Hernandez-Uribe (Garnet Ridge). Constructive reviews by Zeb Page and Ethan Baxter helped us improve the manuscript, and we also appreciate the editorial advice of Marco Scambelluri. This research has been supported by the University of Minnesota Grant-in-Aid program and NSF grant EAR-1949895 to D.L. Whitney.

References

Abers, G.A., van Keken, P.E., Kneller, E.A., Ferris, A., Stachnik, J.C., 2006. The thermal structure of subduction zones constrained by seismic imaging: Implications for slab dehydration and wedge flow. Earth Planet. Sci. Lett. 241, 387–397.

Agard, P., Labrousse, L., Elvevold, S., Lepvrier, C., 2005. Discovery of Paleozoic Fe-Mg carpholite in Motalafjella, Svalbard Caledonides: A milestone for subduction gradients. Geology 33, 761–764. https://doi.org/10.1130/G21693.1.

Agard, P., Monié, P., Gerber, W., Omrani, J., Molinaro, M., Meyer, B., Yamato, P., 2006. transient, synobduction exhumation of Zagros blueschists inferred from P-T, deformation, time, and kinematic constraints: Implications for Neotethyan wedge dynamics. J. Geophys. Res. 111, B11401. https://doi.org/10.1029/2005JB004103.

Agard, P., Yamato, P., Jolivet, L., Burov, E., 2009. Exhumation of oceanic blueschists and eclogites in subduction zones: Timing and mechanisms. Earth Sci. Rev. 92, 53–79.

Altherr, R., Topuz, G., Marschall, H., Zack, T., Ludwig, T., 2004. Evolution of a tourmaline-bearing lawsonite eclogite from the Elekdağ area (Central Pontides, N Turkey): Evidence for infiltration of slab-derived B-rich fluids during exhumation. Contrib. Mineral. Petrol. 148, 409–425.

Angiboust, S., Agard, P., Raimbourg, H., Yamato, P., Huet, B., 2011. Subduction interface processes recorded by eclogite-facies shear zones (Monviso, W. Alps). Lithos 127, 222–238.

Angiboust, S., Langdon, R., Agard, P., Waters, D., Chopin, C., 2012. Eclogitization of the Monviso ophiolite (W. Alps) and implications on subduction dynamics. J. Metamorph. Geol. 30, 37–61. https://doi.org/10.1111/j.1525-1314.2011.00951.x.

Angiboust, S., Agard, P., Glodny, J., Omrani, J., Oncken, O., 2016. Zagros blueschists: Episodic underplating and long-lived cooling of a subduction zone. Earth Planet. Sci. Lett. 443, 48–58. https://doi.org/10.1016/j.epsl.2016.03.017.

Ao, A., Bhowmik, S.K., 2014. Cold subduction of the Neotethys: the metamorphic record from finely banded lawsonite and epidote blueschists and associated metabasalts of the Nagaland Ophiolite Complex, India. J. Metamorph. Geol. 32, 829–860.

Balllevre, M., Pitra, P., Bohn, M., 2003. Lawsonite growth in the epidote blueschists from the Ile de Groix (Armorican Massif, France): a potential geobarometer. J. Metamorph. Geol. 21, 723–735.

Baziotis, I., Proyer, A., Mposkos, E., Windley, F.B., Boukouvala, I., 2019. Exhumation of the high-pressure northwestern Cyclades, Aegean: New P-T constraints, and geodynamic evolution. Lithos 324, 439–453. https://doi.org/10.1016/j.lithos.2018.11.027.

Bebout, G.E., 1991. Field-based evidence for devolatilization in subduction zones: Implications for arc magmatism. Science 251, 413–416.

Bebout, G.E., 2007. Metamorphic chemical geodynamics of subduction zones. Earth Planet. Sci. Lett. 260, 373–393.

Bebout, G.E., Barton, M.D., 1993. Metasomatism during subduction – products and possible paths in the Catalina Schist, California. Chem. Geol. 108, 61–92.

Bebout, G.E., Ryan, J.G., Leeman, W.P., Bebout, A.E., 1999. Fractionation of trace elements by subduction zone metamorphism: Effect of convergent margin thermal evolution. Earth Planet. Sci. Lett. 171, 63–81.

Becker, H., Jochum, K.P., Carlson, R.W., 2000. Trace element fractionation during dehydration of eclogites from high-pressure terranes and the implications for element fluxes in subduction zones. Chem. Geol. 163, 65–99.

Bezacier, L., Reynard, B., Bass, J.D., Wang, J., Mainprice, D., 2010. Elasticity of glaucophane, seismic velocities and anisotropy of the subducted oceanic crust. Tectonophysics 494, 201–210.

Boffa Ballaran, T.B., Angel, R.J., 2003. Equation of state and high-pressure phase transitions in lawsonite. Eur. J. Mineral. 15 (2), 241–246. https://doi.org/10.1127/0935-1221/2003/0015-0241.

Brown, E.H., O'Neil, J.R., 1982. Oxygen isotope geothermometry and stability of lawsonite and pumpellyite in the Shuksan Suite, North Cascades, Washington. Contrib. Mineral. Petrol. 80, 240–244.

Cao, Y., Jung, H., 2016. Seismic properties of subducting oceanic crust: Constraints from natural lawsonite-bearing blueschist and eclogite in Sivrihisar Massif, Turkey. Phys. Earth Planet. Inter. https://doi.org/10.1016/j.pepi.2015.10.003.

Cao, Y., Jung, H., Song, S., 2013. Petro-fabrics and seismic properties of blueschist and eclogite in the North Qilian suture zone, NW China: implications for the low-velocity upper layer in subducting slab, trench-parallel seismic anisotropy and eclogite detectability in the subduction zone. J. Geophys. Res. Solid Earth 118, 3037–3058.

Cao, Y., Jung, H., Song, S., 2014. Microstructures and petro-fabrics of lawsonite blueschist in the North Qilian suture zone, NW China: Implications for seismic anisotropy of subducting oceanic crust. Tectonophysics. https://doi.org/10.1016/j.tecto.2014.04.028.

Caron, J.-M., Péquignot, G., 1986. The transition between blueschists and lawsonite-bearing eclogites based on observations from Corsican metabasalts. Lithos 19, 205–218.

Chinnery, N., Pawley, A.R., Clark, S.M., 2000. The equation of state of lawsonite to 7 GPa and 873 K, and calculation of its high pressure stability. Am. Mineral. 85, 1001–1008.

Clarke, G.L., Aitchison, J.C., Cluzel, D., 1997. Eclogites and blueschists of the Pam Peninsula, NE New Caledonia: A reappraisal. J. Petrol. 38, 843–876.

Clarke, G.L., Powell, R., Fitzherbert, J.A., 2006. The lawsonite paradox: A comparison of field evidence and mineral equilibria modeling. J. Metamorph. Geol. 24, 715–725.

Coleman, R.G., Lee, D.E., 1963. Glaucophane-bearing metamorphic rock types of the Cazadero Area, California. J. Petrol. 4, 260–301.

Collins, N.C., Bebout, G.E., Angiboust, S., Agard, P., Scambelluri, M., Crispini, L., John, T., 2015. Subduction zone metamorphic pathway for deep carbon cycling: II. Evidence from HP/UHP metabasaltic rocks and ophicarbonates. Chem. Geol. 412, 132–150. https://doi.org/10.1016/j.chemgeo.2015.06.012.

Comodi, P., Zanazzi, P.F., 1996. Effects of pressure and temperature on the structure of lawsonite. Am. Mineral. 81, 833–841.

Cordova, J.L., Mulcahy, S.R., Schermer, E.R., Webb, L.E., 2019. Subduction initiation and early evolution of the Easton metamorphic suite, northwest Cascades, Washington. Lithosphere 11, 44–58.

Cotkin, S.J., Cotkin, M.L., Armstrong, R.L., 1993. Early Paleozoic blueschist from the schist of Skookum Gulch, Eastern Klamath Mountains, Northern California. J. Geol. 100, 323–338.

Daniel, I., Fiquet, G., Gillet, P., Schmidt, M.W., Hanfland, M., 2000. High-pressure behavior of lawsonite: A phase transition at 8.6 GPa. Eur. J. Mineral. 12 (4), 721–733. https://doi.org/10.1127/0935-1221/2000/0012-0721.

Davis, G.A., Pabst, A., 1960. Lawsonite and pumpellyite in glaucophane schist, North Berkeley Hills, California, with notes on the X-ray crystallography of lawsonite. Am. J. Sci. 258, 689–704.

Davis, P.B., Whitney, D.L., 2006. Petrogenesis of lawsonite and epidote eclogites and blueschist, Sivrihisar Massif, Turkey. J. Metamorph. Geol. 24, 823–849. https://doi.org/10.1111/j.1525-1314.2006.00671.x.

Davis, P.B., Whitney, D.L., 2008. Petrogenesis and structural petrology of high-pressure metabasalt pods, Sivrihisar, Turkey. Contrib. Mineral. Petrol. 156, 217–241. https://doi.org/10.1007/s00410-008-0282-4.

de Jong, K., Xiao, W., Windley, B.F., Masago, H., Lo, C.-H., 2006. Ordovician ^{40}Ar-^{39}Ar phengite ages from the blueschist-facies Ondor Sum subduction-accretion complex (Inner Mongolia) and implications for the Early Paleozoic history of continental blocks in China and adjacent areas. Am. J. Sci. 306, 799–845.

Domanik, K.J., Holloway, J.R., 1996. The stability and composition of phengitic muscovite and associated phases from 5.5 to 11 GPa: Implications for deeply subducted sediments. Geochim. Cosmochim. Acta 60, 4133–4150.

Du, J.X., Zhang, L.F., Bader, T., Chen, Z.Y., Lu, Z., 2014. Metamorphic evolution of relict lawsonite-bearing eclogites from the (U)HP metamorphic. belt in the Chinese southwestern Tianshan. J. Metamorph. Geol. 32, 575–598. https://doi.org/10.1111/jmg.12080.

El Korh, A., Schmidt, S.T., Ulianov, A., Potel, S., 2009. Trace element partitioning in HP-LT metamorphic assemblages during subduction-related metamorphism, Ile de Groix, France: A detailed LA-ICPMS study. J. Petrol. 50, 1107–1148.

El-Shazly, A.K., 1994. Petrology of lawsonite-, pumpellyite- and sodic amphibole-bearing metabasaites from north-east Oman. J. Metamorph. Geol. 12, 23–48.

Endo, S., Wallis, S.R., 2017. Structural architecture and low-grade metamorphism of the Mikabu-Northern Chichibu accretionary wedge, SW Japan. J. Metamorph. Geol. 35, 695–716. https://doi.org/10.1111/jmg.12251.

Endo, S., Wallis, S.R., Tsbuoi, M., De Leon, R.T., Solari, L.A., 2012. Metamorphic evolution of lawsonite eclogites from the southern Motagua fault zone, Guatemala: Insights from phase equilibria and Raman spectroscopy. J. Metamorph. Geol. 30, 143–164.

Escuder-Viruete, J., Pérez-Estaún, A., 2006. Subduction-related P–T path for eclogites and garnet glaucophanites from the Samaná Peninsula basement complex, northern Hispaniola. Int. J. Earth Sci. 95, 995–1017. https://doi.org/10.1007/s00531-006-0079-5.

Evans, B.W., 1990. Phase relations of epidote-blueschists. Lithos 25, 3–23.

Faber, C., Rowe, C.D., 2019. Late Permian cold subduction in the Yukon-Tanana Terrane, Yukon Territory, Canada: Progressive eclogitization in the lawsonite stailbty field recorded by lawsonite and garnet inclusions in garnet. American Geophysical Union Fall Meeting Abstract V51B-02.

Fedele, L., Tramparulo, F.D.A., Vitale, S., Cappelletti, P., Prinzi, E.P., Mazzoli, S., 2018. Petrogenesis and deformation history of the lawsonite-bearing blueschist facies metabasalts of the Diamante-Terranova oceanic unit (southern Italy). J. Metamorph. Geol. 36, 691–714. https://doi.org/10.1111/jmg.12303.

Fitzherbert, J.A., Clarke, G.L., Powell, R., 2005. Preferential retrogression of high-P metasediments and the preservation of blueschist to eclogite facies metabasite during exhumation, Diahot terrane, NE New Caledonia. Lithos 83, 67–96.

Forbes, R.B., Evans, B.W., Thurston, S.P., 1984. Regional progressive high-pressure metamorphism: Seward Peninsula, Alaska. J. Metamorph. Geol. 2, 43–54.

Fornash, K.F., Whitney, D.L., 2020. Lawsonite-rich layers as records of fluid and element mobility in subducted crust (Sivrihisar Massif, Turkey). Chem. Geol. 533. https://doi.org/10.1016/j.chemgeo.2019.119356.

Fornash, K., Cosca, M., Whitney, D., 2016. Tracking the timing of subduction and exhumation using $^{40}Ar/^{39}Ar$ phengite ages in blueschist and eclogite facies rocks (Sivrihisar, Turkey). Contrib. Mineral. Petrol. 171 (7). https://doi.org/10.1007/s00410-016-1268-2 Article No. 67.

Fornash, K.F., Whitney, D.L., Seaton, N.C.A., 2019. Lawsonite composition and zoning as an archive of metamorphic processes in subduction zones. Geosphere 15, 24–46. https://doi.org/10.1130/GES01455.1.

Forneris, J.F., Holloway, J.R., 2003. Phase equilibria in subducting basaltic crust: Implications for H_2O release from the slab. Earth Planet. Sci. Lett. 214, 187–201.

Fujimoto, Y., Kono, Y., Hirajima, T., Kanagawa, K., Ishikawa, M., Arima, M., 2010. P-wave velocity and anisotropy of lawsonite and epidote blueschists: constraints on water transportation along subducting oceanic crust. Phys. Earth Planet. Inter. 183, 219–228.

Gao, X.Y., Zheng, Y.-F., Chen, Y.-X., 2012. Dehydration melting of ultrahigh-pressure eclogite in the Dabie orogen: Evidence from multiphase solid inclusions in garnet. J. Metamorph. Geol. 30, 193–212.

Garcia Casco, A., Torres-Roldan, R.L., Iturralde-Vinent, M.A., Millan, G., Nunez Cambra, K., Lazaro, C., Rodriguez Vega, A., 2006. High pressure metamorphism of ophiolites in Cuba. Geodin. Acta 4, 63–88.

George, A., Grapes, R., 1987. Lawsonite-bearing veins in Torlesse rocks. New Zealand. J. Geol. Geophys. 30, 203–205.

Gerrits, A.R., Inglis, E.C., Dragovic, B., Starr, P.G., Baxter, E.F., 2019. Release of oxidizing fluids in subduction zones recorded by iron isotope zonation in garnet. Nat. Geosci. 12, 1029–1033. https://doi.org/10.1038/s41561-019-0471-y.

Gerya, T.V., Stöckhert, B., Perchuk, A.L., 2002. Exhumation of high-pressure metamorphic rocks in a subduction channel: A numerical simulation. Tectonics 21, 1–15. https://doi.org/10.1029/2002TC001406.

Ghent, E.D., Stout, M.Z., Erdmer, P., 1993. Pressure-temperature evolution of lawsonite-bearing eclogites, Pinchi Lake, British Columbia. J. Metamorph. Geol. 11, 279–290.

Ghent, E.D., Erdmer, P., Archibald, D.A., Stout, M.Z., 1996. Pressure-temperature and tectonic evolution of Triassic lawsonite-aragonite blueschists from Pinchi Lake, British Columbia. Can. J. Earth Sci. 33, 800–810.

Ghent, E., Tinkham, D., Marr, R., 2009. Lawsonite eclogites from the Pinchi Lake area, British Columbia—new P–T estimates and interpretation. Lithos 109, 248–253.

Gibbons, W., Mann, A., 1983. Pre-Mesozoic lawsonite in Anglesey, northern Wales: Preservation of ancient blueschist. Geology 11, 3–6.

Grevel, K.-D., Schoenitz, M., Skrok, V., Navrotsky, A., Schreyer, W., 2001. Thermodynamic data of lawsonite and zoisite in the system CaO-Al_2O_3-SiO_2-H_2O based on experimental phase equilibria and calorimetric work. Contrib. Mineral. Petrol. 142, 298–308.

Groppo, C., Castelli, D., 2010. Prograde P-T evolution of a lawsonite eclogite from the Monviso meta-ophiolite (Western Alps): Dehydration and redox reactions during subduction of oceanic FeTi-oxide gabbro. J. Petrol. 51, 2489–2514.

Groppo, C., Rolfo, F., Sachan, H.K., Rai, S.K., 2016. Petrology of blueschist from the Western Himalaya (Ladakh, NW India): Exploring the complex behavior of a lawsonite-

bearing system in a paleo-accretionary settings. Lithos 252-253, 41–56. https://doi.org/10.1016/j.lithos.2016.02.014.
Guo, S., Ye, K., Wu, T.F., Chen, Y., Yang, T.H., Zhang, L.M., Liu, J.B., Mao, Q., Ma, Y.G., 2013. A potential method to confirm the previous existence of lawsonite in eclogite: The mass imbalance of Sr and LREEs in multistage epidote (Ganghe, Dabie UHP terrane). J. Metamorph. Geol. 31, 415–435. https://doi.org/10.1111/jmg.12027.
Hacker, B., 2008. H_2O subduction beyond arcs. Geochem. Geophys. Geosyst. 9 (3), Q03001.
Hacker, B.R., Abers, G.A., Peacock, S.M., 2003a. Subduction factory. 1. Theoretical mineralogy, densities, seismic wave speeds, and H_2O contents. J. Geophys. Res. 108, 2029.
Hacker, B.R., Peacock, S.M., Abers, G.A., Holloway, S.D., 2003b. Subduction factory. 2. Are intermediate-depth earthquakes in subducting slabs linked to metamorphic dehydration reactions? J. Geophys. Res. 108, 2030.
Hamelin, C., Brady, J.B., Cheney, J.T., Schumacher, J.C., Able, L.M., Sperry, A.J., 2018. Pseudomorphs after lawsonite from Syros, Greece. J. Petrol. 59, 2353–2383.
Hannula, K.A., McWilliams, M.O., 1995. Reconsideration of the age of blueschist facies metamorphism on the Seward Peninsula, Alaska, based on phengite ^{40}Ar-^{39}Ar results. J. Metamorph. Geol. 13, 125–139.
Hara, T., Tsujimori, T., Chang, Q., Kimura, J.-I., 2018. In situ Sr-Pb isotope geochemistry of lawsonite: A new method to investigate slab fluids. Lithos 320-321, 93–104.
Harlow, G.E., Sisson, V.B., Lallemant, H.G.A., Sorensen, S.S., Seitz, R., 2003. High pressure, metasomatic rocks along the Motagua fault zone, Guatemala. Ofioliti 28, 115–120.
Harlow, G.E., Hemming, S.R., Lallemant, H.G.A., Sisson, V.B., Sorensen, S.S., 2004. Two high-pressure-low-temperature serpentinite-matrix melange belts, Motagua fault zone, Guatemala: A record of Aptian and Maastrichtian collisions. Geology 32, 17–20.
Hernández-Uribe, D., Palin, R.M., 2019. Catastrophic shear-removal of subcontinental lithospheric mantle beneath the Colorado Plateau by the subducted Farallon slab. Sci. Rep. 9, 8153. https://doi.org/10.1038/s41598-019-44628-y.
Hernández-Uribe, D., Gutiérrez-Aguilar, F., Mattinson, C.G., Palin, R.M., Neill, O.K., 2019. A new record of deeper and colder subduction in the Acatlán complex, Mexico: Evidence from phase equilibrium modelling and Zr-in-rutile thermometry. Lithos 324-325, 551–568.
Hetzel, R., Echtller, H.P., Seifer, W., Schulte, B.A., Ivanov, K.S., 1998. Subduction- and exhumation-related fabrics in the Paleozoic high-pressure—low-temperature Maksyutov Complex, Antingan area, southern Urals, Russia. Geol. Soc. Am. Bull. 110, 916–930.
Hirajima, T., Banno, S., Hiroi, Y., Ohta, Y., 1988. Phase petrology of eclogites and related rocks from the Motalafjella high-pressure metamorphic complex in Spitzbergen (Arctic Ocean) and its significance. Lithos 22, 75–97.
Hunziker, D., Burg, J.-P., Moulas, E., Reusser, E., Omrani, J., 2017. Formation and preservation of fresh lawsonite: Geothermobarometry of the North Makran blueschists, southeast Iran. J. Metamorph. Geol. 35, 871–895. https://doi.org/10.1111/jmg.12259.
Iizuka-Oku, R., Soustelle, V., Miyajima, N., Walte, N., Frost, D.J., ad Yagi, T., 2019. Experimentally deformed lawsonite at high pressure and high temperature: Implications for low velocity layers in subduction zones. Phys. Earth Planet. Inter. 295, 106282. https://doi.org/10.1016/j.pepi.2019.106282.
Kang, P., Whitney, D.L., Martin, L., Vitale Brovarone, A., Ghent, E.D., Fornash, K.F., 2019. Lawsonite oxygen isotope and trace element records of subduction fluids. American Geophysical Union Fall Meeting Abstract V43E-0143.
Kawai, T., Windley, B.F., Terabatashi, M., Yamamoto, H., Maruyama, S., Isozaki, Y., 2006. Mineral isograds and metamorphic zones of the Anglesey blueschist belt, UK: Implications for the metamorphic development of a Neoproterozoic subduction-accretion complex. J. Metamorph. Geol. 24, 591–602.
Kelley, K.A., Cottrell, E., 2009. Water and the oxidation state of subduction zone magmas. Science 325, 605–607.
Kelley, K.A., Plank, T., Ludden, J., Staudigel, H., 2003. Composition of altered oceanic crust at ODP Sites 801 and 1149. Geochem. Geophys. Geosyst. 4, 8910. https://doi.org/10.1029/2002GC000435.
Kerrick, D.M., Connolly, J.A.D., 2001. Metamorphic devolatilization of subducted oceanic metabasalts: Implications for seismicity, arc magmatism and volatile recycling. Earth Planet. Sci. Lett. 189, 19–29.
Kim, D., Katayama, I., Michibayashi, K., Tsujimori, T., 2013a. Rheological contrast between glaucophane and lawsonite in naturally deformed blueschist from Diablo Range, California. Island Arc 22, 63–73.
Kim, D., Katayama, I., Michibayashi, K., Tsujimori, T., 2013b. Deformation fabrics of natural blueschists and implications for seismic anisotropy in subducting oceanic crust. Phys. Earth Planet. Inter. 222, 8–21. https://doi.org/10.1016/j.pepi.2013.06.011.
Kim, D., Katayama, I., Wallis, S., Michibayashi, K., Miyake, A., Seto, Y., Azuma, S., 2015. Deformation microstructures of glaucophane and lawsonite in experimentally deformed blueschists: Implications for intermediate-depth intraplate earthquakes. J. Geophys. Res. Solid Earth 120, 1229–1242. https://doi.org/10.1002/2014JB011528.
Kirby, S.H., Stein, S., Okal, E.A., Rubie, D.C., 1996. Metastable mantle phase transformations and deep earthquakes in subducting oceanic lithosphere. Rev. Geophys. 34, 261–306.
Klemd, R., Schröter, F.C., Will, T.M., Gao, J., 2002. P-T evolution of glaucophane-omphacite bearing HP-LT rocks in the western Tianshan Orogen, NW China: new evidence for "Alpine-type" tectonics. J. Metamorph. Geol. 20, 239–254.
Krogh, E.J., Oh, C.W., Liou, J., 1994. Polyphase and anticlockwise P-T evolution for Franciscan eclogites and blueschists from Jenner, California, USA. J. Metamorph. Geol. 12, 121–134.
Li, X.P., Li, Y.L., Shu, G.M., 2005. Breakdown of lawsonite subsequent to peak UHP metamorphism in the Dabie terrane and its implication for fluid activity. Chin. Sci. Bull. 50, 1366–1372.
Li, J.-L., Gao, J., John, T., Klemd, R., Su, W., 2013. Fluid-mediated metal transport in subduction zones and its link to arc-related giant ore deposits: Constraints from a sulfide-bearing HP vein in lawsonite eclogite (Tianshan, China). Geochim. Cosmochim. Acta 120, 326–362.
Libowitzky, E., Armbruster, T., 1995. Low-temperature phase transitions and the role of hydrogen bonds in lawsonite. Am. Mineral. 80, 1277–1285. https://doi.org/10.2138/am-1995-11-1217.
Libowitzky, E., Rossman, G.R., 1996. FTIR spectroscopy of lawsonite between 82 and 325 K. Am. Mineral. 81, 1080–1091.
Liu, J., Bohlen, S.R., Ernst, W.G., 1996. Stability of hydrous phases in subduction oceanic crust. Earth Planet. Sci. Lett. 143, 161–171.
Lopez-Carmona, A., Pitra, P., Abati, J., 2013. Blueschist-facies metapelites from the Malpica–Tui Unit (NW Iberian Massif): Phase equilibria modelling and H_2O and Fe_2O_3 influence in high-pressure assemblages. J. Metamorph. Geol. 31, 263–280.
Lu, Z., Zhang, L., Yue, J., Li, X., 2019. Ultrahigh-pressure and high-P lawsonite eclogites in Muzhaerte, Chinese western Tianshan. J. Metamorph. Geol. 3, 717–743. https://doi.org/10.1111/jmg.12482.
Maekawa, H., Shozui, M., Ishii, T., Fryer, P., Pearce, J.A., 1993. Blueschist metamorphism in an active subduction zone. Nature 364, 520–523.
Malatesta, C., Gerya, T., Scambelluri, M., Federico, L., Crispini, L., Capponi, G., 2012. Intraoceanic subduction of "heterogeneous" oceanic lithosphere in narrow basins: 2D numerical modeling. Lithos 140, 234–251.
Manning, C.E., 2004. The chemistry of subduction-zone fluids. Earth Planet. Sci. Lett. 223, 1–16.
Martin, L.A.J., Hermann, J., 2018. Experimental phase relations in altered oceanic crust: Implications for carbon recycling at subduction zones. J. Petrol. 59, 299–320. https://doi.org/10.1093/petrology/egy031.
Martin, L.A.J., Rubatto, D., Vitale Brovarone, A., Hermann, J., 2011a. Lawsonite eclogite facies metasomatism of a granulite sliver associated to ophiolites in Alpine Corsica. Lithos 125, 620–640.
Martin, L.A.J., Wood, B.J., Turner, S., Rushmer, T., 2011b. Experimental measurements of trace element partitioning between lawsonite, zoisite and fluid and their implication for the composition of arc magmas. J. Petrol. 52, 1049–1075.
Martin, L.A.J., Hermann, J., Gauthiez-Putallaz, L., Whitney, D.L., Vitale Brovarone, A., Fornash, K.F., Evans, N., 2014. Lawsonite geochemistry and stability – Implications for trace element and water cycles in subduction zones. J. Metamorph. Geol. 32, 455–478. https://doi.org/10.1111/jmg.12093.
McKnight, R.E.A., Carpenter, M.A., Darling, T.W., Buckley, A., Taylor, P.A., 2007. Acoustic dissipation associated with phase transitions in lawsonite, $CaAl_2Si_2O_7(OH)_2H_2O$. Am. Mineral. 92, 1665–1672.
Mendoza, O.T., 2000. Mélanges in southern Mexico: Geochemistry and metamorphism of Las Ollas complex (Guerrero terrane). Can. J. Earth Sci. 37, 1309–1320.
Mevel, C., Kienast, J.R., 1980. Chromian jadeite, phengite, pumpellyite, and lawsonite in a high-pressure metamorphosed gabbro from the French Alps. Mineral. Mag. 43, 979–984.
Miyajima, H., Matsubara, S., Miyawaki, R., Ito, K., 1999. Itoigawaite, a new mineral, the Sr analogue of lawsonite, in jadeitite from the Itoigawa-Ohmi District, central Japan. Mineral. Mag. 63, 909–916.
Miyazaki, K., Zulkarnain, I., Sopaheluwakan, J., Wakita, K., 1996. Pressure-temperature conditions and retrograde paths of eclogites, garnet-glaucophane rocks and schists from South Sulawesi, Indonesia. J. Metamorph. Geol. 14, 549–563.
Mulcahy, S.R., King, R.L., Vervoort, J.D., 2011. Lawsonite Lu-Hf geochronology : A new geochronometer for subduction zone processes. Geology 37, 987–990.
Mulcahy, S.R., Vervoort, J.D., Renne, P.R., 2014. Dating subduction-zone metamorphism with combined garnet and lawsonite Lu-Hf geochronology. J. Metamorph. Geol. 32, 515–533.
O'Bannon III, E., Beavers, C.M., Kunz, M., Williams, Q., 2017. The high-pressure phase of lawsonite: A single crystal study of a key mantle hydrous phase. J. Geophys. Res. 122, 6294–6305. https://doi.org/10.1002/2017JB014344.
Oberhänsli, R., Bousquet, R., Moinzadeh, H., Moazzen, M., Arvin, M., 2007. The field of stability of blue jadeite: A new occurrence of jadeitite at Sorkan, Iran, as a case study. Can. Mineral. 45, 1501–1509.
Och, D.J., Leitch, E.C., Caprarelli, G., Watanabe, T., 2003. Blueschist and eclogite in tectonic mélange, Port Macquarie, New South Wales, Australia. Mineral. Mag. 67, 609–624.
Ohtani, E., Litasov, K., Hosoya, T., Kubo, T., Kondo, T., 2004. Water transport into the deep mantle and formation of a hydrous transition zone. Phys. Earth Planet. Inter. 143, 255–269.
Okamoto, K., Maruyama, S., 1999. The high-pressure synthesis of lawsonite in the MORB $+H_2O$ system. Am. Mineral. 84, 362–373.
Okay, A.I., 1980. Mineralogy, petrology, and phase relations of glaucophane-lawsonite zone blueschists from the Tavşanlı region, northwest Turkey. Contrib. Mineral. Petrol. 72, 243–255.
Okay, A.I., 1982. Incipient blueschist metamorphism and metasomatism in the Tavşanlı region, northwest Turkey. Contrib. Mineral. Petrol. 79, 361–367.
Okay, A.I., 1997. Jadeite-K-feldspar rocks and jadeitites from northwest Turkey. Mineral. Mag. 61, 835–844.
Okay, A.I., Whitney, D.L., 2010. Blueschists, eclogites, ophiolites and suture zones in northwest Turkey: A review and a field excursion guide. Ofioliti 35 (2), 131–171.
Okay, A.I., Tüysüz, O., Satır, M., Özkan-Altıner, S., Altıner, D., Sherlock, S., Eren, R.H., 2006. Cretaceous and Triassic subduction-accretion, high-pressure – low-temperature metamorphism, and continental growth in the Central Pontides, Turkey. Geol. Soc. Am. Bull. 118, 1247–1269.
Okazaki, K., Hirth, G., 2016. Dehydration of lawsonite could directly trigger earthquakes in subducting oceanic crust. Nature 530, 81. https://doi.org/10.1038/nature16501.
Ono, S., 1998. Stability limits of hydrous minerals in sediment and mid-ocean ridge basalt compositions: Implications for water transport in subduction zones. J. Geophys. Res. 103, 18253–18267. https://doi.org/10.1029/98JB01351.
Orozbaev, R., Hirajima, T., Bakirov, A., Takasu, A., Maki, K., Yoshida, K., Sakiev, K., Bakirov, A., Hirata, T., Tagiri, M., Togonbaeva, A., 2015. Trace element characteristics of clinozoisite pseudomorphs after lawsonite in talc-garnet-chloritoid schists from the

Makbal UHP Complex, northern Kyrgyz Tian-Shan. Lithos 226, 98–115. https://doi.org/10.1016/j.lithos.2014.10.008.
Parkinson, C.D., 1996. The origin and significance of metamorphosed tectonic blocks in mélanges: Evidence from Sulawesi, Indonesia. Terra Nova 8, 312–323.
Patrick, B.E., Evans, B.W., 1989. Metamorphic evolution of the Seward Peninsula blueschist terrane. J. Petrol. 30, 531–555.
Pawley, A.R., 1994. The pressure and temperature stability limits of lawsonite: Implications for H_2O recycling in subduction zones. Contrib. Mineral. Petrol. 118, 99–108.
Pawley, A.R., Redfern, S.A.T., Holland, T.J.B., 1996. Volume behavior of hydrous minerals at high pressure and temperature: I. Thermal expansion of lawsonite, zoisite, clinozoisite, and diaspore. Am. Mineral. 81, 335–340.
Peacock, S.M., 1993. The importance of blueschist-eclogite dehydration reactions in subducting oceanic crust. Geol. Soc. Am. Bull. 105, 684–694.
Peacock, S.M., 2001. Are the lower planes of double seismic zones caused by serpentine dehydration in subducting oceanic mantle? Geology 29, 299–302.
Pearce, J.A., 1983. Role of the sub-continental lithosphere in magma genesis at active continental margins. In: Hawkesworth, C.J., Norry, M.J. (Eds.), Continental Basalts and Mantle Xenoliths. Shiva Publ. Nantwich, United Kingdom, pp. 230–249.
Penniston-Dorland, S.C., Kohn, M.J., Manning, C.E., 2015. The global range of subduction zone thermal structures from exhumed blueschists and eclogites: Rocks are hotter than models. Earth Planet. Sci. Lett. 428, 243–254. https://doi.org/10.1016/j.epsl.2015.07.031.
Philippon, M., Brun, J.P., Gueydan, F., 2011. Tectonics of the Syros blueschists (Cyclades, Greece): from subduction to Aegean extension. Tectonics 30, TC4001.
Philippon, M., Gueydan, F., Pitra, P., Brun, J.-P., 2013. Preservation of subduction-related prograde deformation in lawsonite pseudomorph-bearing rocks. J. Metamorph. Geol. 31, 571–583. https://doi.org/10.1111/jmg.12035.
Piccoli, F., Vitale Brovarone, A., Beyssac, O., Martinez, I., Ague, J.J., Chaduteau, C., 2016. Carbonation by fluid–rock interactions at high-pressure conditions: Implications for carbon cycling in subduction zones. Earth Planet. Sci. Lett. 44, 146–159. https://doi.org/10.1016/j.epsl.2016.03.045.
Piccoli, F., Vitale Brovarone, A., Ague, J.J., 2018. Field and petrological study of metasomatism and high-pressure carbonation from lawsonite eclogite-facies terrains, Alpine Corsica. Lithos 304-307, 16–37. https://doi.org/10.1016/j.lithos.2018.01.026.
Plunder, A., Agard, P., Chopin, C., Okay, A.I., 2013. Geodynamics of the Tavşanlı zone, western Turkey: Insights into subduction/obduction processes. Tectonophysics 608, 884–903. https://doi.org/10.1016/j.tecto.2013.07.028.
Poli, S., Schmidt, M.W., 1995. H_2O transport and release in subduction zones: Experimental constraints on basaltic and andesitic systems. J. Geophys. Res. 100, 22299–22314.
Poli, S., Schmidt, M.W., 2002. Petrology of subducted slabs. Annu. Rev. Earth Planet. Sci. 30, 207–235.
Poli, S., Franzolin, E., Fumagalli, P., Crottini, A., 2009. The transport of carbon and hydrogen in subducted oceanic crust: an experimental study to 5 GPa. Earth Planet. Sci. Lett. 278, 350–360.
Pommier, A., Williams, Q., Evans, R.L., Pal, I., Zhang, Z., 2019. Electrical investigation of natural lawsonite and application to subduction contexts. J. Geophys. Res. Solid Earth 124, 1430–1442.
Pourteau, A., Scherer, E., Schorn, S., Bast, R., Schmidt, A., 2019. Thermal evolution of an ancient subduction interface revealed by Lu-Hf garnet geochronology, Halilbağı Complex (Anatolia). Geosci. Front. 10, 127–148.
Ravna, E.J.K., Andersen, T.B., Jolivet, L., de Capitani, C., 2010. Cold subduction and the formation of lawsonite eclogite – constraints from the prograde evolution of eclogitized pillow lava from Corsica. J. Metamorph. Geol. 28, 381–395.
Roeske, S.M., Mattinson, J.M., Armstrong, R.L., 1989. Isotopic ages of glaucophane schists on the Kodiak Islands, southern Alaska, and their impllications for the Mesozoic tectonic history of the Border Ranges fault system. Geol. Soc. Am. Bull. 101, 1021–1037.
Ronan, A.C., Tappa, M., Brown, C., Baxter, E., Lefeuvre, B., Agard, P., 2019. Rb/Sr geochemistry and geochronology on lawsonite from the Schiste Lustrés, France. American Geophysical Union Fall Meeting Abstract V43E-1034.
Rubatto, D., Hermann, J., 2003. Zircon formation during fluid circulation in eclogites (Monviso, Western Alps): Implications for Zr and Hf budget in subduction zones. Geochim. Cosmochim. Acta 67, 2173–2187.
Rüpke, L.H., Morgan, J.P., Hort, M., Connolly, J.A.D., 2004. Serpentine and the subduction water cycle. Earth Planet. Sci. Lett. 223, 17–34.
Sato, E., Hirajima, T., Kamimura, K., Fujimoto, Y., 2014. White mica K-Ar ages from lawsonite-blueschist facies Hakoishi subunit and from prehnite-pumpellyite facies Tobiishi sub-unit of the Kurosegawa belt, Kyushu, Japan. J. Mineral. Petrol. Sci. 109, 258–270.
Sato, E., Hirajima, T., Yoshida, K., Kamimura, K., Fujimoto, Y., 2016. Phase relations of lawsonite-blueschists and their role as a water-budget monitor: A case study from the Hakoishi sub-unit. of the Kurosegawa belt, SW Japan. Eur. J. Mineral. 28, 1029–1046.
Scambelluri, M., Philippot, P., 2001. Deep fluids in subduction zones. Lithos 55, 213–227.
Scambelluri, M., Rampone, E., Piccardo, G., 2001. Fluid and element cycling in subducted serpentinite: A trace-element study of the Erro-Tobbio high-pressure ultramafites (Western Alps, NW Italy). J. Petrol. 42, 55–67.
Scambelluri, M., Pettke, T., Cannaò, E., 2015. Fluid-related inclusions in Alpine high-pressure peridotite reveal trace element recycling during subduction-zone dehydration of serpentinized mantle (Cima di Gagnone, Swiss Alps). Lithos 55, 213–227.
Scambelluri, M., Cannaò, E., Gilio, M., 2019. The water and fluid-mobile element cycles during serpentinite subduction. A review. Eur. J. Mineral. 31, 405–428.
Scarsi, M., Malatesta, C., Fornasaro, S., 2018. Lawsonite-bearing eclogite from a tectonic mélange in the Ligurian Alps: new constraints for the subduction plate-interface evolution. Geol. Mag. 155, 280–297.
Schertl, H.P., Maresch, W.V., Stanek, K.P., Hertwig, A., Krebs, M., Baese, R., Sergeev, S.S., 2012. New occurrence of jadeitite, jadeite quartzite and jadeite-lawsonite quartzite in the Dominican Republic, Hispaniola: Petrological and geochronological overview. Eur. J. Mineral. 24, 199–216.
Schmidt, M.W., 1995. Lawsonite: Upper stability and formation of higher density hydrous phases. Am. Mineral. 80, 1286–1292.
Schmidt, M.W., Poli, S., 1994. The stability of lawsonite and zoisite at high pressures: Experiments in CASH to 92 kbar and implications for the presence of hydrous phases in subducted lithosphere. Earth Planet. Sci. Lett. 124, 105–118.
Schmidt, M.W., Poli, S., 1998. Experimentally based water budgets for dehydrating slabs and consequences for arc magma generation. Earth Planet. Sci. Lett. 163, 361–379.
Schneider, J., Bosch, D., Monie, P., Guillot, S., Garcia Casco, A., Lardeaux, J.M., Torres-Roldan, R.L., Millan Trujillo, G., 2004. Origin and evolution of the Escambray Massif (Central Cuba): An example of HP/LT rocks exhumed during intraoceanic subduction. J. Metamorph. Geol. 22, 227–247.
Shatsky, V.S., Usova, L.V., 1989. Lawsonite inclusions in garnets of eclogites of the Atbashinskii Ridge (Kirgiziya). Geol. Geofiz. 30, 134–139.
Sherlock, S.C., Okay, A.I., 1999. Oscillatory zoned chrome lawsonite in the Tavşanlı Zone, northwest Turkey. Mineral. Mag. 63, 687–692.
Sherlock, S., Kelley, S., Inger, S., Harris, N., Okay, A., 1999. $^{40}Ar/^{39}Ar$ and Rb-Sr geochronology of high-pressure metamorphism and exhumation history of the Tavşanlı Zone, NW Turkey. Contrib. Mineral. Petrol. 137, 46–58.
Shibakusa, H., Maekawa, H., 1997. Lawsonite-bearing eclogitic metabasites in the Cazadero area, northern California. Mineral. Petrol. 61, 163–180.
Sicard, E., Potdevin, J.-L., Caron, J.-M., 1984. Coexistence of lawsonite and pseudomorphs in pyrophyllite and kaolinite in Corsican Schistes Lustrés – Role of fluids. Comptes-Rendus de l'Academie des Sciences de Paris II (298), 453–458.
Sicard, E., Caron, J.M., Potdevin, J.L., Dechomets, R., 1986. Mass-transfer and synmetamorphic deformation in a fold, 2. Lawsonite pseudomorphs and characterization of interstitial fluids. Bull. Mineral. 109, 411–422.
Simonov, V.A., Sakiev, K.S., Volkova, N.I., Stupakov, S.I., Travin, A.V., 2008. Conditions of formation of the Atbashi Ridge eclogite (South Tien Shan). Russ. Geol. Geophys. 49, 803–815.
Simons, K.K., Harlow, G.E., Brueckner, H.K., Goldstein, S.L., Sorensen, S.S., Hemming, N.G., Langmuir, C.H., 2010. Lithium isotopes in Guatemalan and Franciscan HP-LT rocks: Insights into the role of sediment-derived fluids during subduction. Geochim. Cosmochim. Acta 74, 3621–3641.
Smith, C.A., Sisson, V.B., Avé Lallemant, H.G., Copeland, P., 1999. Two contrasting pressure-temperature-time paths in the Villa de Cura blueschist belt, Venezuela: Possible evidence for Late Cretaceous initiation of subduction in the Caribbean. Geol. Soc. Am. Bull. 111, 831–848.
Sorensen, S.S., Grossman, J.N., Perfit, M.R., 1997. Phengite-hosted LILE enrichment in eclogite and related rocks: Implications for fluid-mediated mass transfer in subduction zones and arc magma genesis. J. Petrol. 38, 3–34.
Spandler, C., Hermann, J., Arculus, R., Mavrogenes, J., 2003. Redistribution of trace elements during prograde metamorphism from lawsonite blueschist to eclogite facies: Implications for deep subduction-zone processes. Contrib. Mineral. Petrol. 146, 205–222.
Spandler, C., Pettke, T., Rubatto, D., 2011. Internal and external fluid sources for eclogite-facies veins in the Monviso meta-ophiolite, Western Alps: Implications for fluid flow in subduction zones. J. Petrol. 52, 1207–1236.
Staudigel, H., Hart, S.R., Schmincke, H.-U., Smith, B.M., 1989. Cretaceous ocean crust at DSDP sites 417 and 418; carbon uptake from weathering versus loss by magmatic outgassing. Geochim. Cosmochim. Acta 53, 3091–3094.
Syracuse, E.M., van Keken, P.E., Abers, G.A., 2010. The global range of subduction zone thermal models. Phys. Earth Planet. Inter. 183, 73–90.
Tamblyn, R., Hand, M., Kelsey, D., Anczkiewicz, R., Och, D., 2019. Subduction and accumulation of lawsonite eclogite and garnet blueschist in eastern Australia. J. Metamorph. Geol. 38, 157–182. https://doi.org/10.1111/jmg.12516.
Tang, K., Yan, Z., 1993. Regional metamorphism and tectonic evolution of the Inner Mongolian suture zone. J. Metamorph. Geol. 11, 511–522.
Tang, X.C., Zhang, K.-J., 2014. Lawsonite-and glaucophane-bearing blueschists from the NW Qiangtang, northern Tibet, China: Mineralogy, geochemistry, geochronology, and tectonic implications. Int. Geol. Rev. 56, 150–166. https://doi.org/10.1080/00206814.2013.820866.
Teyssier, C., Whitney, D.L., Toraman, E., Seaton, N.C.A., 2010. Lawsonite vorticity and subduction kinematics. Geology 38, 1123–1126.
Theye, T., Seidel, E., 1987. Indicator minerals in high-pressure marbles of Crete: sudoite, lawsonite, aragonite. Fortschr. Mineral. 65, 181.
Tian, Z.L., Wei, C.J., 2013. Metamorphism of ultrahigh-pressure eclogites from the Kebuerte Valley, South Tianshan, NW China: Phase equilibria and P–T path. J. Metamorph. Geol. 31, 281–300.
Topuz, G., Okay, A.I., Altherr, R., Satır, M., Schwarz, W.H., 2008. Late Cretaceous blueschist facies metamorphism in southern Thrace (Turkey) and its geodynamic implications. J. Metamorph. Geol. 26, 895–913.
Tribuzio, R., Messiga, B., Vannucci, R., Bottazzi, P., 1996. Rare earth element distribution during high-pressure – low-temperature metamorphism in ophiolitic Fe-gabbros (Liguria, northwestern Italy): Implications for light REE mobility in subduction zones. Geology 24, 711–714.
Trotet, F., Jolivet, L., Vidal, O., 2001. Tectono-metamorphic evolution of Syros and Sifnos islands (Cyclades, Greece). Tectonophysics 338, 179–206.
Trouw, R.A.J., Simões, L.S.A., Valladares, C.S., 1998. Metamorphic evolution of a subduction complex, South Shetland Islands, Antarctica. J. Metamorph. Geol. 16, 475–490.
Tsuchiya, S., Hirajima, T., 2013. Evidence of the lawsonite eclogite metamorphism from an epidote-glaucophane eclogite in the Kotsu area of the Sanbagawa belt, Japan. J. Mineral. Petrol. Sci. 108, 166–171.

Tsujimori, T., Ernst, W.G., 2014. Lawsonite blueschists and lawsonite eclogites as proxies for palaeo-subduction zone processes: A review. J. Metamorph. Geol. https://doi.org/10.1111/jmg.12057.
Tsujimori, T., Liou, J.G., 2007. Significance of Ca-Na pyroxene-lawsonite-chlorite assemblage in blueschist-facies metabasalts: An example from the Renge metamorphic rocks, Southwest Japan. Int. Geol. Rev. 49, 416–430.
Tsujimori, T., Sisson, V.B., Liou, J.G., Harlow, G.E., Sorensen, S.S., 2006. Very-low temperature record of the subduction process: A review of worldwide lawsonite eclogites. Lithos 92, 609–624.
Turner, S., Hawkesworth, C.J., van Calsteren, P., Heath, E., Macdonald, R., Black, S., 1996. U-series isotopes and destructive plate margin magma genesis in the Lesser Antilles. Earth Planet. Sci. Lett. 142, 191–207.
Ueno, T., 1999. REE-bearing sector-zoned lawsonite in the Sanbagawa pelitic schists of the eastern Kii Peninsula, central Japan. Eur. J. Mineral. 11, 993–998.
Usui, T., Nakamura, E., Kobayashi, K., Maruyama, S., Helmstaedt, H., 2003. Fate of the subducted Farallon plate inferred from eclogite xenoliths in the Colorado Plateau. Geology 31, 589–592.
Usui, T., Nakamura, E., Helmstaedt, H., 2006. Petrology and geochemistry of eclogite xenoliths from the Colorado Plateau: Implications for the evolution of subducted oceanic crust. J. Petrol. 47, 929–964.
van Keken, P.E., Hacker, B.R., Syracuse, E., Abers, G.A., 2011. Subduction factory: 4. Depth-dependent flux of H_2O from subducting slabs worldwide. J. Geophys. Res. 116, B01401.
Vitale Brovarone, A., Agard, P., 2013. True metamorphic isograds or tectonically sliced metamorphic sequence? New high-spatial resolution petrological data for the New Caledonia case study. Contrib. Mineral. Petrol. 166, 451–469.
Vitale Brovarone, A., Beyssac, O., 2014. Lawsonite metasomatism: A new route for water to the deep Earth. Earth Planet. Sci. Lett. 393, 275–284.
Vitale Brovarone, A., Herwartz, D., 2013. Timing of HP metamorphism in the Schistes Lustrés of Alpine Corsica: New Lu-Hf garnet and lawsonite ages. Lithos 172-173, 175–191.
Vitale Brovarone, A., Beltrando, M., Malavieille, J., Giuntoli, F., Tondella, E., Groppo, C., Beyssac, O., Compagnoni, R., 2011a. Inherited Ocean–Continent Transition zones in deeply subducted terranes: Insights from Alpine Corsica. Lithos 124, 273–290.
Vitale Brovarone, A., Groppo, C., Hetényi, G., Compagnoni, R., Malavieille, J., 2011b. Coexistence of lawsonite-bearing eclogite and blueschist: Phase equilibria modelling of Alpine Corsica metabasalts and petrological evolution of subducting slabs. J. Metamorph. Geol. 29, 583–600.
Vitale Brovarone, A., Beyssac, O., Malavieille, J., Molli, G., Beltrando, M., Campagnoni, R., 2013. Stacking and metamorphism of continuous segments of subducted lithosphere in a high-pressure wedge: The example of Alpine Corsica (France). Earth Sci. Rev. 116, 35–56.
Vitale Brovarone, A., Alard, O., Beyssac, O., Martin, L., Picatto, M., 2014a. Lawsonite metasomatism and trace element recycling in subduction zones. J. Metamorph. Geol. 32, 489–514.
Vitale Brovarone, A., Picatto, M., Beyssac, O., Lagabrielle, Y., Castelli, D., 2014b. The blueschist–eclogite transition in the Alpine chain: P–T paths and the role of slow spreading extensional structures in the evolution of HP–LT mountain belts. Tectonophysics 615–616, 96–121.
Vitale Brovarone, A., Agard, P., Monié, P., Chauvet, A., Rabaute, A., 2018. Tectonic and metamorphic architecture of the HP belt of New Caledonia. Earth Sci. Rev. 178, 48–67.
Vitale Brovarone, A., Tumiati, S., Piccoli, F., Ague, J.J., Connolly, J.A., Beyssac, O., 2020. Fluid-mediated selective dissolution of subducting carbonaceous material: Implications for carbon recycling and fluid fluxes at forearc depths. Chem. Geol. https://doi.org/10.1016/j.chemgeo.2020.119682.
Wada, I., Wang, K., 2009. Common depth of slab-mantle decoupling: Reconciling diversity and uniformity of subduction zones. Geochem. Geophys. Geosyst., Q10009 https://doi.org/10.1029/2009GC002570.
Wang, Y., Prelevic, D., Foley, S., 2019. Geochemical characteristics of lawsonite blueschists in tectonic mélange from the Tavşanlı Zone, Turkey: Potential constraints on the origin of Mediterranean potassium-rich magmatism. Am. Mineral. 104, 724–743.
Wei, C.J., Clarke, G.L., 2011. Calculated phase equilibria for MORB compositions: A reappraisal of the metamorphic evolution of lawsonite eclogite. J. Metamorph. Geol. 29, 939–952.
Wei, C.J., Li, Y.J., Yu, Y., Zhang, J.S., 2010. Phase equilibria and metamorphic evolution of glaucophane-bearing UHP eclogites from the Western Dabieshan Terrane, Central China. J. Metamorph. Geol. 28, 647–666.
Whitney, D.L., Davis, P.B., 2006. Why is lawsonite eclogite so rare? Metamorphism and preservation of lawsonite eclogite, Sivrihisar, Turkey. Geology 34, 473–476. https://doi.org/10.1130/G22259.1.
Whitney, D.L., Evans, B.W., 2010. Abbreviations for names of rock-forming minerals. Am. Mineral. 95, 185–187. https://doi.org/10.2138/am.2010.3371.
Whitney, D.L., Teyssier, C., Seaton, N.C.A., Fornash, K.F., 2014. Petrofabrics of high-pressure rocks exhumed at the slab-mantle interface from the 'point of no return' in an oceanic subduction zone (Sivrihisar, Turkey). Tectonics 33, 2315–2341. https://doi.org/10.1002/2014TC003677.
Willlner, A.P., Maresch, W.V., Massonne, H.-J., Sandritter, K., Willner, G., 2016. Metamorphic evolution of blueschists, greenschists, and metagreywackes in the Cretaceous Mt. Hibernia Complex (SE Jamaica). Eur. J. Mineral. 28, 1059–1078.
Willner, A.P., Glodny, J., Gerya, T.V., Godoy, E., Massone, H.-J., 2004. A counterclockwise PTt. path of high-pressure/low-temperature rocks from the Coastal Cordillera accretionary complex of south-central Chile: Constraints for the earliest stage of subduction mass flow. Lithos 75, 283–310. https://doi.org/10.1016/j.lithos.2004.03.002.
Worthing, M.A., Crawford, A.J., 1996. The igneous geochemistry and tectonic setting of metabasites from the Emo Metamorphics, Papua New Guinea; a record of the evolution and destruction of a backarc basin. Mineral. Petrol. 58, 79–100.
Xiao, Y., Niu, Y., Song, S., Davidson, J., Liu, X., 2013. Elemental responses to subduction-zone metamorphism: Constraints from the North Qilian Mountains, China. Lithos 160-161, 55–67.
Zack, T., Rivers, T., Foley, S.F., 2001. Cs-Rb-Ba systematics in phengite and amphibole: An assessment of fluid mobility at 2.0 GPa in eclogites from Trescolmen, Central Alps. Contrib. Mineral. Petrol. 140, 651–669.
Zack, T., Foley, S.F., Rivers, T., 2002. Equilibrium and disequilibrium trace element partitioning in hydrous eclogites (Trescolmen, Central Alps). J. Petrol. 43, 1947–1974.
Zack, T., Rivers, T., Brumm, R., Kronz, A., 2004. Cold subduction of oceanic crust: Implications from a lawsonite eclogite from the Dominican Republic. Eur. J. Mineral. 16, 909–916.
Zhang, J.X., Meng, F.C., Wan, Y.S., 2007. A cold early Palaeozoic subduction zone in the North Qilian Mountains, NW China: Petrological and U-Pb geochronological constraints. J. Metamorph. Geol. 25, 285–304.
Zucali, M., Spalla, I.M., 2011. Prograde lawsonite during the flow of continental crust in the Alpine subduction: Strain vs. metamorphism partitioning, a field-based analysis to infer tectonometamorphic evolutions (Sesia-Lanzo Zone, Western Italian Alps). J. Struct. Geol. 33, 381–398.